

Goodness-of-Fit Tests for High-Dimensional Gaussian Graphical Models via Exchangeable Sampling

Xiaotong Lin¹, Weihao Li¹, Fangqiao Tian², and Dongming Huang¹

¹Department of Statistics and Data Science, National University of Singapore

²Department of Mathematics, National University of Singapore

Abstract

We introduce a general framework for testing goodness-of-fit for Gaussian graphical models in both the low- and high-dimensional settings. This framework is based on a novel algorithm for generating exchangeable copies by conditioning on sufficient statistics. This framework provides exact finite-sample error control regardless of the dimension and allows flexible choices of test statistics to improve power. We explore several candidate test statistics and conduct extensive simulation studies to demonstrate their finite-sample performance compared to existing methods. The proposed tests exhibit superior power, particularly in cases where the true precision matrix deviates from the null hypothesis due to many small nonzero entries. To justify theoretically, we consider a high-dimensional setting where the proposed test achieves rate-optimality under two distinct signal patterns in the precision matrix: (1) dense patterns with many small nonzero entries and (2) strong patterns with at least one large entry. Finally, we illustrate the usefulness of the proposed test through real-world applications.

Keywords: Co-sufficient sampling, Gaussian graphical model, goodness-of-fit, high-dimensional inference, minimax hypothesis testing.

1 Introduction

Gaussian graphical models (GGMs) have been widely used for analysing complex dependencies among high-dimensional variables in various fields. By using graphs to represent conditional independence in multivariate Gaussian distributions, GGMs provide visual interpretations for relationships among variables. For example, GGMs have been applied to recover gene association networks [Schäfer and Strimmer, 2005, Dobra, 2009, Castelletti and Consonni, 2021], to model functional brain networks [Belilovsky et al., 2016, Smith et al., 2011, Varoquaux et al., 2010], and to model cross-sectional and time-series data in psychological studies [Epskamp et al., 2018].

Consider a p -dimensional random vector $X = (X_1, X_2, \dots, X_p)^\top$ following a multivariate normal distribution $\mathbf{N}_p(\boldsymbol{\mu}, \boldsymbol{\Sigma})$ with mean $\boldsymbol{\mu}$ and covariance matrix $\boldsymbol{\Sigma}$. The GGM concerns the precision matrix $\boldsymbol{\Omega} = \boldsymbol{\Sigma}^{-1}$, where an off-diagonal entry $\omega_{ij} = 0$ implies X_i and X_j are conditionally independent given the remaining variables [Dempster, 1972]. Using this property, the GGM imposes constraints on the pattern of zero entries of $\boldsymbol{\Omega}$ to satisfy its conditional independence structure of the distribution. The structure is represented by a graph $G = (\mathcal{V}, \mathcal{E})$, where $\mathcal{V} = \{1, 2, \dots, p\}$ is the node set and \mathcal{E} is the edge set that include (i, j) if $i \neq j$ and ω_{ij} is allowed to be nonzero. Formally, the p -dimensional GGM with graph $G = (\mathcal{V}, \mathcal{E})$ is defined as:

$$\mathcal{M}_G = \{\mathbf{N}_p(\boldsymbol{\mu}, \boldsymbol{\Omega}^{-1}) : \boldsymbol{\mu} \in \mathbb{R}^p, \boldsymbol{\Omega} \succ \mathbf{0}, \omega_{i,j} = 0 \text{ if } i \neq j \text{ and } (i, j) \notin \mathcal{E}\}. \quad (1.1)$$

Additional details on GGMs can be found in Lauritzen [1996] and Anderson [2007].

This paper considers goodness-of-fit testing in GGMs, which tests whether the data-generating distribution belongs to the GGM with a given candidate graph.

Table 1: Comparison of goodness-of-fit (GoF) testing and graph selection for graphical models

Aspect	GoF Testing	Graph Selection
Goal	Assess a candidate graph G_0 before downstream analyses	Identify the underlying graph G to represent conditional independence
Focus	Test if G_0 includes all true edges, regardless of false edges	Select as many true edges as possible while avoiding false edges
Null Hypothesis	Single hypothesis that G_0 includes all true edges	Multiple individual hypotheses about the absence of each edge
Output	A testing decision or a p-value	A graph with selected edges
Error Control	Rejection probability when G_0 includes all true edges	False discovery rate of selected edges

1.1 Motivation

To apply a GGM for data analysis, it is important to determine the graph. This involves estimating the graph structure and assessing the adequacy of the GGM. Graph selection has been studied extensively, with important advancements such as the Graphical Lasso (GLasso) [Yuan and Lin, 2007] and Neighbourhood Lasso [Meinshausen and Bühlmann, 2006]. However, goodness-of-fit (GoF) testing for GGMs has received comparatively less attention.

GoF testing evaluates whether a prespecified graph sufficiently captures all true edges. Unlike graph selection, which aims to *identify as many true edges as possible while avoiding false ones*, GoF testing aims to determine whether *a specific candidate graph includes all true edges even if false edges are present*. The definition of Type-I error also differs: in graph selection, it means *selecting any false edge*, while in GoF testing, it means *rejecting the candidate graph when it already contains all true edges*. These conceptual differences lead to distinct methodologies, which are summarised in Table 1. Appendix A.1 provides a literature review of both problems.

In GoF testing, a candidate graph may be derived from domain expertise or historical data. Validating a candidate graph is important before using it for subsequent inference. For example, in analysing U.S. precipitation data, assessing whether the GGM based on geographic adjacency is appropriate can enhance the credibility of downstream analyses. In the model-X framework, if we are sure that the distribution of predictors belongs to a GGM, then we can reliably implement a conditional knockoff filter to select important variables for a response of interest with false discovery control. Appendix A.2 provides more details on this matter.

1.2 Problem formulation

Suppose the rows of the observed data \mathbf{X} are independent and identically distributed (i.i.d.) samples from some population P . Let $[p] := \{1, 2, \dots, p\}$. Given a graph $G_0 = ([p], \mathcal{E}_0)$, the goal is to test the null hypothesis that

$$H_0 : P \in \mathcal{M}_{G_0}, \tag{1.2}$$

where \mathcal{M}_{G_0} is the GGM w.r.t. G_0 , as defined in (1.1).

The statement $P \in \mathcal{M}_{G_0}$ allows G_0 to include additional false edges, which is more flexible than the *faithfulness* that requires each edge in G_0 corresponds to an off-diagonal nonzero entry of the precision matrix. In addition, the statement does not concern combinatorial properties of the graph, such as connectivity and the maximum degree. Both faithfulness testing and combinatorial inference are very different from GoF testing, and Appendices A.3 and A.4 discuss these differences.

While several GoF tests for GGMs exist, none are fully satisfactory. Classical tests like the generalised likelihood ratio test are inapplicable in high dimensions. The multiplicity adjustment of pairwise tests by Drton and Perlman [2007] and the procedures by Verzelen and Villers [2009] remain suboptimal in certain situations, especially when signals are *dense but weak*—that is, when the true precision matrix has many small nonzero entries absent from the null model. Furthermore, they cannot incorporate prior structural information. These limitations motivate the development of more powerful and flexible GoF tests.

To overcome the aforementioned challenges, we construct a valid randomisation test using arbitrary test statistics. Suppose we can sample M copies $\tilde{\mathbf{X}}^{(m)}$ of the observed data \mathbf{X} so that $\{\mathbf{X}, \tilde{\mathbf{X}}^{(1)}, \dots, \tilde{\mathbf{X}}^{(M)}\}$ are exchangeable under the null hypothesis. Let $T(\mathbf{X})$ be a statistic chosen such that larger (positive) values are regarded as evidence against the null, and $T(\tilde{\mathbf{X}}^{(m)})$ represents the corresponding test statistic of each copy. If we define a p-value by

$$\text{pVal}(\mathbf{X}, \tilde{\mathbf{X}}^{(1)}, \dots, \tilde{\mathbf{X}}^{(M)}) = \frac{1}{M+1} \left(1 + \sum_{m=1}^M \mathbb{1} \left\{ T(\tilde{\mathbf{X}}^{(m)}) \geq T(\mathbf{X}) \right\} \right), \quad (1.3)$$

then it is guaranteed that $\mathbf{P}(\text{pVal} \leq \alpha) \leq \alpha$ under the null hypothesis, where α is any predefined significance level. The general idea of this approach has been well-explored and is known as Monte Carlo testing (see Appendix A.5 for a review). The validity of the p-value defined in (1.3) does not rely on the choice of $T(\cdot)$, and the computation does not require any knowledge about the sampling distribution of $T(\mathbf{X})$. Therefore, users have the freedom to choose any test statistic to improve power, such as by incorporating prior knowledge about potential alternatives.

The main requirement for this approach is the exchangeability among the observed data \mathbf{X} and the generated copies $\tilde{\mathbf{X}}^{(m)}$. This could be achieved by *co-sufficient sampling*, which generates i.i.d. Monte Carlo samples from the conditional distribution given the value of a sufficient statistic; see Appendix A.6 for a review. Although co-sufficient sampling has been applied to many parametric models, it is not straightforward to implement co-sufficient sampling for GGMs. The idea of conditioning on sufficient statistics has also been explored for model-X knockoff generation [Huang and Janson, 2020]. However, their methods cannot satisfy the exchangeability requirement due to the fundamental differences between knockoff and exchangeable copies; see Appendix A.5 for a detailed discussion. Moreover, it remains unclear how to choose the test statistic to achieve high power.

1.3 Main contributions

To fill the aforementioned gaps, we provide the following contributions:

1. In Section 2, we propose an efficient algorithm for generating exchangeable copies of the observed data under GGMs, which leverages the geometry of Gaussian conditional distributions and the properties of Markov chains.
2. In Section 3, we propose the MC-GoF test for (1.2) using the exchangeable copies. This method yields a valid p-value with any test statistic function and can be applied with any dimension. Furthermore, we propose several test statistic functions and extend the method to test the local Markov property.
3. Section 4 presents a theoretical framework for the power properties of the MC-GoF test in high dimensions. We show that the MC-GoF test can achieve rate-optimality under two distinct alternative hypotheses about how the precision matrix violates the null hypothesis: (1) a dense alternative with many small nonzero entries, and (2) a strong alternative with at least one large entry. In both cases, the signal strength required by the MC-GoF test to have full power matches the lower bound on the separation rate for any consistent test.
4. We conduct extensive simulations to investigate the finite-sample performance of the MC-GoF test across various graph structures in Section 5. Our proposed method is shown to be competitive in general, and significantly outperforms existing methods when the signal pattern is dense but weak.

We exemplify the usefulness of our methods through their applications to real-world datasets in Section 6. Section 7 discusses future directions, including adapting our methodologies to other graphical models. The supplementary material provides complete details of the literature review, algorithms, theoretical derivations, proofs, simulation results, and data analyses.

2 Sampling Exchangeable Copies

Suppose $G = (\mathcal{V}, \mathcal{E})$ is a given graph and the rows of \mathbf{X} are n i.i.d. samples from a distribution in \mathcal{M}_G . We propose an algorithm to generate copies $\tilde{\mathbf{X}}^{(m)}$ ($1 \leq m \leq M$) so that $\mathbf{X}, \tilde{\mathbf{X}}^{(1)}, \dots, \tilde{\mathbf{X}}^{(M)}$ are exchangeable. Our method is based on the idea of conditioning on sufficient statistics and the properties of Markov chains.

Let \mathbf{x}_i^\top be the i -th row of \mathbf{x} and $f_{\mu, \Omega}(\mathbf{x})$ be the density function for \mathbf{X} . Since $\Omega_{i,j} = 0$ for $(i, j) \notin \mathcal{E}$, a sufficient statistic is given by $\psi_G(\mathbf{X})$, where $\psi_G(\cdot)$ is defined as $\psi_G(\mathbf{x}) := (\sum_{i=1}^n \mathbf{x}_i, (\mathbf{x}^\top \mathbf{x})_{i,j} : i = j \text{ or } (i, j) \in \mathcal{E})$ for $\mathbf{x} \in \mathbb{R}^{n \times p}$.

Let $\Psi = \psi_G(\mathbf{X})$ be the observed sufficient statistic. If the value of $\psi_G(\mathbf{x})$ is fixed to be Ψ , the density function $f_{\mu, \Omega}(\mathbf{x})$ is free of \mathbf{x} . Therefore, the conditional distribution of \mathbf{X} given Ψ is uniform on a support defined as $\mathcal{X}_\Psi := \{\mathbf{x} \in \mathbb{R}^{n \times p} : \psi_G(\mathbf{x}) = \Psi\}$. Note that \mathcal{X}_Ψ is an algebraic variety in a high-dimensional space and, except for special cases such as the one presented in Appendix B.1, it generally lacks a simple structure. As a result, it is difficult to sample directly from the uniform distribution on \mathcal{X}_Ψ . Instead, we construct Markov chains to generate exchangeable copies using the idea in Besag and Clifford [1989], where we sequentially update the columns of the data matrix one at a time. It should be clarified that we are not using the Markov Chain Monte Carlo method to sample approximately from the conditional distribution; instead, we construct Markov chains to generate exchangeable copies.

Our sampling method will be presented in two steps: we first introduce the one-step update in Section 2.1, and then introduce the construction of the Markov chains in Section 2.2.

2.1 Residual Rotation

In our method, we update each column \mathbf{X}_i by sampling from its conditional distribution given the other columns and the sufficient statistic Ψ . Under the Gaussian graphical model, this conditional distribution is uniform over a certain linear constraint set in \mathbb{R}^n . To sample from this uniform distribution, we hold the projection of \mathbf{X}_i onto the column space of $[\mathbf{1}_n, \mathbf{X}_{N_i}]$ fixed and then rotate the residual component uniformly at random. We name this procedure the *residual rotation* and summarise it in Algorithm 1, with derivations provided in Appendix B.2. Proposition 1 states the desired properties, namely, the output $\tilde{\mathbf{X}}_i$ and the input \mathbf{X}_i are conditionally exchangeable given \mathbf{X}_{-i} .

Algorithm 1 Sampling one column via residual rotation

- Input:** $n \times p$ data matrix \mathbf{X} , index i of the variable to sample, neighbourhood N_i of i
 If $n \leq |N_i| + 1$, output $\tilde{\mathbf{X}}_i = \mathbf{X}_i$; otherwise, proceed to the following steps.
Step 1: Apply least squares linear regression to \mathbf{X}_i on $[\mathbf{1}_n, \mathbf{X}_{N_i}]$
Step 2: Obtain the fitted vector \mathbf{F} and the residual vector \mathbf{R} from the regression
Step 3: Apply linear regression to a standard normal n -vector on $[\mathbf{1}_n, \mathbf{X}_{N_i}]$ and obtain the residual $\tilde{\mathbf{R}}$
Step 4: Compute and output $\tilde{\mathbf{X}}_i = \mathbf{F} + \tilde{\mathbf{R}} \frac{\|\mathbf{R}\|}{\|\tilde{\mathbf{R}}\|}$
-

Proposition 1. *Suppose the rows of \mathbf{X} are i.i.d. samples from a distribution in \mathcal{M}_G . Let $\tilde{\mathbf{X}}_i$ be the output of Algorithm 1 with index i , N_i be its neighbourhood, and $\tilde{\mathbf{X}}$ be a matrix formed by replacing the i -th column of \mathbf{X} with $\tilde{\mathbf{X}}_i$. Then, $\psi_G(\mathbf{X}) = \psi_G(\tilde{\mathbf{X}})$ and the conditional distribution of $\tilde{\mathbf{X}}$ given $\mathbf{X} = \mathbf{x}$ is the same as that of \mathbf{X} for almost every $\mathbf{x} \in \mathbb{R}^{n \times p}$. Furthermore, if $n \geq 3 + |N_i|$, then $\tilde{\mathbf{X}}_i \neq \mathbf{X}_i$, a.s.*

2.2 Sampling Exchangeable Copies from Markov Chains

To generate exchangeable copies of \mathbf{X} , we construct forward and backward Markov chains using the residual rotation method. First, we run the residual rotation across all variables in turn to create a forward Markov chain $\mathcal{C}_1 = (\mathbf{X}, \vec{\mathbf{X}}^{(1)}, \dots, \vec{\mathbf{X}}^{(p)})$. Then, starting from this endpoint, we run a similar procedure backward with the reversed order of variables to obtain a backward Markov chain $\mathcal{C}_2 = (\vec{\mathbf{X}}^{(p)}, \overleftarrow{\mathbf{X}}^{(p-1)}, \dots, \overleftarrow{\mathbf{X}}^{(0)})$. If the distribution of \mathbf{X} belongs to \mathcal{M}_G , Proposition 1 implies that

$$(\vec{\mathbf{X}}^{(p)}, \overleftarrow{\mathbf{X}}^{(p-1)}, \dots, \overleftarrow{\mathbf{X}}^{(0)}) \stackrel{d.}{=} (\vec{\mathbf{X}}^{(p)}, \vec{\mathbf{X}}^{(p-1)}, \dots, \vec{\mathbf{X}}^{(1)}, \mathbf{X}).$$

Therefore, conditioning on $\vec{\mathbf{X}}^{(p)}$, we have that \mathbf{X} and $\overleftarrow{\mathbf{X}}^{(0)}$ are i.i.d. We can independently conduct the backward sampling multiple times to obtain multiple copies $\tilde{\mathbf{X}}^{(m)}$ for $m = 1, 2, \dots, M$ that are exchangeable jointly with \mathbf{X} . Derivations and illustrations are provided in Appendix B.3.

Our approach is inspired by the *parallel* method introduced by Besag and Clifford [1989]. The starting point of the backward chains is called the *hub* since it is the common centre of all chains. When generating each chain, we can repeat the iteration for L times to prolong the chain, but $L = 1$ already suffices to provide satisfactory results. More discussions on the choice of L can be found in Appendix B.3.2. The order \mathcal{I} of variables to apply residual rotation can be customised as long as the backward chain uses the exact reverse order of updates.

The general procedure is summarised in Algorithm 2. It is well-suited to high-dimensional settings where $p \gg n$. First, the output copies have columns that differ from those of \mathbf{X} if $n - 2$ exceeds the degree of variables, regardless of p . In addition, it is computationally efficient because it supports independent sampling of M Markov chains via parallel computing, and each chain has computational complexity $O(Lpnd^2)$ scaling linearly in p .

Algorithm 2 Sampling exchangeable copies for a GGM

Input: $n \times p$ data matrix \mathbf{X} , graph G , number of copies M , number of iterations L (set to 1 by default), permutation \mathcal{I} of a subset $\mathcal{T} \subset [p]$.

Step 1: Start from \mathbf{X} and run Algorithm 1 according to the order \mathcal{I} for L times to generate $\mathbf{X}^{(hub)}$.

Step 2: For $m = 1, 2, \dots, M$, independently start from $\mathbf{X}^{(hub)}$ and run Algorithm 1 according to the reversed order of \mathcal{I} for L times to generate $\tilde{\mathbf{X}}^{(m)}$.

Output: $\tilde{\mathbf{X}}^{(1)}, \dots, \tilde{\mathbf{X}}^{(M)}$.

Proposition 2 summarises the desirable exchangeability of the output of Algorithm 2. It serves as the foundation for the test in Section 3, as exchangeability can be used to construct exactly valid randomisation tests (see Davison and Hinkley [1997, Chapter 4]).

Proposition 2. *Let G be a graph and suppose the rows of \mathbf{X} are i.i.d. samples from a distribution in \mathcal{M}_G . Let $\{\tilde{\mathbf{X}}^{(m)}\}_{m=1}^M$ be generated by Algorithm 2 with $\mathcal{T} \subseteq [p]$. Then (1) $\mathbf{X}, \tilde{\mathbf{X}}^{(1)}, \dots, \tilde{\mathbf{X}}^{(M)}$ are exchangeable, (2) $\tilde{\mathbf{X}}_{-\mathcal{T}}^{(m)} = \mathbf{X}_{-\mathcal{T}}$ for all m , and (3) $\mathbf{X}_{\mathcal{T}}, \tilde{\mathbf{X}}_{\mathcal{T}}^{(1)}, \dots, \tilde{\mathbf{X}}_{\mathcal{T}}^{(M)}$ are conditionally exchangeable given $\mathbf{X}_{-\mathcal{T}}$.*

3 Goodness-of-Fit Test

We will exploit the exchangeable copies to construct goodness-of-fit tests for Gaussian graphical models in Section 3.1 and then propose several test statistics in Section 3.2. In Section 3.3, we adapt the method for testing the local Markov property.

3.1 Construction of p-values

To test the null hypothesis H_0 that \mathbf{X} follows a distribution in \mathcal{M}_{G_0} for a graph G_0 , we generate $\tilde{\mathbf{X}}^{(1)}, \dots, \tilde{\mathbf{X}}^{(M)}$ using Algorithm 2. Under H_0 , Proposition 2 ensures $T(\mathbf{X}), T(\tilde{\mathbf{X}}^{(1)}), \dots, T(\tilde{\mathbf{X}}^{(M)})$ are ex-

changeable for any chosen test statistic T . As a result, the p-values computed as in (1.3) are exactly valid at any significance level α .

Algorithm 3 Monte Carlo goodness-of-fit (MC-GoF) test for GGMs

Input: $n \times p$ data matrix \mathbf{X} , graph G_0 , test statistic $T(\cdot)$, number of copies M

Step 1: Apply Algorithm 2 with $G = G_0$ and $\mathcal{I} = (1, 2, \dots, p)$ to obtain $\tilde{\mathbf{X}}^{(1)}, \dots, \tilde{\mathbf{X}}^{(M)}$

Step 2: Calculate the statistics $T(\mathbf{X}), T(\tilde{\mathbf{X}}^{(1)}), T(\tilde{\mathbf{X}}^{(2)}), \dots, T(\tilde{\mathbf{X}}^{(M)})$

Step 3: Compute and output the (one-sided) p-value in (1.3)

We summarise the testing procedure in Algorithm 3 and call it the *Monte Carlo goodness-of-fit* (MC-GoF) test for GGMs. The test statistic $T(\cdot)$ can be any function where larger values provide stronger evidence against H_0 ; extensions to tie-breaking and two-sided rules can be found in Appendix B.3.1. Proposition 3 established the validity of the MC-GoF test for H_0 .

Proposition 3. *For any test statistic $T(\cdot)$, the p-value obtained by Algorithm 3 is valid: for any level $\alpha \in (0, 1)$, we have $\mathbf{P}(\text{pVal}_T \leq \alpha) \leq \alpha$ if $P \in \mathcal{M}_{G_0}$.*

Based on this result, the MC-GoF test guarantees finite-sample Type-I error control with no constraint on the dimension p and no need to know about the sampling distribution of the test statistic. It also bypasses the need to estimate any unknown parameters so \mathcal{M}_{G_0} is allowed to have much more unknown parameters than the sample size n , which is particularly advantageous for high-dimensional settings where $p \gg n$. Specifically, the MC-GoF test remains applicable even when all degrees of G_0 reach $n/2$, while many existing methods impose sparsity assumptions that the maximum degree is at the order of $o(\sqrt{n/\log p})$.

Although the MC-GoF test does not require G_0 to be sparse, we focus on graphs with maximum degree d at most moderate relative to n (e.g., $d \leq n/2$) for practical reasons: extremely dense graphs are difficult to estimate with limited data, and they are rarely encountered in applications of graphical models.

The number of copies M does not affect the validity of the test, but it should not be too small as this may reduce the power. For significance level $\alpha = 0.05$, setting $M = 100$, or more generally $M \geq 2/\alpha$, is sufficient, as further increasing M yields minimal benefit. Setting the number of the iteration $L = 1$ already achieves desirable power properties in simulations, even for moderately dense null graphs. Detailed discussions on the choice of M and L are provided in Appendix B.3.2.

3.2 Choice of test statistic

The MC-GoF testing framework (Algorithm 3) ensures valid Type-I error control for any chosen test statistic $T(\cdot)$. However, to achieve high power, $T(\cdot)$ should effectively capture deviations from the null hypothesis. This section introduces three classes of test statistics and a fourth principle to incorporate prior knowledge. We provide an overview of the motivations and aggregation schemes. Detailed derivations are deferred to Appendix B.4.

Consider alternatives where the population belongs to a GGM, but the true graph G includes some edges absent from the null graph $G_0 = (\mathcal{V}, \mathcal{E}_0)$ in (1.2). The problem reduces to testing $H_0 : \forall(i, j) \notin \mathcal{E}_0, \omega_{ij} = 0$ versus $H_a : \exists(i, j) \notin \mathcal{E}_0, \omega_{ij} \neq 0$. We propose three strategies to measure the “distributional difference” between H_0 and H_a :

1. **Partial-Correlation-Based Statistics:** These statistics measure the conditional dependence between pairs of variables not connected in G_0 . The motivation is that if G contains edges that G_0 omits, some partial correlations will be nonzero. See more details in Appendix B.4.1.
2. **Conditional-Regression-Based Statistics:** Based on the idea of nodewise regressions, these statistics evaluate the regression of each variable on its neighbours in G_0 and test whether adding any omitted variable improves the fit. See more details in Appendix B.4.2.

3. Likelihood-Ratio-Based Statistics: These statistics compare the likelihoods under the null model with G_0 and a full model fitted using regularisation (e.g., GLasso). See more details in Appendix B.4.3.

For partial-correlation-based and conditional-regression-based approaches, we first derive pairwise or nodewise measures that reflect potential departures from G_0 and then combine these local measures into one statistic. Two aggregation schemes are:

- (i) Sum-Type Aggregation: Summing up local measures is effective if we consider the *dense-but-weak* alternative, where there are many small deviations from G_0 . For example, from partial correlation measures, we define the SRC statistic as $T_{\text{SRC}}(\mathbf{X}) = \sum_{(i,j) \notin \mathcal{E}_0} \hat{\gamma}_{ij}^2$, where $\hat{\gamma}_{ij}$ is a residual correlation measure derived from regressing i and j on the union of their neighbours in G_0 . Other statistics of this type are PRC and ERC defined in Appendix B.4.1, and F_{Σ} in Appendix B.4.2.
- (ii) Max-Type Aggregation: Taking the maximum of local measures is effective if we consider the *strong-but-sparse* alternative, where there are one or a few large deviations from G_0 . For example, from partial correlation measures, the MRC statistic is defined as $T_{\text{MRC}}(\mathbf{X}) = \max_{(i,j) \notin \mathcal{E}_0} \hat{\gamma}_{ij}^2$ in Appendix B.4.1. Another example of this type is F_{max} defined in Appendix B.4.2, where its relation to the M^1P_1 and M^1P_2 procedures proposed in Verzelen and Villers [2009] is further discussed.

The likelihood ratio approach inherently provides a single global statistic, so it does not require an additional aggregation step. For example, in Appendix B.4.3, the GLR- ℓ_1 statistic is defined as $T_{\text{GLR-}\ell_1} = 2 \log \ell(\hat{\Omega}_{ML})$, where $\hat{\Omega}_{GL}$ is a modified GLasso estimator that penalises only edges absent in G_0 and is tailored for high-dimensional settings.

When additional knowledge suggests that certain edges not in G_0 are more likely to exist, one can modify the test statistic to reflect this information. For example, if $w_{ij} \geq 0$ encodes prior beliefs about the existence of an edge (i, j) , then a weighted version of the SRC statistic is defined as $T_{\text{SRC-}w}(\mathbf{X}) = \sum_{(i,j) \notin \mathcal{E}_0} w_{ij} \hat{\gamma}_{ij}^2$. Appendix B.4.4 discusses this idea in detail, and Appendix F.4 illustrates the advantage of this approach with numerical examples. More advanced methods, such as Bayesian approaches, demand future exploration.

3.3 Testing local Markov property

Instead of a global test, some applications of GGMs may require a localised evaluation, such as testing the *local Markov property* for a subset of nodes. For node i , this property states that X_i is independent of other variables outside its neighbourhood N_i given X_{N_i} . Testing the local Markov property for a subset $\mathcal{T} \subseteq [p]$ involves verifying

$$H_0 : X \text{ is normal and } X_i \perp\!\!\!\perp X_{B_i} \mid X_{N_i}, \quad (3.1)$$

where B_i excludes i and N_i . When $\mathcal{T} = [p]$, (3.1) becomes the global hypothesis (1.2).

To obtain a valid p-value for such a local test, we modify Step 1 of Algorithm 3 by using a permutation of \mathcal{T} only (rather than a permutation of $[p]$). We call this modified algorithm the *local MC-GoF test* for GGMs and prove its validity for testing (3.1) in Appendix E.4. We can also adjust test statistics to focus on nodes in \mathcal{T} ; for example, a localised version of SRC can be defined as $T_{\text{SRC}}^{(loc)}(\mathbf{X}) = \sum_{i \in \mathcal{T}} \sum_{j \in B_i} \hat{\gamma}_{ij}^2$.

This localised framework is more efficient in terms of both computation and power when only a part of the graph is of interest. It also serves as a diagnostic tool for identifying nodes that contribute to a global model misspecification.

4 Power Analysis

This section establishes a theoretical framework for analysing the power properties of the MC-GoF test in high-dimensional settings, where both p and n grow to infinity, with p potentially much larger than n . We will quantify when the MC-GoF test can distinguish between the null hypothesis and structured alternatives, and will establish rate-optimal detection boundaries.

4.1 Setup and Framework

The power analysis involves understanding the following two aspects regarding the observed statistic $T(\mathbf{X})$ and the Monte Carlo copies $T(\tilde{\mathbf{X}}^{(m)})$:

- (A) the empirical distribution of $T(\tilde{\mathbf{X}}^{(m)})$, $m \in [M]$;
- (B) the distribution of $T(\mathbf{X})$ under a meaningful alternative hypothesis.

It is challenging to analyse Aspect (A) under general null graphs due to the complexity of Markov chains involved in the generation of $\tilde{\mathbf{X}}^{(m)}$. To achieve a tractable theory, we assume the null graph $G_0 = ([p], \mathcal{E}_0)$ belongs to the class of *clique-star shaped graphs*: the graph is a split graph with a clique \mathcal{H} and an independent set \mathcal{C} such that every node in \mathcal{C} is connected to all nodes in \mathcal{H} . Such structures simplify the null model so we can explicitly characterise the distributions of the generated copies. Remark 1 discusses the necessity and novelty of this simplification.

To study Aspect (B), we focus on normal populations and consider two distinct signal patterns: (1) the **dense-but-weak** pattern, where many off-diagonal entries of $\{\boldsymbol{\Omega}_{ij} : (i, j) \notin \mathcal{E}_0\}$ are nonzero but each is too small to detect individually, and (2) the **strong-but-sparse** pattern, where most off-diagonal entries of $\{\boldsymbol{\Omega}_{ij} : (i, j) \notin \mathcal{E}_0\}$ are zero except for at least one significant. These alternatives bridge between Aspect (B) and recent advances in correlation matrix inference.

Concretely, suppose the n rows of \mathbf{X} are i.i.d. sampled from $P = \mathbf{N}_p(\boldsymbol{\mu}, \boldsymbol{\Omega}^{-1})$. For a set Θ of precision matrices, we write $\boldsymbol{\Omega} \in \Theta$ to indicate $P \in \{\mathbf{N}_p(\boldsymbol{\mu}, \boldsymbol{\Omega}^{-1}) : \boldsymbol{\mu} \in \mathbb{R}^p, \boldsymbol{\Omega} \in \Theta\}$. Consider the null $H_0 : P \in \mathcal{M}_{G_0}$ under the following condition.

Condition 1. $G_0 = ([p], \mathcal{E}_0)$ is clique-star shaped with clique \mathcal{H} and independent set \mathcal{C} such that $|\mathcal{H}| \leq n-3$ and $q = |\mathcal{C}|$. Furthermore, either $p \geq n$ or $p = q$ holds.

Under Condition 1, $P \in \mathcal{M}_{G_0} \Leftrightarrow$ the submatrix $\boldsymbol{\Omega}_{\mathcal{C}}$ is a diagonal matrix, and so does its inverse. We measure deviations from the null using the following quantity:

$$D(\boldsymbol{\Omega}_{\mathcal{C}}, s) = \|\mathbf{R}(\boldsymbol{\Omega}_{\mathcal{C}}^{-1}) - \mathbf{I}_q\|_s,$$

where $\mathbf{R}(\mathbf{M}) = \text{diag}(\mathbf{M})^{-1/2} \mathbf{M} \text{diag}(\mathbf{M})^{-1/2}$ is the diagonal normalisation and the symbol $s \in \{F, \infty\}$ denotes the Frobenius norm or the maximum norm of a matrix, respectively. For both $s = F$ and $s = \infty$, we have $D(\boldsymbol{\Omega}_{\mathcal{C}}, s) = 0 \Leftrightarrow P \in \mathcal{M}_{G_0}$. Remark 2 provides detailed discussions and concrete examples for this metric. As we will see, the power of the MC-GoF test depends on the magnitude of $D(\boldsymbol{\Omega}_{\mathcal{C}}, s)$.

4.2 Theoretical Results

For dense alternatives where many of the off-diagonal entries of $\boldsymbol{\Omega}_{\mathcal{C}}$ are nonzero, we use $D(\boldsymbol{\Omega}_{\mathcal{C}}, F)$ to quantify the deviation from the null. For strong alternatives where some of the off-diagonal entries of $\boldsymbol{\Omega}_{\mathcal{C}}$ are separated from zero, we use $D(\boldsymbol{\Omega}_{\mathcal{C}}, \infty)$ to quantify the deviation. Our goal is to characterise how large these deviations must be (relative to n , p , and q) for the MC-GoF test to achieve high power, and to show that the rates of these deviations cannot be improved by any other test. For any $\alpha \in (0, 1)$ and any statistic T , we denote the power of the α -level MC-GoF test with statistic T as

$$\beta_n(P; \alpha, T) := \mathbb{P} \left(\frac{1}{M+1} \left[1 + \sum_{m=1}^M \mathbf{1} \left\{ T(\tilde{\mathbf{X}}^{(m)}) \geq T(\mathbf{X}) \right\} \right] \leq \alpha \right),$$

where $\tilde{\mathbf{X}}^{(m)}$ are generated by Algorithm 3 with G_0 . We now present the main results. All formal statements and further discussion are provided in Appendix C.

Dense alternatives. Consider the alternative $H_a : \boldsymbol{\Omega} \in \Theta_{n1}(b)$, where $\Theta_{n1}(b) := \left\{ \mathbf{A} \in \mathbb{S}_+^p : D(\mathbf{A}_{\mathcal{C}}, F) \geq b \sqrt{\frac{q}{n}} \right\}$, for a fixed $b_0 \geq 1$. In this case, the SRC statistic is suitable and can be expressed as $T_1(\mathbf{X}) = \sum_{i,j \in \mathcal{C}, i \neq j} \hat{\gamma}_{ij}^2$.

Theorem 1. *Suppose Condition 1 holds and $\lim_{n \rightarrow \infty} \frac{q}{n} = \gamma > 0$. Then, the followings hold:*

- (a) For any $\epsilon > 0$, there exists a constant b such that if $\boldsymbol{\Omega} \in \boldsymbol{\Theta}_{n1}(b)$, it holds $\liminf_n \beta_n(P; \alpha, T_1) \geq 1 - \epsilon$, provided that $M \geq \max(2\alpha^{-1}, \log(2\epsilon^{-1}))$.
- (b) Suppose the condition number of $\boldsymbol{\Omega}_{\mathcal{C}}$ is bounded and $D(\boldsymbol{\Omega}_{\mathcal{C}}, F) \rightarrow \infty$. If α_n and M scale appropriately, then $\lim_{n \rightarrow \infty} \beta_n(P; \alpha_n, T_1) = 1$.
- (c) Let $0 < \alpha < \beta < 1$. Suppose $q/n \leq \kappa$ for some constant $\kappa < \infty$. Then, there exists a constant b such that

$$\limsup_{n \rightarrow \infty} \left\{ \sup_{\phi} \inf_{\boldsymbol{\Omega} \in \boldsymbol{\Theta}_{n1}(b)} \mathbb{E}(\phi) \right\} < \beta.$$

where \sup_{ϕ} is taken over any α -level test ϕ for $H_0 : P \in \mathcal{M}_{G_0}$.

Strong alternatives. Consider the alternative $H_a : \boldsymbol{\Omega} \in \boldsymbol{\Theta}_{n2}(b)$, where $\boldsymbol{\Theta}_{n2}(b) = \{\mathbf{A} \in \mathbb{S}_+^p : D(\mathbf{A}_{\mathcal{C}}, \infty) \geq b\sqrt{\log(q)/n}\}$. In this case, the MRC statistic is suitable and can be expressed as $T_2(\mathbf{X}) = \max_{i,j \in \mathcal{C}, i \neq j} \hat{\gamma}_{ij}^2$.

Theorem 2. Suppose Condition 1 holds and that $\log q/n \rightarrow 0$. Then, the followings hold:

- (a) For any $\epsilon > 0$, if $n > \max(10/\alpha, 32 \log(16/\epsilon), 8/\epsilon)$ and $M > \max(2\alpha^{-1}, \log(2\epsilon^{-1}))$, then $\inf_{\boldsymbol{\Omega} \in \boldsymbol{\Theta}_{n2}(16)} \beta_n(P; \alpha, T_2) \geq 1 - \epsilon$.
- (b) If α_n and M scale appropriately, then $\lim_{n \rightarrow \infty} \inf_{\boldsymbol{\Omega} \in \boldsymbol{\Theta}_{n2}(16)} \beta_n(P; \alpha_n, T_2) = 1$.
- (c) Suppose $\log(q)/n \leq \kappa$ for some constant $\kappa < \infty$. Then, for any constant $b \in (0, \min(1, \kappa^{-1}))$, the following holds:

$$\limsup_{n \rightarrow \infty} \left\{ \sup_{\phi} \inf_{\boldsymbol{\Omega} \in \boldsymbol{\Theta}_{n2}(b)} \mathbb{E}(\phi) \right\} \leq \alpha,$$

where \sup_{ϕ} is taken over all α -level test for $H_0 : P \in \mathcal{M}_{G_0}$.

Union Alternative. We finally consider the scenario where the true precision $\boldsymbol{\Omega}$ lies in a union of dense and strong alternative sets. Consider the alternative $H_a : \boldsymbol{\Omega} \in \boldsymbol{\Theta}_{n3}(b) = \boldsymbol{\Theta}_{n1}(b) \cup \boldsymbol{\Theta}_{n2}(b)$. What makes this interesting is that $\boldsymbol{\Omega}$ can deviate from the null either via many small entries or at least one large entry, but not both simultaneously. Accordingly, we define a combined statistic $T_3(\mathbf{X}) = \max\left(\frac{n}{2q}[T_1(\mathbf{X}) - q(q-1)/n], nT_2(\mathbf{X}) - 4 \log q + \log \log q\right)$.

Theorem 3. Suppose Condition 1 holds and $q/n \rightarrow \gamma \in (0, \infty)$. Then, the followings hold:

- (a) For any $\epsilon > 0$, there exists a constant b such that if $\boldsymbol{\Omega} \in \boldsymbol{\Theta}_{n3}(b)$, it holds $\liminf_n \beta_n(P; \alpha, T_3) \geq 1 - \epsilon$, provided that $M \geq \max(2\alpha^{-1}, \log(2\epsilon^{-1}))$.
- (b) Let $0 < \alpha < \beta < 1$. Suppose $q/n \leq \kappa$ for some constant $\kappa < \infty$. Then, there exists a constant b such that

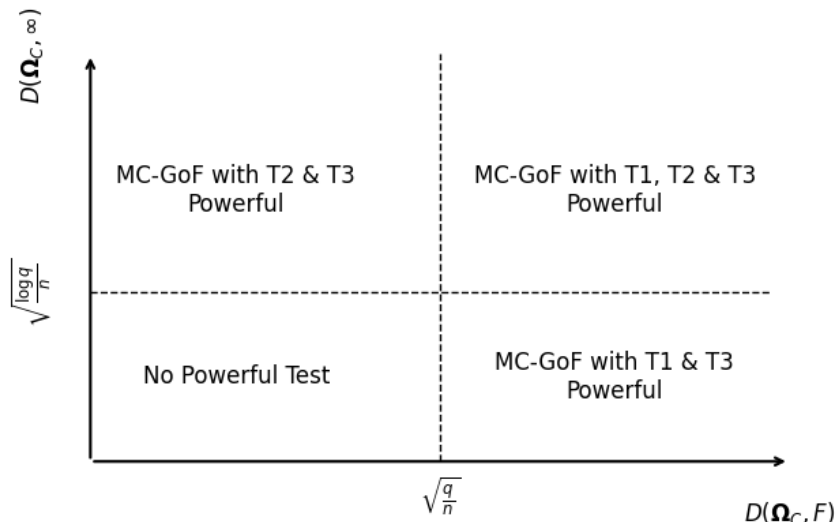
$$\limsup_{n \rightarrow \infty} \left\{ \sup_{\phi} \inf_{\boldsymbol{\Omega} \in \boldsymbol{\Theta}_{n3}(b)} \mathbb{E}(\phi) \right\} < \beta.$$

where \sup_{ϕ} is taken over any α -level test ϕ for $H_0 : P \in \mathcal{M}_{G_0}$.

For each alternative, the theorem first shows that the MC-GoF test, with a suitable statistic, achieves high power when the signal is sufficiently large, and then provides lower bounds on the detection limit that match the required signal levels up to a constant. Hence, the MC-GoF test is both powerful and rate-optimal.

Figure 1 summarises the feasibility of distinguishing the null from the alternative based on $D(\boldsymbol{\Omega}_{\mathcal{C}}, F)$ and $D(\boldsymbol{\Omega}_{\mathcal{C}}, \infty)$. It illustrates the regimes where the MC-GoF test achieves rate-optimal detection.

Figure 1: Goodness-of-fit detection boundaries and powerful tests. The four quadrants represent different signal regimes: top-left (dense-but-weak), top-right (dense-and-strong), bottom-right (strong-but-sparse), and bottom-left (weak-and-sparse).



Our theoretical analysis focuses on the large-sample power with clique-star-shaped null graphs. To complement the theory, we conduct extensive simulation studies in Section 5 and Appendix F to evaluate the finite-sample performance of the MC-GoF test under general null graphs. These simulations demonstrate that the MC-GoF test remains robust and powerful across diverse graph structures. This suggests that the theoretical insights obtained for clique-star-shaped null graphs apply more broadly.

Remark 1. *The reduction to clique-star-shaped null graphs is a necessary and strategic choice for developing a rigorous theory for the MC-GoF test. This reduction makes the characterisation of the MC-GoF test analytically tractable, which allows us to derive results on the power properties of the test that would otherwise remain inaccessible. As the analysis of alternative hypotheses is clear by focusing on these null graphs, we established the rate-optimal results for two distinct and meaningful signal patterns that, to the best of our knowledge, have not previously been examined in the literature on goodness-of-fit testing for GGMs. Furthermore, deriving these results for clique-star-shaped null graphs already demands substantial theoretical effort, which suggests that extending the theory to general null graph structures would be even more challenging. Nonetheless, the insights and benchmarks gained here provide a foundation for future extensions.*

Remark 2. *We provide some intuitions about the metric $D(\Omega_C, s)$, which is the key quantity for characterising the power of the MC-GoF test. Suppose $X = (X_1, \dots, X_p)^\top \sim \mathbf{N}_p(\mathbf{0}, \Omega^{-1})$ and $\mathcal{H} = [p] \setminus \mathcal{C}$. We have*

$$D(\Omega_C, \infty) = \max_{i,j \in \mathcal{C}} |\text{cor}(X_i, X_j \mid X_{\mathcal{H}})|,$$

$$D(\Omega_C, F)^2 \geq \frac{1}{\lambda} \sum_{i,j \in \mathcal{C}} \tilde{\Omega}_{i,j}^2,$$

where λ is the condition number of Ω_C and $\tilde{\Omega}_C = \mathbf{R}(\Omega_C)$. These suggest that $D(\Omega_C, \infty)$ measures the largest magnitude of the partial correlations that violate the null hypothesis, and the square of $D(\Omega_C, F)$ serves as a proxy for the sum of squared entries of the normalised Ω_C . To illustrate the difference between $D(\Omega_C, \infty)$ and $D(\Omega_C, F)$, we provide two simple examples.

Example (Dense but weak). Let b be a positive constant and $\rho = b/\sqrt{n(q-1)}$. Define $\mathbf{J} = (1-\rho)\mathbf{I}_q + \rho\mathbf{1}_q\mathbf{1}_q^\top$ where $\mathbf{1}_q$ is the q -vector with all entries being 1. Suppose $\boldsymbol{\Omega}_C = \mathbf{J}^{-1}$, then we have $D(\boldsymbol{\Omega}_C, F) = b\sqrt{q/n}$ while $D(\boldsymbol{\Omega}_C, \infty) = \rho = b/\sqrt{n(q-1)} \ll \sqrt{\log(q)/n}$. According to Figure 1, the precision matrix in this example lies in the regime where the signals are dense but weak (the bottom right region).

Example (Strong but sparse). Let $\rho = b\sqrt{\log(q)/n}$ and define $\mathbf{J} = \mathbf{I}_q + \rho\mathbf{E}$ where $\mathbf{E} = 1_{\{i=1, j=2\}} + 1_{\{i=2, j=1\}}$. Suppose $\boldsymbol{\Omega}_C = \mathbf{J}^{-1}$, then we have $D(\boldsymbol{\Omega}_C, \infty) = b\sqrt{\log(q)/n}$ while $D(\boldsymbol{\Omega}_C, F) = b\sqrt{2\log(q)/n} \ll \sqrt{q/n}$. According to Figure 1, the precision matrix in this example lies in the regime where the signals are strong but sparse (the upper left region).

5 Simulation Studies

We conduct numerical experiments to evaluate the finite-sample performance of the proposed MC-GoF test compared to two baseline methods: the M^1P_1 procedure by Verzelen and Villers [2010] and the Bonferroni-adjusted approach (Bonf) from Drton and Perlman [2007]. We implement the MC-GoF test with four test statistic functions: PRC, ERC, F_Σ , and GLR- ℓ_1 defined in Appendix B.4. To conserve space, we present an overview here and refer readers to Appendix D for full simulation details, along with an illustration of valid Type I error control of all methods and an examination of the M^1P_2 procedure.

We first consider three representative classes of graphs: band graphs, hub graphs, and Erdős–Rényi–Gilbert random graphs. In each setting, we define a true distribution with precision matrix $\boldsymbol{\Omega}$ and a null graph G_0 with different configurations of population parameters. To clarify the impact of signals, we focus on scenarios where G_0 is a subgraph of the true graph so that any violation of the null reveals itself clearly through additional edges with varying signal strengths. We measure these signals by parameters s or ξ that control the Kullback–Leibler divergence between the true distribution and the null model. Each scenario isolates specific aspects of graph structure, signal strength, dimension, and sample size.

Simulation results show that the MC-GoF test consistently outperforms or matches the power of M^1P_1 and Bonf. Some more observations are

(1) The MC-GoF test with F_Σ is consistently among the top performers, making it our recommended default.

(2) The power of the MC-GoF test tends to increase as the dimension p increases. In contrast, the baseline methods M^1P_1 and Bonf suffer from a loss of power in the high-dimensional cases. This indicates that our proposed method is more applicable to high-dimensional problems than existing methods.

(3) When many edges are absent from the null but each is relatively weak, baseline methods struggle to detect deviations from the null, while the MC-GoF test achieves high power. This observation matches our theoretical results in Theorem 1, which shows the rate-optimality of the MC-GoF test for detecting dense-but-weak signals.

(4) Additional simulations in Appendix F.3 demonstrate that our tests are highly competitive with M^1P_1 for detecting strong-but-sparse signals.

We also extend the experiments to more complex graph structures. Appendix F.2 presents experiments with tree, spatial, small-world, and scale-free graphs, which may be more commonly seen in real-world applications. Appendix F.1 includes an example with moderately dense null graphs, where the minimum degree is not small relative to the sample size. These additional experiments consider cases where the null graph is not a subgraph of the true graph and can be relatively dense. Across all these challenging scenarios, MC-GoF tests, especially with F_Σ , significantly outperform the baseline methods. These findings reinforce the superior performance and broad applicability of our proposed method.

6 Real-World Examples

This section empirically illustrates the effectiveness of our proposed methods through case studies in environmental science and finance.

6.1 Average Daily Precipitation in the United States

Modelling daily precipitation is essential in various fields, such as agriculture [Naylor et al., 2007], hydrology [Hamududu and Killingtveit, 2012], and climate [Cloke and Pappenberger, 2009]. Here, we intend to model the average daily precipitation in each year across the contiguous United States. We collected data from 48 states from 1979 to 2011, excluding several states due to their geographical isolation, from the North American Land Data Assimilation System. This dataset has $n = 33$ observations, and the dimension of variables is $p = 48$. Appendix G.1 reports details of data preprocessing as well as data analyses, for which we provide a summary below.

The null hypothesis states that the precipitation across states can be modelled by a GGM with G_0 , the graph representing geographic adjacency. The maximum and median degrees of G_0 are 8 and 4 respectively. The testing procedures are identical to those in Section 5, namely, the MC-GoF tests with statistics F_Σ , $\text{GLR-}\ell_1$, PRC, and ERC, as well as the benchmark methods M^1P_1 and Bonf.

We first conducted a simulation study to confirm that all methods control the Type-I error, and then reported the p-values of the GoF test applied to real data. The MC-GoF test using the F_Σ and the $\text{GLR-}\ell_1$ statistic reject the null hypothesis with p-values smaller than 0.05, which suggests that a GGM defined by the geographic adjacency of the states falls short of modelling the precipitation. A plausible explanation is that the data are strongly associated with precipitation in neighbouring regions outside the U.S. (Canada, Mexico, and the oceans), and the absence of the precipitation data in these regions breaks the conditional independence between non-adjacent states. Besides, the other tests fail to reject the null hypothesis.

We further examine how sample size affects the GoF tests by analysing random subsamples. In summary, the MC-GoF test with the $\text{GLR-}\ell_1$ statistic remains robust performance across varying subsample sizes, while the F_Σ statistic rejects the null more often as the sample size increases. Other methods show little improvement as more data are included. This example demonstrates the effectiveness of our MC-GoF test in detecting the deficiency of GGMs for modelling high-dimensional data.

6.2 Modelling stock returns

In stock market analysis, building a graphical model for stock returns can uncover dependencies among stocks and identify clusters or sector-specific interactions. We apply our MC-GoF test to assess the GGM for modelling 103 large-cap U.S. stocks spanning 11 industry sectors. The data consists of 92 weekly average returns from September 1, 2020, to June 30, 2022, obtained from Yahoo Finance. The dataset has $n = 92$ observations, and the dimension is $p = 103$. Appendix G.2 reports technical details of data preprocessing and results of statistical analyses, for which we provide a summary below.

To estimate a suitable graph G , we use a modified GLasso that leaves within-sector edges unpenalised. This approach incorporates industry knowledge to produce a super-graph \hat{G} that may include extra edges but still yields an adequate GGM. The resulting graph has a maximum node degree of 30, a median degree of 19, and about 18.4% of node pairs connected.

We validate the adequacy of the GGM with \hat{G} using the MC-GoF test with statistic F_Σ (the overall winner in the simulation studies), as well as two benchmark methods (M^1P_1 and Bonf). All the resulting p-values exceed 0.3, which confirms that the GGM with \hat{G} is sufficient for modelling the stock data. This validation supports the suitability of the estimated graph for downstream tasks such as model-X inference for portfolio analysis or risk assessment.

7 Discussion

In this work, we introduced the MC-GoF test for Gaussian graphical models (GGMs), which provides finite-sample Type-I error control in any dimension. This test is a randomisation test based on a novel algorithm for generating exchangeable copies alongside the observation under the GGM. Additionally, the test is flexible in choosing the test statistic function to accommodate different alternatives and to incorporate prior information. These advantages make the MC-GoF test especially effective in high-dimensional inference.

We developed a theoretical framework to analyse the power of the MC-GoF test in high-dimensional settings. We considered the *dense-but-weak* alternative and the *strong-but-sparse* alternative separately, where the MC-GoF test is proved to be not only powerful but also rate-optimal. Numerical studies further demonstrate the superior performance of the MC-GoF test compared to existing GoF tests, especially for dense-but-weak signals.

Our work raises several future research directions. First, while we focused on GGMs, similar techniques may extend to other first-order Markov random fields with suitable sufficient statistics. For instance, discrete undirected graphical models might be handled by conditional sampling schemes inspired by our approach. Future research may extend these ideas to exponential family graphical models [Wainwright et al., 2008]. Second, while Bayesian inference offers a general framework for embedding prior information into test statistics in our method, as illustrated in Appendix B.4.4, efficient implementations remain open challenges. Third, while our theory focuses on clique-star-shaped null graphs, extending these results to more general null graphs would be a natural next step. Relaxing these structural constraints introduces complex Markov chain dynamics and intricate dependency patterns, which require the development of new theoretical tools. Finally, while the MC-GoF test can validate assumptions of downstream tasks such as model-X variable selection, it would be valuable to develop a unified framework that integrates the MC-GoF test with model-X inference.

Acknowledgements

D. Huang was partially supported by NUS Start-up Grant A-0004824-00-0 and Singapore Ministry of Education AcRF Tier 1 Grant A-8000466-00-00.

References

- Juliane Schäfer and Korbinian Strimmer. An empirical bayes approach to inferring large-scale gene association networks. *Bioinformatics*, 21(6):754–764, 2005.
- Adrian Dobra. Variable selection and dependency networks for genomewide data. *Biostatistics (Oxford, England)*, 10(4):621–639, 2009.
- Federico Castelletti and Guido Consonni. Bayesian inference of causal effects from observational data in Gaussian graphical models. *Biometrics*, 77(1):136–149, 2021.
- Eugene Belilovsky, Gaël Varoquaux, and Matthew B Blaschko. Testing for differences in Gaussian graphical models: Applications to brain connectivity. In D. Lee, M. Sugiyama, U. Luxburg, I. Guyon, and R. Garnett, editors, *Advances in Neural Information Processing Systems*, volume 29. Curran Associates, Inc., 2016.
- Stephen M. Smith, Karla L. Miller, Gholamreza Salimi-Khorshidi, Matthew Webster, Christian F. Beckmann, Thomas E. Nichols, Joseph D. Ramsey, and Mark W. Woolrich. Network modelling methods for fMRI. *NeuroImage*, 54(2):875–891, 2011.
- Gaël Varoquaux, Alexandre Gramfort, Jean-Baptiste Poline, and Bertrand Thirion. Brain covariance selection: better individual functional connectivity models using population prior. In J. Lafferty, C. Williams,

- J. Shawe-Taylor, R. Zemel, and A. Culotta, editors, *Advances in Neural Information Processing Systems*, volume 23. Curran Associates, Inc., 2010.
- Sacha Epskamp, Lourens J. Waldorp, René Møttus, and Denny Borsboom. The Gaussian graphical model in cross-sectional and time-series data. *Multivariate Behavioral Research*, 53(4):453–480, 2018.
- Arthur P. Dempster. Covariance selection. *Biometrics*, 28(1):157–175, 1972.
- Steffen L. Lauritzen. *Graphical Models*. Oxford Statistical Science Series. Oxford University Press, 1996.
- Theodore Wilbur Anderson. *An Introduction to Multivariate Statistical Analysis*. Wiley, 3 edition, 2007.
- Ming Yuan and Yi Lin. Model selection and estimation in the gaussian graphical model. *Biometrika*, 94(1):19–35, 2007.
- Nicolai Meinshausen and Peter Bühlmann. High-dimensional graphs and variable selection with the Lasso. *The Annals of Statistics*, 34(3):1436–1462, 2006.
- Mathias Drton and Michael D. Perlman. Multiple testing and error control in Gaussian graphical model selection. *Statistical Science*, 22(3):430–449, 2007.
- Nicolas Verzelen and Fanny Villers. Tests for Gaussian graphical models. *Computational Statistics & Data Analysis*, 53(5):1894–1905, 2009.
- Dongming Huang and Lucas Janson. Relaxing the assumptions of knockoffs by conditioning. *The Annals of Statistics*, 48(5):3021–3042, 2020.
- Julian Besag and Peter Clifford. Generalized Monte Carlo significance tests. *Biometrika*, 76(4):633–642, 1989.
- A. C. Davison and D. V. Hinkley. *Tests*, page 136–190. Cambridge Series in Statistical and Probabilistic Mathematics. Cambridge University Press, 1997. doi: 10.1017/CBO9780511802843.005.
- Nicolas Verzelen and Fanny Villers. Goodness-of-fit tests for high-dimensional gaussian linear models. *The Annals of Statistics*, 38(2):704–752, 2010.
- Rosamond L Naylor, David S Battisti, Daniel J Vimont, Walter P Falcon, and Marshall B Burke. Assessing risks of climate variability and climate change for Indonesian rice agriculture. *Proceedings of the National Academy of Sciences*, 104(19):7752–7757, 2007.
- Byman Hamududu and Aanund Killingtveit. Assessing climate change impacts on global hydropower. *Energies*, 5(2):305–322, 2012.
- Hannah L Cloke and Florian Pappenberger. Ensemble flood forecasting: A review. *Journal of hydrology*, 375(3-4):613–626, 2009.
- Martin J Wainwright, Michael I Jordan, et al. Graphical models, exponential families, and variational inference. *Foundations and Trends® in Machine Learning*, 1(1-2):1–305, 2008.
- Alexandre d’Aspremont, Onureena Banerjee, and Laurent El Ghaoui. First-order methods for sparse covariance selection. *SIAM Journal on Matrix Analysis and Applications*, 30(1):56–66, 2008.
- Jerome H. Friedman, Trevor Hastie, and Robert Tibshirani. Sparse inverse covariance estimation with the graphical lasso. *Biostatistics*, 9(3):432–441, 2008.
- Adam J. Rothman, Peter J. Bickel, Elizaveta Levina, and Ji Zhu. Sparse permutation invariant covariance estimation. *Electronic Journal of Statistics*, 2:494–515, 2008.

- Clifford Lam and Jianqing Fan. Sparsistency and rates of convergence in large covariance matrix estimation. *The Annals of Statistics*, 37(6B):4254 – 4278, 2009.
- Pradeep Ravikumar, Martin J. Wainwright, Garvesh Raskutti, and Bin Yu. High-dimensional covariance estimation by minimizing ℓ_1 -penalized log-determinant divergence. *Electronic Journal of Statistics*, 5: 935–980, 2011.
- Ming Yuan. High dimensional inverse covariance matrix estimation via linear programming. *The Journal of Machine Learning Research*, 11:2261–2286, 2010.
- Tony Cai, Weidong Liu, and Xi Luo. A constrained ℓ_1 minimization approach to sparse precision matrix estimation. *Journal of the American Statistical Association*, 106(494):594–607, 2011.
- Anja Wille and Peter Bühlmann. Low-order conditional independence graphs for inferring genetic networks. *Statistical Applications in Genetics and Molecular Biology*, 5(1), 2006.
- Mathias Drton and Michael D. Perlman. Model selection for Gaussian concentration graphs. *Biometrika*, 91(3):591–602, 2004.
- Mathias Drton and Michael D. Perlman. A SINful approach to Gaussian graphical model selection. *Journal of Statistical Planning and Inference*, 138(4):1179–1200, 2008.
- Weidong Liu. Gaussian graphical model estimation with false discovery rate control. *The Annals of Statistics*, 41(6):2948–2978, 2013.
- Jinzhou Li and Marloes H. Maathuis. GGM knockoff filter: False discovery rate control for Gaussian graphical models. *Journal of the Royal Statistical Society Series B: Statistical Methodology*, 83(3):534–558, 2021.
- Olha Bodnar and Elena Farahbakhsh Touli. Exact test theory in Gaussian graphical models. *Journal of Multivariate Analysis*, 196:105185, 2023.
- Emmanuel Candès, Yingying Fan, Lucas Janson, and Jinchi Lv. Panning for gold: ‘model-X’ knockoffs for high dimensional controlled variable selection. *Journal of the Royal Statistical Society Series B: Statistical Methodology*, 80(3):551–577, 01 2018.
- Thien-Minh Le, Ping-Shou Zhong, and Chenlei Leng. Testing the graph of a Gaussian graphical model, 2022.
- Matey Neykov, Junwei Lu, and Han Liu. Combinatorial inference for graphical models. *The Annals of Statistics*, 47(2):795 – 827, 2019. doi: 10.1214/17-AOS1650. URL <https://doi.org/10.1214/17-AOS1650>.
- Rina Foygel Barber and Lucas Janson. Testing goodness-of-fit and conditional independence with approximate co-sufficient sampling. *The Annals of Statistics*, 50(5):2514 – 2544, 2022.
- Wanrong Zhu and Rina Foygel Barber. Approximate co-sufficient sampling with regularization. *arXiv preprint arXiv:2309.08063*, 2023.
- Maurice Stevenson Bartlett. Properties of sufficiency and statistical tests. *Proceedings of the Royal Society of London. Series A - Mathematical and Physical Sciences*, 160(901):268–282, 1937.
- Alan Agresti. A survey of exact inference for contingency tables. *Statistical science*, 7(1):131–153, 1992.
- Steinar Engen and Magnar Lillegard. Stochastic simulations conditioned on sufficient statistics. *Biometrika*, 84(1):235–240, 1997.

- Bo Henry Lindqvist, Gunnar Taraldsen, Magnar Lillegård, and Steinar Engen. A counterexample to a claim about stochastic simulations. *Biometrika*, 90(2):489–490, 2003.
- Bo Henry Lindqvist and Gunnar Taraldsen. Monte Carlo conditioning on a sufficient statistic. *Biometrika*, 92(2):451–464, 2005.
- Bo Henry Lindqvist and Gunnar Taraldsen. Conditional Monte Carlo based on sufficient statistics with applications. In *Advances in statistical modeling and inference: Essays in honor of Kjell A Doksum*, pages 545–561. World Scientific, 2007.
- Persi Diaconis and Bernd Sturmfels. Algebraic algorithms for sampling from conditional distributions. *The Annals of statistics*, 26(1):363–397, 1998.
- Richard A. Lockhart, Federico J. O’Reilly, and Michael A. Stephens. Use of the Gibbs sampler to obtain conditional tests, with applications. *Biometrika*, 94(4):992–998, 2007.
- Richard A. Lockhart, Federico J. O’Reilly, and Michael A. Stephens. Exact conditional tests and approximate bootstrap tests for the von Mises distribution. *Journal of Statistical Theory and Practice*, 3: 543–554, 2009.
- L. Gracia-Medrano and Federico J. O’Reilly. Transformations for testing the fit of the inverse-Gaussian distribution. *Communications in Statistics-Theory and Methods*, 33(4):919–924, 2005.
- Federico O’Reilly and Leticia Gracia-Medrano. On the conditional distribution of goodness-of-fit tests. *Communications in Statistics—Theory and Methods*, 35(3):541–549, 2006.
- James D Santos and Nelson L Souza Filho. A Metropolis algorithm to obtain co-sufficient samples with applications in conditional tests. *Communications in Statistics-Simulation and Computation*, 48(9): 2655–2659, 2019.
- Rina Foygel Barber and Emmanuel J Candès. Controlling the false discovery rate via knockoffs. *The Annals of statistics*, pages 2055–2085, 2015.
- Thomas B. Berrett, Yi Wang, Rina Foygel Barber, and Richard J. Samworth. The conditional permutation test for independence while controlling for confounders. *Journal of the Royal Statistical Society Series B: Statistical Methodology*, 82(1):175–197, 2020.
- Michael Howes. Markov chain monte carlo significance tests. *arXiv preprint arXiv:2310.04924*, 2023.
- Jana Janková and Sara van de Geer. Inference in high-dimensional graphical models. In *Handbook of Graphical Models*, pages 325–350. CRC Press, 2018.
- Donald R. Williams, Philippe Rast, Luis R Pericchi, and Joris Mulder. Comparing Gaussian graphical models with the posterior predictive distribution and Bayesian model selection. *Psychological Methods*, 25(5):653–672, 2020.
- Alberto Roverato. Hyper inverse wishart distribution for non-decomposable graphs and its application to Bayesian inference for Gaussian graphical models. *Scandinavian Journal of Statistics*, 29(3):391–411, 2002.
- Aliye Atay-Kayis and H elene Massam. A monte carlo method for computing the marginal likelihood in nondecomposable Gaussian graphical models. *Biometrika*, 92(2):317–335, 2005.
- Adrian Dobra, Alex Lenkoski, and Abel Rodriguez. Bayesian inference for general Gaussian graphical models with application to multivariate lattice data. *Journal of the American Statistical Association*, 106(496):1418–1433, 2011.

- A.(Reza) Mohammadi and Ernst Wit. Bayesian Structure Learning in Sparse Gaussian Graphical Models. *Bayesian Analysis*, 10(1):109 – 138, 2015.
- Shurong Zheng, Guanghui Cheng, Jianhua Guo, and Hongtu Zhu. Test for high dimensional correlation matrices. *Annals of statistics*, 47(5):2887, 2019.
- Jiti Gao, Xiao Han, Guangming Pan, and Yanrong Yang. High dimensional correlation matrices: The central limit theorem and its applications. *Journal of the Royal Statistical Society Series B: Statistical Methodology*, 79(3):677–693, 2017.
- T Tony Cai and Tiefeng Jiang. Limiting laws of coherence of random matrices with applications to testing covariance structure and construction of compressed sensing matrices. *Annals of statistics*, 39(3):1496–1525, 2011.
- Varun Jog and Po-Ling Loh. On model misspecification and KL separation for Gaussian graphical models. In *2015 IEEE International Symposium on Information Theory (ISIT)*, pages 1174–1178, 2015.
- Erich L. Lehmann and Joseph P. Romano. *Testing Statistical Hypotheses*. Springer Texts in Statistics. Springer International Publishing, 2022.
- Michael Kearns and Lawrence Saul. Large deviation methods for approximate probabilistic inference. In *Proceedings of the Fourteenth conference on Uncertainty in artificial intelligence*, pages 311–319, 1998.
- T Tony Cai and Zongming Ma. Optimal hypothesis testing for high dimensional covariance matrices. *Bernoulli*, pages 2359–2388, 2013.
- Duncan J Watts and Steven H Strogatz. Collective dynamics of ‘small-world’ networks. *nature*, 393(6684): 440–442, 1998.
- Albert-László Barabási and Réka Albert. Emergence of scaling in random networks. *science*, 286(5439): 509–512, 1999.
- North America Land Data Assimilation System (NLDAS). Daily Precipitation years 1979-2011 on CDC WONDER Online Database, 2012. URL <https://wonder.cdc.gov/NASA-Precipitation.html>.
- Shantaram P. Hegde and John B. McDermott. The market liquidity of DIAMONDS, Q’s, and their underlying stocks. *Journal of Banking & Finance*, 28(5):1043–1067, 2004.

Appendix

Notation

We use the following notations in the main text and this supplementary material. For any set U , let $|U|$ be its cardinality. Define $[p] := \{1, \dots, p\}$ for any positive integer p . For $S \subseteq [p]$ and a vector X , let X_S be the sub-vector $(X_j)_{j \in S}$; and for a matrix \mathbf{X} , let \mathbf{X}_j be the j th column and \mathbf{X}_S the submatrix formed by the columns corresponding to S . Also, let $X_{-S} := (X_j)_{j \notin S}$ and $\mathbf{X}_{-S} := \mathbf{X}_{S^c}$. For a square matrix \mathbf{A} , $\text{diag}(\mathbf{A})$ is the diagonal matrix with the same diagonal entries as \mathbf{A} .

We write $\mathbf{A} \succ \mathbf{0}$ if \mathbf{A} is positive definite. Let $\mathbf{N}_p(\boldsymbol{\mu}, \boldsymbol{\Sigma})$ denote a p -dimensional normal distribution with mean $\boldsymbol{\mu}$ and covariance $\boldsymbol{\Sigma}$, and define $\boldsymbol{\Omega} := \boldsymbol{\Sigma}^{-1}$ with entries ω_{ij} . We consider undirected graphs without loops or multiple edges. For a graph $G = (\mathcal{V}, \mathcal{E})$ with node set \mathcal{V} and edge set \mathcal{E} , denote the neighborhood of node i by $N_i = \{j \in \mathcal{V} : j \neq i, (i, j) \in \mathcal{E}\}$. We use the terms ‘node’ ($j \in [p]$) and ‘variable’ (X_j) interchangeably. We write \mathcal{M}_G for the GGM w.r.t. G .

A Connections with existing works

A.1 Comparison between GoF testing and graph selection

In the past two decades, high-dimensional GGM estimation has gained a significant amount of attention. The current primary methodologies can be categorized into two types. The first involves utilizing penalized likelihood with an ℓ_1 penalty on entries of the precision matrix for variable selection [Yuan and Lin, 2007, d’Aspremont et al., 2008, Friedman et al., 2008]. In particular, Friedman et al. [2008] propose an efficient algorithm called Graphical Lasso (GLasso) for solving the ℓ_1 penalized likelihood estimation. Rates of convergence and model selection consistency have then been developed [Rothman et al., 2008, Lam and Fan, 2009, Ravikumar et al., 2011]. In addition to the ℓ_1 penalized likelihood, several related methods have also been introduced; for example, the neighborhood selection [Meinshausen and Bühlmann, 2006], graphical Dantzig selector [Yuan, 2010], and CLIME [Cai et al., 2011]. The second branch of research in GGM estimation focuses on edge selection through multiple-testing procedures to control either the family-wise error rate or the false discovery rate; see, for example, Schäfer and Strimmer [2005], Wille and Bühlmann [2006], Drton and Perlman [2004, 2007, 2008], Liu [2013], Li and Maathuis [2021].

While the estimation of precision matrices has been well-explored, research on goodness-of-fit hypothesis testing within high-dimensional GGMs is relatively less developed. Nonetheless, several advancements have been made in this area. For instance, edge selection methods with family-wise error control, such as those in Drton and Perlman [2007], can be adapted for GoF testing. Verzelen and Villers [2009] introduced a general GoF test by connecting the local Markov property and conditional regression of a Gaussian random variable. However, this test is unable to achieve high power when the signals are dense but weak. Bodnar and Touli [2023] proposed finite-sample tests for particular precision matrix structures (e.g., block-diagonal, AR(1), factor structures), but their approach requires that $n > p$. These above tests focus on specific test statistics, while our method is flexible to choose any test statistic.

There are fundamental distinctions between GoF testing and graph selection. GoF testing aims to determine whether a specific candidate graph includes all true edges, regardless of the presence of additional false edges. In contrast, graph selection aims to identify as many true edges as possible while minimizing the inclusion of false ones. These differences extend to the definition of Type-I error: in GoF testing, it corresponds to rejecting the null hypothesis when the candidate graph already contains all true edges, whereas in graph selection, it corresponds to the inclusion of any false edge in the estimated graph. Consequently, the methodologies and theoretical frameworks for GoF testing are very different from those for graph selection. These distinctions, along with their practical implications, are summarized in Table 1 in the main text.

A.2 Connection between GoF testing and model-X inference

GoF testing is important in the *model-X framework* for high-dimensional inference. Unlike traditional methods that model the conditional distribution of a response Y given the predictor X , the model-X framework shifts the focus to modeling the distribution F_X of X . For methods like the model-X knockoff filter [Candès et al., 2018], which identifies important predictor variables for Y while controlling the false discovery rate, accurate modeling of F_X is essential. In particular, when F_X is modeled by a GGM and the underlying graph is a subgraph of a known graph G , the model-X knockoff filter can be efficiently implemented [Huang and Janson, 2020]. The validity of this approach relies on the assumption that $F_X \in \mathcal{M}_G$, which can be assessed statistically through GoF testing.

A.3 Comparison between GoF and faithfulness

In GGMs, the population P is said to be *faithful* to a graph if $\omega_{ij} \neq 0 \Leftrightarrow i$ and j are connected. It is associated with the following model

$$\overline{\mathcal{M}}_G = \{\mathbf{N}_p(\boldsymbol{\mu}, \boldsymbol{\Omega}^{-1}) : \boldsymbol{\mu} \in \mathbb{R}^p, \boldsymbol{\Omega} \succ \mathbf{0}, \Omega_{i,j} = 0 \text{ if and only if } i \neq j \text{ and } (i, j) \notin \mathcal{E}\}.$$

Compared to (1.1), we have $\overline{\mathcal{M}}_G \subsetneq \mathcal{M}_G$. Therefore, faithfulness testing is different from GoF testing. Recently, Le et al. [2022] introduced asymptotic tests for testing the faithfulness to a prespecified graph, which is more restricted than the hypothesis for GoF testing in (1.2). In addition, their theory requires the sparsity assumption that the maximum degree is $o(\sqrt{n/\log p})$, and thus, their tests do not apply in the settings of this paper.

We adopt the hypothesis (1.2) as the null hypothesis for GoF testing in GGMs because our focus lies in validating the adequacy of the GGM \mathcal{M}_{G_0} . Once validated, the model \mathcal{M}_{G_0} can be used in subsequent analyses, such as implementing model-X knockoff filter to identify important predictor variables, even if G_0 may include false edges.

A.4 Comparison between GoF testing and combinatorial testing

Neykov et al. [2019] studied testing for some characteristics of the graph structure such as the connectivity, the presence of a cycle, and the maximum degree. These tests target specific global characteristics of the underlying graph, rather than assessing the goodness-of-fit for a prespecified graph, where the mapping between node and variable is fixed. In principle one could formulate a structural property as a composite null hypothesis that includes a large set of graphs, where these graphs are invariant to changes in the mapping between nodes and variables. However, since this composite null hypothesis could contain an exponentially growing number of graphs, how to extend a GoF test to handle such a hypothesis remains an open challenge.

A.5 Review of Monte Carlo tests

Our GoF test belongs to the class of Monte Carlo tests. For problems where sampling from the null distribution is impracticable, Besag and Clifford [1989] proposed two methods to generate exchangeable copies of the data using Markov chains. A related line of research lies in the use of approximate sufficiency for asymptotic GoF testing, which could be expedient if finding an appropriate sufficient statistic is hard. Barber and Janson [2022] considered sampling data conditional on an asymptotically efficient estimator and derived bounds on the finite-sample Type-I error inflation of their method. Recently, Zhu and Barber [2023] developed an extension to constrained and penalized maximum likelihood estimation. These methods are approximative in nature and require additional assumptions about the distribution, the dimension of variables, and the sample size, and thus are not directly comparable to our method.

A.6 Review of co-sufficient sampling

Our GoF test for GGMs is closely related to the framework of co-sufficient sampling. Under this framework, GoF testing is achieved by sampling copies from the conditional distribution of the data given a sufficient statistic. This idea can be traced back at least to Bartlett [1937], and the general problem of Monte Carlo computation of the conditional expectation given a sufficient statistic has been explored by various researchers [Agresti, 1992, Engen and Lillegard, 1997, Lindqvist et al., 2003, Lindqvist and Taraldsen, 2005, 2007]. Diaconis and Sturmfels [1998] proposed Markov chain algorithms for sampling from discrete exponential families conditional on a sufficient statistic. Lockhart et al. [2007] and Lockhart et al. [2009] considered using the Gibbs sampler for co-sufficient sampling for the Gamma distribution and the von Mises distribution. Gracia-Medrano and O’Reilly [2005] and O’Reilly and Gracia-Medrano [2006] studied the conditional sampling for inverse-Gaussian distributions, and Santos and Filho [2019] proposed a Metropolis-Hasting algorithm for exponential families with doubly transitive sufficient statistics. To the best of our knowledge, existing literature has not considered co-sufficient sampling for GGMs with dimensions of variables larger than sample sizes, as considered by the current paper. While Huang and Janson [2020] studied conditioning on sufficient statistics to construct high-dimensional model-X knockoff variables, their construction is limited to knockoff generation and does not extend to co-sufficient sampling. We provide a further discussion on the comparison between knockoff and exchangeable samples in Appendix A.7.

A.7 Comparison between knockoffs and exchangeable copies

Algorithm 2 generates copies $\tilde{\mathbf{X}}^{(m)}$ of \mathbf{X} such that $\{\mathbf{X}, \tilde{\mathbf{X}}^{(1)}, \dots, \tilde{\mathbf{X}}^{(M)}\}$ are exchangeable, that is, the joint distribution is invariant to permuting any subset of these datasets. Sampling these copies $\tilde{\mathbf{X}}^{(m)}$ may appear similar to the knockoff construction [Barber and Candès, 2015, Candès et al., 2018], but there is a crucial difference. We use the model-X knockoff framework proposed in Candès et al. [2018] as an example, and the discussion below easily extends to the fixed-X knockoff framework used in Barber and Candès [2015] and Li and Maathuis [2021].

In the model-X knockoff framework, a single dataset $\tilde{\mathbf{X}}$ is constructed to replicate the dependencies in the original dataset \mathbf{X} . The key property of the knockoff construction, known as the swap invariance property, requires that for each variable j , swapping the j -th column of \mathbf{X} with the corresponding column of $\tilde{\mathbf{X}}$ leaves their joint distribution unchanged. Formally, for any $j \in \{1, 2, \dots, p\}$, we have the distributional equivalence

$$[\mathbf{X}, \tilde{\mathbf{X}}]_{\text{swap}(j)} \stackrel{d}{=} [\mathbf{X}, \tilde{\mathbf{X}}].$$

The swap invariance property is the foundation of the FDR control of the knockoff filter in variable selection.

To connect with the focus of the current paper, the swap invariance property also guarantees that the original and knockoff datasets, as a pair, are exchangeable. However, when multiple knockoffs $\{\tilde{\mathbf{X}}^{(1)}, \dots, \tilde{\mathbf{X}}^{(M)}\}$ are generated, the pairwise exchangeability does not automatically extend to the joint exchangeability. Since each knockoff dataset is generated by conditioning on the observed data \mathbf{X} , \mathbf{X} plays a distinguished role that the knockoffs do not share. This distinction is critical: while the swap invariance property ensures pairwise exchangeability between \mathbf{X} and $\tilde{\mathbf{X}}^{(m)}$, it does not guarantee joint exchangeability across multiple knockoffs and \mathbf{X} together.

In fact, exchanging the position of \mathbf{X} with any of the knockoffs $\tilde{\mathbf{X}}^{(m)}$ will change the joint distribution. For instance,

$$[\mathbf{X}, \tilde{\mathbf{X}}^{(1)}, \dots, \tilde{\mathbf{X}}^{(M)}] \text{ and } [\tilde{\mathbf{X}}^{(1)}, \mathbf{X}, \dots, \tilde{\mathbf{X}}^{(M)}]$$

do not follow the same distribution in general.

B Details on Algorithms

B.1 Special sampling with complete graphs

There is a special case where sampling from the uniform distribution of \mathcal{X}_Ψ is simple: when G is a complete graph, which means that every node is connected to all other nodes. In this case, $\mathcal{E} = \{(i, j) : \forall i, j \in [p], i \neq j\}$, and the minimal sufficient statistic ψ_G consists of the sample mean and the sample Gram matrix. The conditional distribution of \mathbf{X} is the uniform distribution on all $n \times p$ matrices with the same sample mean and sample Gram matrix as the observed ones. We can sample from this conditional distribution using the construction $\tilde{\mathbf{X}} = \mathbf{1}\mathbf{1}^\top \mathbf{X} + \mathbf{\Gamma}\mathbf{H}\mathbf{\Gamma}^\top \mathbf{X}$, where $\mathbf{\Gamma}$ is an $n \times (n-1)$ orthonormal matrix that is orthogonal to the vector $\mathbf{1}$ and \mathbf{H} is a uniform random $(n-1) \times (n-1)$ orthonormal matrix. The astute reader may notice a connection between this simple generation and the fixed-X knockoff construction in Barber and Candès [2015]. The difference is that the generated copy $\tilde{\mathbf{X}}$ is not a knockoff matrix and the matrix \mathbf{H} needs to be random. The case where G is the complete graph only serves for pedagogical purposes, since the model \mathcal{M}_G includes all p -dimensional multivariate normal distributions and is not interesting in graphical modeling.

B.2 Derivation of Residual Rotation

The Lebesgue density of the joint distribution of \mathbf{X} is given by

$$f_{\boldsymbol{\mu}, \boldsymbol{\Omega}}(\mathbf{x}) = (2\pi)^{-np/2} \det(\boldsymbol{\Omega})^{n/2} \exp\left(-\frac{1}{2} \sum_{i=1}^n (\mathbf{x}_i - \boldsymbol{\mu})^\top \boldsymbol{\Omega} (\mathbf{x}_i - \boldsymbol{\mu})\right), \quad \forall \mathbf{x} \in \mathbb{R}^{n \times p}, \quad (\text{B.1})$$

where \mathbf{x}_i^\top is the i th row of \mathbf{x} .

Consider updating one column \mathbf{X}_i according to its conditional distribution given all other columns \mathbf{X}_{-i} as well as the sufficient statistic Ψ . We first study the conditional distribution of \mathbf{X}_i given \mathbf{X}_{-i} and then the conditional distribution given (\mathbf{X}_{-i}, Ψ) .

By the properties of the multivariate normal distribution [Anderson, 2007], the conditional distribution of \mathbf{X}_i given \mathbf{X}_{-i} is $\mathbf{N}_n(\mu_i \mathbf{1}_n + (\mathbf{X}_{-i} - \mathbf{1}_n \mu_{-i}^\top) \Omega_{-i,i} \Omega_{i,i}^{-1}, \Omega_{i,i}^{-1} \mathbf{1}_n)$, where μ_i is the i -th entry of $\boldsymbol{\mu}$. Under the model \mathcal{M}_G , if j is not a neighbor of i , then $\Omega_{j,i} = 0$. Therefore, $\mathbf{X}_{-i} \Omega_{-i,i} \Omega_{i,i}^{-1} = \mathbf{X}_{N_i} \boldsymbol{\alpha}$ for some $|N_i|$ -dimensional parameter $\boldsymbol{\alpha}$ that depends on Ω .

For this conditional distribution, a sufficient statistic is given by

$$\psi_G^i(\mathbf{X}) := \left[\mathbf{X}_i^\top \mathbf{1}_n, \mathbf{X}_i^\top \mathbf{X}_i, \mathbf{X}_i^\top \mathbf{X}_{N_i} \right].$$

Denote by Ψ^i the observed value of this statistic. Recall the definition of ψ_G that

$$\psi_G(\mathbf{x}) := \left(\sum_{i=1}^n \mathbf{x}_i, (\mathbf{x}^\top \mathbf{x})_{i,j} : i = j \text{ or } (i, j) \in \mathcal{E} \right), \quad \forall \mathbf{x} \in \mathbb{R}^{n \times p}, \quad (\text{B.2})$$

and note that $\psi_G^i(\mathbf{x})$ is contained by $\psi_G(\mathbf{x})$. Therefore, according to the Lebesgue density of the joint distribution in (B.1), the conditional distribution of \mathbf{X}_i given (\mathbf{X}_{-i}, Ψ) is the uniform distribution on

$$\mathcal{X}_\Psi^i := \{ \mathbf{x}_i \in \mathbb{R}^n : \psi_{G,i}(\mathbf{x}) = \Psi^i \}. \quad (\text{B.3})$$

Algorithm 1 in the main text provides a simple way to sample from this uniform distribution. The idea of this algorithm is to fix the projection of \mathbf{X}_i onto the column space of $[\mathbf{1}_n, \mathbf{X}_{N_i}]$ and to rotate the residual uniformly and independently. We name this procedure the *residual rotation*. Given (\mathbf{X}_{-i}, Ψ) , the output $\tilde{\mathbf{X}}_i$ is a conditionally i.i.d. copy of \mathbf{X}_i . As long as $n \geq |N_i| + 3$, the output $\tilde{\mathbf{X}}_i$ is different from \mathbf{X}_i almost surely.

B.3 Details on Algorithm 2

To generate exchangeable copies of \mathbf{X} , we introduce a method that updates the individual columns one at a time to generate Markov chains. This method combines the residual rotation (Algorithm 1) in Section 2.1 of the main paper and the parallel method introduced in Besag and Clifford [1989].

When Algorithm 1 is executed repeatedly with index running from 1 to p , we obtain a Markov chain $\mathcal{C}_1 = (\mathbf{X}, \overrightarrow{\mathbf{X}}^{(1)}, \dots, \overrightarrow{\mathbf{X}}^{(p)})$, where the endpoint $\overrightarrow{\mathbf{X}}^{(p)}$ is an entirely new sample and the arrow pointing right overhead in the notation $\overrightarrow{\mathbf{X}}^{(i)}$ emphasizes that this Markov chain is going forward.

This is illustrated in Figure 2, where each row shows one step of residual rotation.

If we start from $\overrightarrow{\mathbf{X}}^{(p)}$ and independently run Algorithm 1 backward along the reversed order (from p to 1), we obtain a second Markov chain $\mathcal{C}_2 = (\overleftarrow{\mathbf{X}}^{(p)}, \overleftarrow{\mathbf{X}}^{(p-1)}, \dots, \overleftarrow{\mathbf{X}}^{(0)})$, where the arrow pointing left overhead in the notation $\overleftarrow{\mathbf{X}}^{(i)}$ emphasizes that this chain is going backward.

If the distribution of \mathbf{X} belongs to \mathcal{M}_G , the backward Markov chain \mathcal{C}_2 has the same distribution as the reversed chain of \mathcal{C}_1 , as seen by applying Proposition 1 at each residual rotation. In other words, we have

$$(\overrightarrow{\mathbf{X}}^{(p)}, \overleftarrow{\mathbf{X}}^{(p-1)}, \dots, \overleftarrow{\mathbf{X}}^{(0)}) \stackrel{d.}{=} (\overrightarrow{\mathbf{X}}^{(p)}, \overrightarrow{\mathbf{X}}^{(p-1)}, \dots, \overrightarrow{\mathbf{X}}^{(1)}, \mathbf{X}).$$

Therefore, conditioning on $\overrightarrow{\mathbf{X}}^{(p)}$, we can conclude that \mathbf{X} and $\overleftarrow{\mathbf{X}}^{(0)}$ are independent and identically distributed, and thus \mathbf{X} and $\overleftarrow{\mathbf{X}}^{(0)}$ are conditionally exchangeable. Since the backward sampling can be conducted independently multiple times, we can obtain multiple versions of $\overleftarrow{\mathbf{X}}^{(0)}$ (denoted as $\tilde{\mathbf{X}}^{(m)}$ for $m = 1, 2, \dots, M$) that are exchangeable jointly with \mathbf{X} .

In the generation of each Markov chain, we can repeat the residual rotation with the index running from 1 to p (or from p to 1) for L iterations so that each Markov chain is lengthened from p to pL .

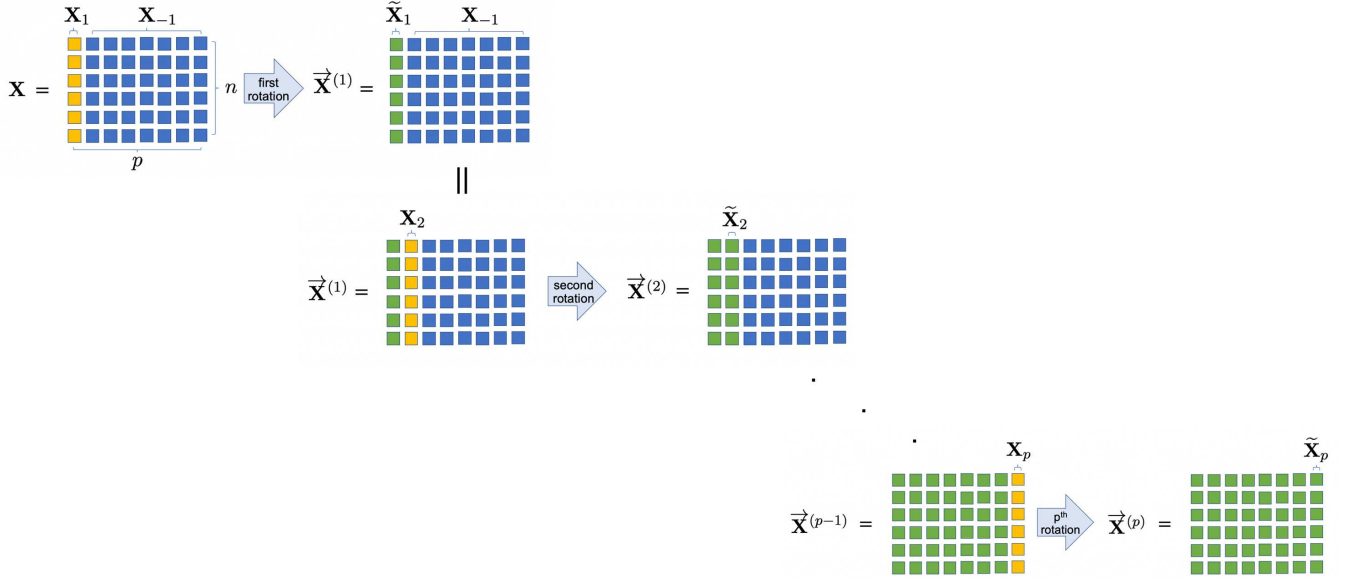


Figure 2: Forward sampling process. Each mini square represents an entry of the data matrix. At each step, Algorithm 1 is applied to the yellow column \mathbf{X}_i , producing the green column. The updated matrix is used as input for the next step. Iterating column by column yields a fully updated matrix.

Unlike traditional MCMC, which requires sufficiently long chains to approximate target distributions, our algorithm generates exchangeable copies even with $L = 1$. Although increasing L seems beneficial for reducing the correlation between the endpoint and the starting point of the chain, further analyses in Appendix F.1 show that choosing $L = 1$ suffices to provide satisfactory results.

The sampling procedure is illustrated in Figure 3 and is summarized in Algorithm 2. In Algorithm 2 in the main paper, the residual rotation is applied following any order \mathcal{I} , and the endpoint of the forward Markov chain \mathcal{C}_1 is called the *hub* since it is the common center of all Markov chains. Our Markov chain construction is based on the *parallel* method introduced by Besag and Clifford [1989], which has been revisited recently by Berrett et al. [2020], Barber and Janson [2022], Howes [2023].

By setting the argument \mathcal{I} as a permutation of $[p]$, Algorithm 2 allows updating the columns in any chosen order. Exchangeability is maintained as long as the backward sampling in Step 2 follows the reverse sequence of \mathcal{I} . For example, we can arrange the nodes in the graph based on their degrees such that $d_{j_1} \leq d_{j_2} \leq \dots \leq d_{j_p}$, and we set $\mathcal{I} = (j_1, j_2, \dots, j_p)$. Besides, \mathcal{I} can be chosen as a permutation of a subset of $[p]$ so that some columns of the output remain unchanged. This approach is useful for constructing the test for the local Markov property in Section 3.3 of the main paper.

B.3.1 Extensions to randomized and two-sided tests

In Algorithm 3, the function $T(\cdot)$ can be any test statistic function such that larger values are regarded as evidence against the null hypothesis. Here, we discuss how we can use randomized tests to boost power and two-sided tests for more general choices of test statistics. The p-values defined below are both valid under the condition of Proposition 3. We include the justification for completeness in Appendix E.3.

1. The p-value defined in Algorithm 3 is conservative when there are ties. Alternatively, one can break the ties randomly. We simplify the notation $T(\mathbf{X})$ and $T(\tilde{\mathbf{X}}^{(m)})$ as T_0 and T_m . Let $\kappa = \sum_{i=1}^M \mathbb{1}\{T_i = T_0\}$, and let S be a random integer from $\{1, 2, \dots, \kappa + 1\}$. We define the randomized p-value as follows:

$$\frac{1}{1 + M} \left(S + \sum_{i=1}^M \mathbb{1}\{T_i > T_0\} \right).$$

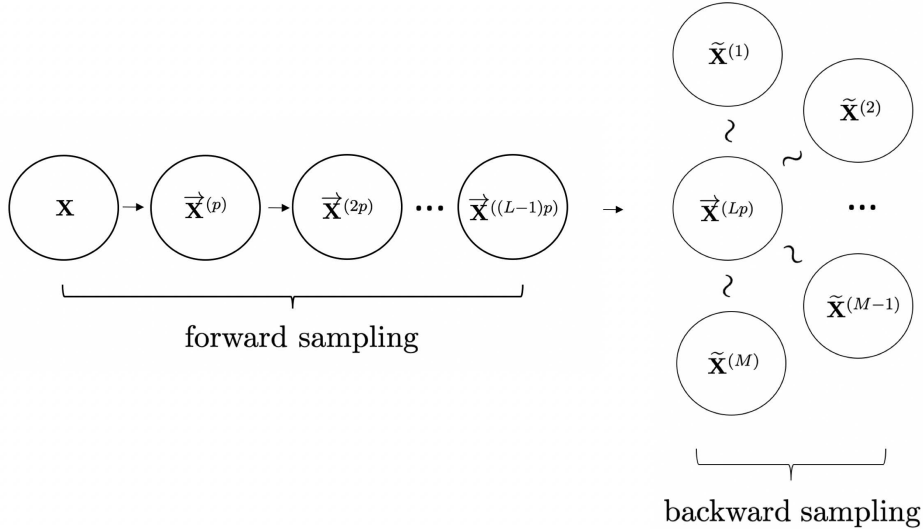


Figure 3: Sampling exchangeable copies of \mathbf{X} . Left: Forward sampling from \mathbf{X} , and each right arrow represents L -time forward residual rotation. Right: Backward sampling from the hub $\vec{\mathbf{X}}^{(Lp)}$, and each wavy line represents a backward sampling of a Markov chain of length Lp .

- Algorithm 3 is stated in terms of a one-sided test, which treats larger values of T as evidence for rejecting the null hypothesis. We can also consider a two-sided test that rejects the null when T is either too large or too small. With S and κ defined in the first point, we define the two-sided p-value as follows:

$$\frac{2}{1+M} \left[S + \min \left(\sum_{i=1}^M \mathbb{1}\{T_i > T_0\}, \sum_{i=1}^M \mathbb{1}\{T_i < T_0\} \right) \right].$$

B.3.2 Choices of parameters in Algorithm 3

The number M of copies in Algorithm 2 has a minor impact on the test. Proposition 3 guarantees that the validity of the p-value is unaffected by M . However, M should not be too small in order to achieve good power. Given a significance level α , setting $M \geq 2/\alpha$ ensures that the computed p-values can be smaller than $\alpha/2$. Both theory and empirical results suggest that as long as M exceeds a moderate threshold, further increases have little impact. Specifically, the theoretical results in Section 4 of the main paper show that taking $M = 2 \max(\alpha^{-1}, \log n)$ is sufficient to achieve essentially full power when the alternative is well separated from the null (see Corollaries 1 and 2). In practice, $M = 100$ already suffices for commonly used significance levels such as $\alpha = 0.05$, and increasing M beyond that offers minimal further benefit.

The number of iterations L in Algorithm 2 controls the length of the generated Markov chains. As discussed in Section 2.2 in the main paper and Appendix F.1, $L = 1$ is sufficient in most practical scenarios even when the graph is moderately dense.

Moreover, the asymptotic theory on the power property in Section 4 of the main paper holds for any L , including $L = 1$. In our numerical studies, choosing $L = 3$ achieves desirable power performance, with no noticeable improvement observed for larger values of L . Hence, we recommend choosing L between 1 and 3.

B.4 Derivations of Test Statistics

Algorithm 3 is valid in controlling the Type-I error with any test statistic function, but to achieve high power, we aim to choose a function that is likely to be large when the null hypothesis is false. The general principle is to find a statistic that captures the “distributional difference” between possible alternative

hypotheses and the null hypothesis. Motivated by the classical inference methods such as the likelihood ratio test, we propose three types of test statistics in Appendix B.4.1, B.4.2, and B.4.3. We further discuss in Appendix B.4.4 how a practitioner can construct problem-specific test statistics when prior knowledge about plausible alternative hypotheses is available.

To address the most common scenarios in GoF testing for GGMs, we focus on alternatives where the population belongs to a GGM, but the underlying graph differs from $G_0 = (\mathcal{V}, \mathcal{E}_0)$, the graph stipulated by the null hypothesis. In the following, we denote by $X = (X_1, X_2, \dots, X_p)^\top \in \mathbb{R}^p$ a multivariate normal random vector from $\mathbf{N}_p(\boldsymbol{\mu}, \boldsymbol{\Sigma})$ and the precision matrix is $\boldsymbol{\Omega} = (\omega_{ij})_{1 \leq i, j \leq p} = \boldsymbol{\Sigma}^{-1}$. Suppose that the distribution of X is *pairwise faithful* to the graph $G = (\mathcal{V}, \mathcal{E})$ in the sense that for any distinct pairs of i and j , $\omega_{ij} = 0 \Leftrightarrow (i, j) \notin \mathcal{E}$. Under this assumption, the testing problem for the hypothesis in (1.2) is reduced to testing $H_0 : \mathcal{E} \subset \mathcal{E}_0$ versus $H_a : \mathcal{E} \not\subset \mathcal{E}_0$, which is equivalent to testing

$$H_0 : \forall (i, j) \notin \mathcal{E}_0, \omega_{i,j} = 0 \quad \text{versus} \quad H_a : \exists (i, j) \notin \mathcal{E}_0, \omega_{i,j} \neq 0. \quad (\text{B.4})$$

We propose several choices of test statistics that aim to estimate some measures of “distributional difference” between the null hypothesis and the alternative hypothesis in (B.4). Although these statistics are rooted in standard practices for GoF testing, they are particularly suited for high-dimensional problems. The simulation studies in Section 5 of the main paper demonstrate that our MC-GoF testing procedure using any of these test statistics has competitive finite-sample performance. It should be emphasized that the testing problem in (B.4) merely serves as a motivation for deriving our test statistics, and the MC-GoF test continues to be valid for testing the null hypothesis stated in (1.2).

In the simulations of the main paper, we examined the following four test statistic functions: PRC (B.11), ERC (B.13) in Appendix B.4.1, F_Σ (B.17) in Appendix B.4.2, $\text{GLR-}\ell_1$ (B.21) in Appendix B.4.3.

B.4.1 Pairwise partial correlation

Our first test statistic is based on the estimation of partial correlations. The ij -th partial correlation ρ_{ij} is the correlation between X_i and X_j in their conditional distribution given other variables. By the properties of the normal distribution, the partial correlation can be expressed as

$$\rho_{ij} = \frac{-\omega_{ij}}{\sqrt{\omega_{ii}\omega_{jj}}}, \quad (\text{B.5})$$

and thus $\omega_{ij} = 0$ if and only if $\rho_{ij} = 0$. Therefore, the testing problem in (B.4) can be converted to the testing of

$$H_0 : \forall (i, j) \notin \mathcal{E}_0, \rho_{ij} = 0 \quad \text{versus} \quad H_a : \exists (i, j) \notin \mathcal{E}_0, \rho_{i,j} \neq 0.$$

This null hypothesis is a composition of $H_0^{ij} : \rho_{ij} = 0$ for all (i, j) not in \mathcal{E}_0 . It is natural to consider using the ij -th sample partial correlation as the test statistic for each H_0^{ij} . When the sample size n is larger than the dimension p , sample partial correlations can be computed by replacing the elements of $\boldsymbol{\Omega}$ in (B.5) with the corresponding elements of the inverse of the sample covariance matrix. See Drton and Perlman [2007] for an application of sample partial correlations for GGM selection.

Instead of using the sample partial correlations, we utilize the graph G_0 stipulated in the null hypothesis to formulate a statistic that can be computed even when $p \gg n$.

By the properties of the normal distribution [Anderson, 2007], X_i can be expressed as

$$X_i = X_{-i}^\top \theta^{(i)} + \epsilon_i, \quad (\text{B.6})$$

where $\epsilon_i \sim N(0, \omega_{ii}^{-1})$ is independent of X_{-i} , and $\theta^{(i)} \in \mathbb{R}^{p-1}$ is a vector such that $\theta^{(i)} = -\boldsymbol{\Omega}_{-i,i}/\omega_{ii}$, where $\boldsymbol{\Omega}_{-i,i}$ is the i -th column of $\boldsymbol{\Omega}$ excluding the i -th entry. For any pairs of distinct i and j , (ϵ_i, ϵ_j) is normally distributed and the ij -th partial correlation satisfies that

$$\text{Cor}(\epsilon_i, \epsilon_j) = -\rho_{ij}.$$

This suggests that we can first perform local linear regression to X_i and X_j respectively, and then consider the correlation between the residuals as a test statistic for the hypothesis H_0^{ij} .

The detailed derivation is as follows. Suppose $(i, j) \notin \mathcal{E}_0$. Let U be the union of the neighborhoods N_i and N_j , and denote by u the cardinality of U . If $u + 2 < n$, $[\mathbf{1}_n, \mathbf{X}_U]$ has full column rank almost surely. In this case, we can regress \mathbf{X}_i on \mathbf{X}_U (with the intercept term) using least squares estimation and obtain the residual vector \mathbf{r}_i . Similar estimation can be applied for \mathbf{X}_j to obtain \mathbf{r}_j . Define the pairwise residual correlation $\hat{\gamma}_{ij}$ as

$$\hat{\gamma}_{ij} := \mathbf{r}_i^\top \mathbf{r}_j / (\|\mathbf{r}_i\| \|\mathbf{r}_j\|). \quad (\text{B.7})$$

For simplicity, we define $\hat{\gamma}_{ij} := 1$ if $n \leq u + 2$. A simple test statistic can be defined as

$$T_{\text{SRC}}(\mathbf{X}) = \sum_{(i,j) \notin \mathcal{E}_0} \hat{\gamma}_{ij}^2, \quad (\text{B.8})$$

where SRC stands for the sum of squared pairwise residual correlations. Aggregation via summation effectively captures dense (but potentially weak) signals, which means the true precision matrix has many small nonzero entries not indicated by the null graph G_0 . Another simple choice of test statistic is

$$T_{\text{MRC}}(\mathbf{X}) = \max_{(i,j) \notin \mathcal{E}_0} \hat{\gamma}_{ij}^2, \quad (\text{B.9})$$

where MRC stands for the maximum of pairwise residual correlations. Aggregation by taking the maximum effectively captures strong (but potentially sparse) signals, which means that the true precision matrix has at least one nonzero entry not indicated by the null graph G_0 .

Although simple, the power of the MC-GoF test with SRC or MRC can be theoretically studied. In Section 4 of the main paper, we prove that when the alternative hypothesis has a dense signal (or a strong signal), the MC-GoF with T_{SRC} (or with T_{MRC}) can achieve high power asymptotically with the optimal rate.

By considering the distribution of $\hat{\gamma}_{ij}$ under the null hypothesis if $n > 2 + u$, we transform it as $\hat{t}_{ij} = \sqrt{(n-2-u)}\hat{\gamma}_{ij}/\sqrt{1-\hat{\gamma}_{ij}^2}$ and define

$$p_{ij} := 2F_{t, n-2-u_j}(-|\hat{t}_{ij}|), \quad (\text{B.10})$$

where $F_{t,a}$ is the cumulative distribution function (CDF) of the t-distribution with a degrees of freedom. If $n \leq u + 2$, we define $p_{ij} := 1$. We define the z-score for p_{ij} as

$$z_{ij} = -\Phi^{-1}(p_{ij}/2),$$

where Φ^{-1} is the inverse CDF of the standard normal distribution. To aggregate p_{ij} 's in (B.10) while preventing the signals from being overwhelmed by noises, we filter out large p_{ij} 's. Specifically, let δ be a pre-specified constant (0.05 by default). We define $\Xi = \{(i, j) \notin \mathcal{E}_0 : p_{ij} \leq \delta\}$ and define

$$T_{\text{PRC}}(\mathbf{X}) = \sum_{(i,j) \in \Xi} z_{ij}^2. \quad (\text{B.11})$$

Since this statistic is obtained from the aggregation of pairwise residual correlations, we call it the PRC statistic.

The computation of the PRC statistic could become burdensome when p is large, since it requires the computation of all pairwise residual correlations $\hat{\gamma}_{ij}$, each of which involves fitting two local linear regressions of \mathbf{X}_i and \mathbf{X}_j on variables in the union of their neighborhoods. We can improve the computational efficiency by fitting a local linear regression for each \mathbf{X}_i on its own neighborhood N_i to obtain the residual \mathbf{r}_i . We then define the residual correlation $\tilde{\gamma}_{ij}$ as in (B.7). Unlike $\hat{\gamma}_{ij}$, the exact distribution of $\tilde{\gamma}_{ij}$ is not

easy to obtain. Inspired by the Fisher's variance stabilizing transformation [Drton and Perlman, 2007, Proposition 2], we define

$$\tilde{\xi}_{ij} := \frac{\sqrt{n-2-\tilde{u}}}{2} \log \left(\frac{1+\tilde{\gamma}_{ij}}{1-\tilde{\gamma}_{ij}} \right), \quad (\text{B.12})$$

where $\tilde{u} = \min(|N_i|, |N_j|)$. If $n \leq \tilde{u} + 2$, we define $\tilde{\xi}_{ij} := 0$. Define $\tilde{p}_{ij} = 2\Phi(-|\tilde{\xi}_{ij}|)$ and $\tilde{\Xi} = \{(i, j) \notin \mathcal{E}_0 : \tilde{p}_{ij} \leq \delta\}$. A computationally efficient statistic is defined as

$$T_{\text{ERC}} = \sum_{(i,j) \in \tilde{\Xi}} \tilde{\xi}_{ij}^2. \quad (\text{B.13})$$

Since this statistic is obtained from the aggregation of an efficient computation of pairwise residual correlations, we call it the ERC statistic.

B.4.2 Conditional regression

We propose a powerful test statistic by taking advantage of a method originated in Verzelen and Villers [2009]. Based on the conditional regression of X_i on the other variables, as expressed in (B.6), the null hypothesis in (B.4) can be decomposed into the following hypotheses for all $i \in [p]$:

$$H_0^{(i)} : \forall k \notin N_i, \theta_k^{(i)} = 0,$$

where N_i is the neighborhood of i in the graph G . Following the Bonferroni adjustment, the overall significance level α is divided among the tests as $\alpha = \sum_{i \in [p]} \alpha_i$. Given a node i and any nonempty index set $A \subset (\{i\} \cup N_i)^c$, an alternative hypothesis can be $H_A^{(i)} : \theta_A^{(i)} \neq \mathbf{0}$. The Fisher test statistic for testing $H_0^{(i)}$ versus $H_A^{(i)}$ for the normal linear model in (B.6) is given by

$$\phi_A(\mathbf{X}_i, \mathbf{X}_{-i}) := \frac{\|\Pi_{N_i \cup A} \mathbf{X}_i - \Pi_{N_i} \mathbf{X}_i\|^2 / |A|}{\|\mathbf{X}_i - \Pi_{N_i \cup A} \mathbf{X}_i\|^2 / (n - h_i - |A|)}, \quad (\text{B.14})$$

where $|A|$ is the size of A , h_i equals to $|N_i| + 1$, Π_S is the orthogonal projection from \mathbb{R}^n onto the column spaces of $[\mathbf{1}_n, \mathbf{X}_S]$. If $n < h_i + |A|$, we define $\phi_A(\mathbf{X}_i, \mathbf{X}_{-i}) := 0$ for simplicity. In practice, the statistic in (B.14) can be computed by fitting linear regressions via standard statistical software, such as the `anova` function in the **R** language.

For simplicity, we define the collection of all singleton subsets of $(\{i\} \cup N_i)^c$ as

$$\mathcal{A}_i = \{ \{a\} : a \in (\{i\} \cup N_i)^c \}, \quad (\text{B.15})$$

and we consider $A \in \mathcal{A}_i$. To aggregate the statistics $\phi_A(\mathbf{X}_i, \mathbf{X}_{-i})$ for all $A \in \mathcal{A}_i$, Verzelen and Villers [2009] proposed to use a Bonferroni correction with $\sum_{A \in \mathcal{A}_i} \alpha_A^{(i)} = \alpha_i$ and define the test as

$$T_{\alpha_i} = \sup_{A \in \mathcal{A}_i} \left\{ \phi_A(\mathbf{X}_i, \mathbf{X}_{-i}) - \bar{F}_{1, n-h_i-1}^{-1} \left(\alpha_A^{(i)} \right) \right\},$$

where $\bar{F}_{a,b}(u)$ is the probability for a Fisher variable with a and b degrees of freedom to be larger than u . $\alpha_A^{(i)}$ may be set equal to $\alpha_i / (p - h_i)$ for all $A \in \mathcal{A}_i$. In the numerical experiments in Verzelen and Villers [2009], this testing procedure with $\alpha_i = 0.05/p$ proved nearly as powerful as the more complicated alternative methods in most cases. We refer to this testing procedure as $M^1 P_1$ and will use it as one of the benchmarks for comparison in our numerical studies in Section 5 of the main paper.

Motivated by the $M^1 P_1$ procedure, we propose to compute either the maximal value or the summation of ϕ_A . More concretely, we define the following test statistics

$$T_{F_{\max}}(\mathbf{X}) = \max_{i \in [p]} \max_{A \in \mathcal{A}_i} \phi_A(\mathbf{X}_i, \mathbf{X}_{-i}) \quad (\text{B.16})$$

and

$$T_{F_\Sigma}(\mathbf{X}) = \sum_{i \in [p]} \sum_{A \in \mathcal{A}_i} \phi_A(\mathbf{X}_i, \mathbf{X}_{-i}), \quad (\text{B.17})$$

and call them the F_{\max} statistic and the F_Σ statistic, respectively. In the simulation studies in Section 5 of the main paper, we demonstrate that our MC-GoF test with the F_Σ statistic consistently outperforms most competitors in terms of power, and thus we recommend it as the default choice. Besides, we expect that the performance of F_{\max} is similar to the M^1P_1 procedure in Verzelen and Villers [2009] and confirm this in an additional simulation in Appendix F.3.

Remark 3. Verzelen and Villers [2009] also proposed a procedure called M^1P_2 , which adaptively selects the quantity $\alpha_A^{(i)}$ using a Monte Carlo method. Specifically, it computes the α_i -quantile of the following random variable conditional on \mathbf{X}_{-i} :

$$\inf_{A \in \mathcal{A}_i} \bar{F}_{1, n-h_i-1}(\phi_A(\mathbf{Z}, \mathbf{X}_{-i})), \quad (\text{B.18})$$

where \mathbf{Z} is an independent standard normal vector of dimension n . The procedure then sets $\alpha_A^{(i)}$ to this quantile for all $A \in \mathcal{A}_i$.

Compared to the M^1P_1 procedure, M^1P_2 avoids splitting α_i into smaller components for subsets A . However, the improvement in power is marginal, as shown in the simulation studies in Verzelen and Villers [2009]. Both M^1P_2 and M^1P_1 are designed to detect strong signals rather than to aggregate weak signals. Consequently, they lose power in dense-but-weak signal scenarios compared to the MC-GoF test with the F_Σ statistic. We examine the power properties of the M^1P_2 in Appendix D.4 and confirm that its performance is only slightly better than that of M^1P_1 and does not compete with the MC-GoF test.

Another critical limitation of the M^1P_2 procedure lies in its computational scalability. Computing the quantile in (B.18) requires at least α_i^{-1} Monte Carlo replications for each variable i . For example, with $p = 120$ and $\alpha = 5\%$, at least 2400 replications are needed per variable. The total number of replications grows as $\sum_i \alpha_i^{-1} \geq p^2 / (\sum_i \alpha_i) = p^2 / \alpha$ (by the generalized mean inequality). This computational burden makes the M^1P_2 procedure impractical for high-dimensional inference.

Remark 4. The power of the MC-GoF test is maximized when the chosen test statistic aligns with the signal pattern of the alternative hypothesis. We offer practical guidance to help practitioners select an appropriate test statistic based on the expected structure of the alternative hypothesis.

Motivated by the theoretical results in Section 4 and the experimental findings in Section 5 of the main paper, we identify two distinct and meaningful types of alternative hypotheses: (a) the dense-but-weak alternative, where many small nonzero entries in the precision matrix violate the null hypothesis, and (b) the strong-but-sparse alternative, where at least one large entry in the precision matrix violates the null hypothesis. The test statistics introduced so far can be broadly categorized into two types:

- (1) **sum-type statistics** including SRC, PRC, ERC, and F_Σ ;
- (2) **max-type statistics** including MRC and F_{\max} .

For alternatives expected to be strong but sparse, we recommend the use of max-type statistics. Conversely, for alternatives expected to be dense but weak, sum-type statistics are more effective. In the case of strong and dense alternatives—a comparatively easier scenario—any of these statistics is appropriate.

B.4.3 Generalized likelihood ratio test

Our third strategy to construct a GoF test statistic is based on the generalized likelihood ratio (GLR) test for comparing two nested models: a null model and a more complex model (full model). For the GoF testing problem, we consider the full model \mathcal{M}_{full} that comprises all p -dimensional normal distributions and consider testing for

$$H_0 : P \in \mathcal{M}_{G_0} \text{ versus } H_a : P \in \mathcal{M}_{full}.$$

Suppose $\ell(\boldsymbol{\Omega})$ is the profile likelihood function that replaced the unknown mean by the sample mean. The GLR test statistic depends on $\ell(\boldsymbol{\Omega})$, the maximum likelihood estimator (MLE) $\widehat{\boldsymbol{\Omega}}_{ML}$ under the full model, and the restricted MLE $\widehat{\boldsymbol{\Omega}}_{ML}^{(G_0)}$ under \mathcal{M}_{G_0} . The test statistic is expressed as

$$T_{\text{GLR}} = 2 \log \ell(\widehat{\boldsymbol{\Omega}}_{ML}) - 2 \log \ell(\widehat{\boldsymbol{\Omega}}_{ML}^{(G_0)}). \quad (\text{B.19})$$

When T_{GLR} is used in Algorithm 3, the second term in (B.19) can be eliminated. This is because every $\widetilde{\mathbf{X}}^{(m)}$ and \mathbf{X} share the same value of the sufficient statistic for the model \mathcal{M}_{G_0} , and consequently, the same value of $\ell(\widehat{\boldsymbol{\Omega}}_{ML}^{(G_0)})$.

The computation for $\ell(\widehat{\boldsymbol{\Omega}}_{ML})$ can be challenging, especially in high-dimensional problems where the sample sizes are not sufficiently large relative to the dimensions. In this case, one should instead use a regularized estimator. For example, $\widehat{\boldsymbol{\Omega}}_{ML}$ in (B.19) can be replaced by the following modified GLasso estimator [Friedman et al., 2008]:

$$\widehat{\boldsymbol{\Omega}}_{GL} = \arg \min_{\boldsymbol{\Omega} \succ 0} \left\{ \text{tr}(\widehat{\boldsymbol{\Sigma}}\boldsymbol{\Omega}) - \log \det(\boldsymbol{\Omega}) + \lambda \sum_{(i,j) \notin \mathcal{E}_0, i \neq j} \sqrt{\widehat{\boldsymbol{\Sigma}}_{ii} \widehat{\boldsymbol{\Sigma}}_{jj}} |\Omega_{ij}| \right\}, \quad (\text{B.20})$$

where the minimization is taken over all positive definite matrices with dimension $p \times p$, and $\widehat{\boldsymbol{\Sigma}}$ is the sample covariance matrix. The estimator in (B.20) takes into account the scaling of different coordinates, which is also considered by Jankova and van de Geer [2018]. In addition, the penalty is imposed only on edges not included in the null graph G_0 . For implementation in the **R** language, one can compute $\widehat{\boldsymbol{\Omega}}_{GL}$ by properly setting the argument “rho” as a matrix in the **glasso** function. The tuning parameter λ is often selected by cross-validation, but to speed up the computation, we may simply set $\lambda = 2\sqrt{\log p/n}$ based on existing theory on GLasso; see Rothman et al. [2008, Theorem 1] and Jankova and van de Geer [2018, Proposition 1]. To this end, we propose the following GLR- ℓ_1 test statistic:

$$T_{\text{GLR-}\ell_1} = 2 \log \ell(\widehat{\boldsymbol{\Omega}}_{ML}). \quad (\text{B.21})$$

B.4.4 Incorporating prior information

In the presence of prior information about the underlying graph, we could construct test statistic functions that incorporate this information. Although a comprehensive discussion is beyond our scope, we provide three examples of such constructions.

We begin with a scenario where we have prior information that specific pairs of variables, unconnected in the null graph $G_0 = (\mathcal{V}, \mathcal{E}_0)$, have high (or low) chances of connection in the actual graph. To incorporate this prior information quantitatively, we introduce a non-negative weighting factor w_{ij} for each pair $(i, j) \notin \mathcal{E}_0$. By default, w_{ij} is set to 1 and can be adjusted according to the prior information about the chance that an edge exists between nodes i and j . We can then modify the PRC statistic in (B.11) into the following statistic:

$$T_{\text{PRC-w}}(\mathbf{X}) = \sum_{(i,j) \in \Xi} w_{ij} \cdot z_{ij}^2, \quad (\text{B.22})$$

which is called the PRC-w statistic since it is a weighted version of the PRC statistic. Similarly, we can define the weighted version of the ERC statistic and call it the ERC-w statistic. In Appendix F.4, we present a numerical example where these weighted statistics achieve higher power compared to the other statistics that do not incorporate prior information.

We next consider a general Bayesian approach to construct GoF test statistics for GGMs. Using the framework of Bayesian inference, beliefs about which edges are likely to exist can be directly integrated into the prior distribution and will be reflected in the posterior distribution. A test statistic can then be formulated based on the posterior distribution, such as the posterior predictive p-value, which measures

how well the Bayesian model predicts new data. See Williams et al. [2020] for more details about model comparison methods using posterior predictive distributions and Bayes factors.

To illustrate how the Bayesian inference can be used to construct test statistic functions for our MC-GoF test, we consider a situation where there is prior information about some possible alternative graphs (denoted by $G^{(i)}$) that are suspected to be the true graph. We can specify a hyper-prior distribution $\pi(\mathcal{M})$ on the null model \mathcal{M}_{G_0} and the alternative models $\mathcal{M}_{G^{(i)}}$. For each of these models, we place a prior $\gamma_i(\boldsymbol{\Omega})$ on the precision matrix $\boldsymbol{\Omega}$ so that the constraints of the model $\mathcal{M}_{G^{(i)}}$ are fulfilled. Subsequently, the reciprocal of the posterior probability of the null model $\pi(\mathcal{M}_{G^{(0)}} | \mathbf{X})$ can serve as a test statistic.

The Bayesian approach is flexible in the incorporation of prior knowledge. We point out that a promising choice for the prior on the precision matrix w.r.t. a graph is the G-Wishart prior [Roverato, 2002], which is a conjugate prior and has been studied extensively in Bayesian literature; see for example Atay-Kayis and Massam [2005], Dobra et al. [2011], Mohammadi and Wit [2015]. However, the Bayesian approach requires the posterior computation to be conducted for not only \mathbf{X} but also all the M copies $\tilde{\mathbf{X}}^{(m)}$, which can be intensive in computation. We left the exploration of this method for future investigations.

C Details on power theory

The power analysis is based on contrasting the distribution of the observed statistic $T(\mathbf{X})$ against the empirical distribution of $T(\tilde{\mathbf{X}}^{(m)})$, $m \in [M]$, computed from the generated copies. This analysis involves understanding the following two aspects:

(A) the distribution of copies $\tilde{\mathbf{X}}^{(m)}$ and statistics $T(\tilde{\mathbf{X}}^{(m)})$;

(B) the distribution of $T(\mathbf{X})$ under a meaningful alternative hypothesis.

Since Algorithm 2 is a Monte Carlo procedure based on Markov chains, the distribution of its output is not always analytically tractable for a general graph. To make tangible progress, we focus on the following class of null graphs whose structure enables an explicit and tractable analysis.

Definition 1. A graph $G = ([p], \mathcal{E})$ is said to be clique-star shaped if there exists a subset $\mathcal{H} \subsetneq [p]$ such that $\mathcal{E} = \{(i, j) : \forall i \in [p], j \in \mathcal{H}\}$.

If $P \in \mathcal{M}_{G_0}$ and G_0 is clique-star shaped, then every node in the clique set \mathcal{H} is connected to all other variables, and the variables in \mathcal{H}^c are conditionally independent given the variables in \mathcal{H} . Using these two properties, we can explicitly characterize the distribution of the output of Algorithm 2 and thus address the challenge in studying Aspect (A).

Under Condition 1 in the main paper, we denote $\mathcal{C} = \mathcal{H}^c$, $q = |\mathcal{C}|$, and denote by $\boldsymbol{\Omega}_{\mathcal{C}}$ the submatrix of $\boldsymbol{\Omega}$ consisting the rows and columns indexed by \mathcal{C} . For normal populations, we have

$$P \in \mathcal{M}_{G_0} \Leftrightarrow \boldsymbol{\Omega}_{\mathcal{C}} \text{ is a diagonal matrix.}$$

This equivalence motivates the following metric for quantifying the deviation of the population P from the null hypothesis:

$$D(\boldsymbol{\Omega}_{\mathcal{C}}, s) = \|\mathbf{R}(\boldsymbol{\Omega}_{\mathcal{C}}^{-1}) - \mathbf{I}_q\|_s,$$

where $\mathbf{R}(\mathbf{M}) = \text{diag}(\mathbf{M})^{-1/2} \mathbf{M} \text{diag}(\mathbf{M})^{-1/2}$ is the diagonal normalization and the symbol s can be either F or ∞ , corresponding to the Frobenius norm or the maximum norm of a matrix, respectively. The metric $D(\boldsymbol{\Omega}_{\mathcal{C}}, s)$ serves as a measure of signal strength under the alternative hypothesis. In particular, for both $s = F$ and $s = \infty$, we have $D(\boldsymbol{\Omega}_{\mathcal{C}}, s) = 0$ if and only if $\boldsymbol{\Omega}_{\mathcal{C}}$ is a diagonal matrix, which indicates no deviation from the null hypothesis. Appendix C.1 provides a detailed discussion on this metric. As we will see, the power of the MC-GoF test depends on the magnitude of $D(\boldsymbol{\Omega}_{\mathcal{C}}, s)$.

We now provide an overview of our theory as follows:

- Dense alternative: When many of the off-diagonal entries of $\boldsymbol{\Omega}_{\mathcal{C}}$ are nonzero, we use $D(\boldsymbol{\Omega}_{\mathcal{C}}, F)$ to quantify the deviation from the null hypothesis. In Appendix C.2, we show that when both n and p

diverge to infinity proportionally, if $D(\boldsymbol{\Omega}_C, F) \gg \sqrt{q/n}$, then the asymptotic power of the MC-GoF test with some statistic T_1 converges to 1. Additionally, we show that no α -level test can distinguish between the null and alternative hypotheses with power tending to one when the separation rate in terms of $D(\boldsymbol{\Omega}_C, F)$ is of order $\sqrt{q/n}$. This result implies that the MC-GoF test with T_1 is rate-optimal for dense alternatives.

- Strong alternative: When some of the off-diagonal entries of $\boldsymbol{\Omega}_C$ are separated from zero, we use $D(\boldsymbol{\Omega}_C, \infty)$ to quantify the deviation from the null hypothesis. In Appendix C.3, we show that when $D(\boldsymbol{\Omega}_C, \infty) = 16\sqrt{\log q/n}$, the power of the MC-GoF test with some statistic T_2 converges to 1 as $n \rightarrow \infty$. Additionally, we show that any test will be powerless if the separation rate in terms of $D(\boldsymbol{\Omega}_C, \infty)$ is of order smaller than $\sqrt{\log q/n}$. This result implies that the MC-GoF test with T_2 is rate-optimal for strong alternatives.
- Dense or strong alternative: The union of the aforementioned alternative hypotheses can also be tested using the MC-GoF test with a properly designed test statistic T_3 . In Section C.4, we show that when either $D(\boldsymbol{\Omega}_C, F) \gg \sqrt{q/n}$ or $D(\boldsymbol{\Omega}_C, \infty) \geq 16\sqrt{\log q/n}$, the power of the MC-GoF test with T_3 converges to 1. Again, this test is rate-optimal for the union alternative.

We provide a proof sketch in Section C.5 and place the complete proof in Appendix E.6.

C.1 Metric of deviation

Before we study the power, we provide some intuitions about the metric $D(\boldsymbol{\Omega}_C, s)$, which is the key quantity for characterizing the power of the MC-GoF test as illustrate in Figure 1 in the main text. To connect this metric with some common population quantities, we provide the following result.

Proposition 4. *Suppose $X = (X_1, \dots, X_p)^\top \sim \mathbf{N}_p(\mathbf{0}, \boldsymbol{\Omega}^{-1})$. Let \mathcal{C} be a nonempty subset of $[p]$ and let $\mathcal{H} = [p] \setminus \mathcal{C}$. Then we have*

$$D(\boldsymbol{\Omega}_C, \infty) = \max_{i,j \in \mathcal{C}} |\text{cor}(X_i, X_j \mid X_{\mathcal{H}})|.$$

Furthermore,

$$D(\boldsymbol{\Omega}_C, F)^2 \geq \frac{1}{\lambda} \sum_{i,j \in \mathcal{C}} \tilde{\boldsymbol{\Omega}}_{i,j}^2,$$

where λ is the condition number of $\boldsymbol{\Omega}_C$ and $\tilde{\boldsymbol{\Omega}}_C = \mathbf{R}(\boldsymbol{\Omega}_C)$.

Proposition 4 suggests that $D(\boldsymbol{\Omega}_C, \infty)$ measures the largest magnitude of the partial correlations that violate the null hypothesis, and the square of $D(\boldsymbol{\Omega}_C, F)$ serves as a proxy for the sum of squared entries of the normalized $\boldsymbol{\Omega}_C$.

C.2 Dense alternative

We first consider the case where the true precision $\boldsymbol{\Omega}$ deviates from the model assumption of the null hypothesis with many small entries. In such a case, we consider the SRC statistic in (B.8). Under Condition 1, this statistic is expressed as

$$T_1(\mathbf{X}) = \sum_{i,j \in \mathcal{C}, i \neq j} \hat{\gamma}_{ij}^2,$$

where $\hat{\gamma}_{ij}$ is the pairwise residual correlation statistic defined in (B.7). To examine the power, we use the metric $D(\cdot, F)$ to quantify the deviation from the null hypothesis and define

$$\Theta_{n1}(b) := \left\{ \mathbf{A} \in \mathbb{S}_+^p : D(\mathbf{A}_C, F) \geq b\sqrt{\frac{q}{n}}, \quad \lambda_{\max}(\mathbf{A}_C)/\lambda_{\min}(\mathbf{A}_C) \leq b_0 \right\}, \quad \forall b > 0,$$

where $b_0 \geq 1$ can be any fixed constant. We are interested in the dense alternative hypothesis defined as

$$H_a : \boldsymbol{\Omega} \in \Theta_{n1}(b). \quad (\text{C.1})$$

Theorem 4. *Suppose that Condition 1 holds and that $q/n \rightarrow \gamma \in (0, \infty)$. For any $\epsilon > 0$, there exists a positive constant b such that for any sequence of populations with $\boldsymbol{\Omega} \in \Theta_{n1}(b)$, it holds*

$$\liminf_n \beta_n(P; \alpha, T_1) \geq 1 - \epsilon,$$

provided that the number of copies M is at least $\max(2\alpha^{-1}, \log(2\epsilon^{-1}))$.

Remark 5. *In the proof, we specifically choose $b = \sqrt{2z_1 + 4b_0^4\gamma z_2}$, where z_1 and z_2 are the $(\alpha^2/16)$ - and $(\epsilon/2)$ -upper quantiles of the standard normal distribution respectively. In other words, b depends on ϵ at the order of $\sqrt{\log(\epsilon^{-1})}$.*

Theorem 4 shows that the MC-GoF test can distinguish between the null (1.2) and the dense alternative (C.1) with power tending to 1 when $b = b_n \rightarrow \infty$. In particular, we have the following corollary on the consistency of the MC-GoF test against the dense alternative.

Corollary 1. *Suppose that Condition 1 holds and that $q/n \rightarrow \gamma \in (0, \infty)$. For a sequence of populations such that the condition number of $\boldsymbol{\Omega}_{\mathcal{C}}$ is bounded and $D(\boldsymbol{\Omega}_{\mathcal{C}}, F)$ diverges to infinity, if the MC-GoF test is conducted with level α_n at least $1/\log(n)$ and with M at least $2 \max(\alpha_n^{-1}, \log n)$, then*

$$\lim_{n \rightarrow \infty} \beta_n(P; \alpha_n, T_1) = 1.$$

Although Theorem 4 and Corollary 1 require q to grow proportionally in n , they allow the limit of q/n to be much larger than 1 so they are applicable in high-dimensional settings where the dimension is much larger than the sample size. When q/n is bounded, the result in Corollary 1 cannot be improved. Specifically, the following theorem proves that if $D(\boldsymbol{\Omega}_{\mathcal{C}}, F)$ is at the order of $\sqrt{q/n}$, then no α -level test for $H_0 : P \in \mathcal{M}_{G_0}$ can differentiate between the null hypothesis and the dense hypothesis with power tending to one as n and q grow.

Theorem 5. *Let $0 < \alpha < \beta < 1$. Suppose that as $n \rightarrow \infty, q \rightarrow \infty$ and that Condition 1 holds. Suppose $q/n \leq \kappa$ for some constant $\kappa < \infty$ and all n . Then there exists a constant $b = b(\kappa, \beta - \alpha)$ such that*

$$\limsup_{n \rightarrow \infty} \left\{ \sup_{\phi} \inf_{\boldsymbol{\Omega} \in \Theta_{n1}(b)} \mathbb{E}(\phi) \right\} < \beta.$$

where \sup_{ϕ} is taken over any α -level test ϕ for $H_0 : P \in \mathcal{M}_{G_0}$.

Theorem 5 shows that no level α test for (1.2) can distinguish between the two hypotheses with power tending to 1 as n and p grow when the separation rate ε_n is of order $\sqrt{q/n}$. Thus, it provides a lower bound on the separation rate. Comparing with the power guarantee given in Theorem 4, we see that the MC-GoF test with T_1 is rate-optimal for dense alternatives.

C.3 Strong alternative

We consider the case where the true precision $\boldsymbol{\Omega}$ deviates from the model assumption of the null hypothesis with at least one large entry. In such a case, we choose the following test statistic

$$T_2(\mathbf{X}) = \max_{i,j \in \mathcal{C}, i \neq j} \hat{\gamma}_{ij}^2,$$

where $\hat{\gamma}_{ij}$ is the pairwise residual correlation statistic defined in (B.7).

To examine the power, we consider the quantity $D(\cdot, \infty)$ and define

$$\Theta_{n2}(b) = \left\{ \mathbf{A} \in \mathbb{S}_+^p : D(\mathbf{A}_C, \infty) \geq b \sqrt{\frac{\log q}{n}} \right\},$$

and consider the following alternative:

$$H_a : \boldsymbol{\Omega} \in \Theta_{n2}(b).$$

Theorem 6. *Suppose that Condition 1 holds and that $\log q/n \rightarrow 0$. For any $\epsilon > 0$, if the sample size $n > \max(10/\alpha, 32 \log(16/\epsilon), 8/\epsilon)$ and $M > \max(2\alpha^{-1}, \log(2\epsilon^{-1}))$, then*

$$\inf_{\boldsymbol{\Omega} \in \Theta_{n2}(16)} \beta_n(P; \alpha, T_2) \geq 1 - \epsilon.$$

Corollary 2. *Suppose that Condition 1 holds and that $\log q/n \rightarrow 0$. If the MC-GoF test is conducted with level α_n at least $1/\log(n)$ and with M at least $2 \max(\alpha_n^{-1}, \log n)$, then*

$$\lim_{n \rightarrow \infty} \inf_{\boldsymbol{\Omega} \in \Theta_{n2}(16)} \beta_n(P; \alpha_n, T_2) = 1.$$

The following theorem proves that if $D(\boldsymbol{\Omega}_C, \infty)$ is not sufficiently large compared to $\sqrt{\log(q)/n}$, then any test for $H_0 : P \in \mathcal{M}_{G_0}$ cannot differentiate between the null hypothesis and the sparse hypothesis as n and q grow.

Theorem 7. *Let $0 < \alpha < 1$. Suppose that Condition 1 holds and that as $n \rightarrow \infty, q \rightarrow \infty$ and that $\log(q)/n \leq \kappa$ for some constant $\kappa < \infty$ and all n . Then for any constant $b \in (0, \min(1, \kappa^{-1}))$, the following holds:*

$$\limsup_{n \rightarrow \infty} \left\{ \sup_{\phi} \inf_{\boldsymbol{\Omega} \in \Theta_{n2}(b)} \mathbb{E}(\phi) \right\} \leq \alpha,$$

where \sup_{ϕ} is taken over all α -level test for $H_0 : P \in \mathcal{M}_{G_0}$.

Theorem 7 provides a lower bound on the separation rate between the null hypothesis and the sparse alternative hypothesis required by any consistent test. Together with the power guarantee in Theorem 6, we see that the MC-GoF test with T_2 is rate-optimal for sparse alternatives.

C.4 Union Alternative

In this section, we consider the case where the true precision $\boldsymbol{\Omega}$ has either many small entries or has at least one large entry but not both. In other words, we are interested in the union alternative defined as

$$H_a : \boldsymbol{\Omega} \in \Theta_{n3}(b) = \Theta_{n1}(b) \cup \Theta_{n2}(b).$$

For this alternative, we propose the following test statistic T_3 that incorporates both T_1 and T_2 :

$$T_3(\mathbf{X}) = \max \left(\frac{n}{2q} (T_1(\mathbf{X}) - q(q-1)/n), nT_2(\mathbf{X}) - 4 \log q + \log \log q \right).$$

Theorem 8. *Suppose that Condition 1 holds and $q/n \rightarrow \gamma \in (0, \infty)$. For any $\epsilon > 0$, there exists a positive constant b such that for any sequence of populations with $\boldsymbol{\Omega} \in \Theta_{n3}(b)$, it holds*

$$\liminf_n \beta_n(P; \alpha, T_3) \geq 1 - \epsilon,$$

provided that the number of copies M is at least $\max(2\alpha^{-1}, \log(2\epsilon^{-1}))$.

The following theorem is a corollary of Theorem 5 and Theorem 7, which shows that the MC-GoF test with T_3 is rate-optimal for the union alternative.

Theorem 9. Let $0 < \alpha < \beta < 1$. Suppose that Condition 1 holds and that as $n \rightarrow \infty, q \rightarrow \infty$ and $q/n \leq \kappa$ for some constant $\kappa < \infty$ and all n . Then there exists a constant $b = b(\kappa, \beta - \alpha)$ such that

$$\limsup_{n \rightarrow \infty} \left\{ \sup_{\phi} \inf_{\Omega \in \Theta_{n3}(b)} \mathbb{E}(\phi) \right\} < \beta.$$

where \sup_{ϕ} is taken over any α -level test ϕ for $H_0 : P \in \mathcal{M}_{G_0}$.

C.5 Proof sketch for upper bounds

In this section, we provide an overview of our proof of the power guarantee of the MC-GoF test. For each of the tests being considered, the proof will follow the following three steps:

Step 1. We first bound the power from below with some constant t as

$$\mathbb{P}(\text{Reject } H_0) \geq \mathbb{P}(T(\mathbf{X}) > t) - \mathbb{P}\left(\frac{1}{M+1} \left[1 + \sum_{m=1}^M \mathbf{1}\{T(\tilde{\mathbf{X}}^{(m)}) \geq t\}\right] > \alpha\right),$$

where the value of t depends on the choice of the test statistic and the setting of the alternative hypothesis.

Step 2. Next, we show that the distribution of the statistics $T(\mathbf{X})$ and $T(\tilde{\mathbf{X}}^{(m)})$ can be characterized using the distribution of $T(\mathbf{U})$ and $T(\tilde{\mathbf{U}}^{(m)})$, where \mathbf{U} is a $(n-1-|\mathcal{H}|) \times q$ matrix with i.i.d. rows sampled from $N_q(\mathbf{0}, \mathbf{R}(\Omega_c^{-1}))$, and $\tilde{\mathbf{U}}^{(m)}$ is a $(n-1-|\mathcal{H}|) \times q$ matrix with i.i.d. rows sampled from $N_q(\mathbf{0}, \mathbf{I}_q)$.

Step 3. Based on the characterization in the last step, we derive an upper bound on the probability $\mathbb{P}\left(\frac{1}{M+1} \left[1 + \sum_{m=1}^M \mathbf{1}\{T(\tilde{\mathbf{U}}^{(m)}) \geq t\}\right] > \alpha\right)$ for each choice of statistic T . Furthermore, we will analyze the asymptotic property of $T(\mathbf{U})$ to derive a tight lower bound on $\mathbb{P}(T(\mathbf{U}) > t)$.

The details of the proof are provided in Appendix E.6. In the proof, Step 3 is the most important and it requires more technical analyses on the asymptotic properties of sample correlation statistics. Step 2 is proved by using the properties of Algorithm 2. This step is essential because it provides a tractable characterization that allows us to study the asymptotic properties of the MC-GoF test using the techniques developed for studying high-dimensional sample correlation tests.

Our theoretical results are related to high-dimensional hypothesis testing for correlation matrices [Zheng et al., 2019, Gao et al., 2017, Cai and Jiang, 2011]. Specifically, when the null graph G_0 does not have any edge, $\mathcal{H} = \emptyset$ and testing whether $P \in \mathcal{M}_{G_0}$ is equivalent to testing whether the correlation matrix equals to the identity matrix. In this scenario, our results imply that the MC-GoF test can achieve rate-optimal power, which matches the test for correlation matrices proposed in Zheng et al. [2019].

D Details on Simulations in Section 5

We compare the power performance of our method against two baseline methods: the M^1P_1 procedure in Verzelen and Villers [2010] and the Bonferroni adjustment of multiple testing for the composite null hypothesis in (B.4) as suggested in Drton and Perlman [2007]. These two methods are referred to as M^1P_1 and Bonf. Specifically, the Bonferroni-adjusted p-value of the Bonf method is defined as

$$\min\{1, Kp_{ij} : i < j, (i, j) \notin \mathcal{E}\}, \tag{D.1}$$

where K equals to the number of pairs of distinct i and j that are not connected in G , and p_{ij} is the statistic defined in (B.10).

The MC-GoF test (Algorithm 3) will be conducted using four test statistic functions discussed in Section B.4, including PRC and ERC in Appendix B.4.1, F_Σ in Appendix B.4.2, GLR- ℓ_1 in Appendix B.4.3. For simplicity, we fix the procedure parameters $M = 100$ and $L = 3$.

In Appendix D.1, we first explain the experimental settings. Appendix D.2 demonstrates the theoretically valid Type-I error control for all methods. Then in Appendix D.3, we compare power of each method for each setting with different configurations of population parameters. Appendix D.4 presents the numerical results of a baseline method, the M^1P_2 procedure, which performs similarly to the M^1P_1 procedure but incurs significantly higher computational costs as discussed in Remark 3.

D.1 Setup

For illustration, we consider three types of graphs, each with distinct topological properties. In each of the following items, we define the precision matrix $\mathbf{\Omega} = (\omega_{ij})_{i,j \in [p]}$ and the corresponding graph G for the true distribution of the data, and define another graph G_0 for the null hypothesis.

- **Band Graph:** The precision matrix $\mathbf{\Omega}$ satisfies that for $i, j \in \{1, \dots, p\}$:

$$\omega_{i,j} = \begin{cases} 1 & \text{if } i = j, \\ s & \text{if } 1 \leq |i - j| \leq K, \\ 0 & \text{if } |i - j| > K, \end{cases}$$

where K is the bandwidth and $s \in (0, 0.2)$ is the signal magnitude. We define the graph G_0 for a null hypothesis as a band graph with bandwidth K_0 .

- **Hub Graph:** The nodes are divided into separate groups of size $h = 10$, and within each group, members are only connected to a hub node. Specifically, for each positive integer $k \leq p/h$, let $i = h(k - 1) + 1$, $\omega_{ij} = \omega_{ji} = 1$ for $j \in \{(i + 1), \dots, (i + h - 1)\}$, and let all other off-diagonal entries equal to zero. Then each of the diagonal entries is set to be the summation of absolute values along the row plus a parameter $\xi > 0$:

$$\omega_{ii} = \sum_{i \neq j} |\omega_{ij}| + \xi,$$

which guarantees that $\mathbf{\Omega} = (\omega_{ij})_{1 \leq i, j \leq p}$ is positive definite. The parameter ξ controls the signal magnitude: a larger value of ξ corresponds to weaker signals.

To define the graph for a null hypothesis, we consider a subgraph G_0 by randomly removing the existing edges independently with probability 0.7.

- **Erdős–Rényi–Gilbert Random Graph:** There is an edge between a pair of distinct nodes independently and randomly with probability q . We begin with constructing a random matrix $\mathbf{A} = (a_{ij})_{1 \leq i, j \leq p}$. Let $a_{ii} = 1$, for $i \in \{1, \dots, p\}$. For any pair of $i < j$, let $a_{ij} = a_{ji} = u_{ij} \cdot \delta_{ij}$, where u_{ij} is uniformly distributed on $(s/2, 3s/2)$ and δ_{ij} is an independent Bernoulli random variable with success probability q . Let λ be the smallest eigenvalue of \mathbf{A} . The precision matrix is defined as

$$\mathbf{\Omega} = \mathbf{A} + (|\lambda| + 0.05) \mathbf{I}.$$

To define the graph for a null hypothesis, we consider a subgraph G_0 whose edges exist with probability q_0 . This can be obtained by randomly removing the existing edges in G independently with probability $1 - q_0/q$. In our experiment, we fix $q_0 = 0.08$.

In the construction of a band graph, the population parameter s will be referred to as the *signal magnitude*. This is because if the constructed normal distribution does not belong to \mathcal{M}_{G_0} , then the result given by Jog and Loh [2015, Corollary 1] ensures that the Kullback-Leibler (KL) divergence between this distribution and any distribution in \mathcal{M}_{G_0} is at least $\eta_-(s) := -2^{-1} \log(1 - s^2)$, which is an increasing

function of s^2 . For a hub graph model and an Erdős–Rényi–Gilbertrandom graph, similar lower bounds for the KL divergence between the true distribution and any distribution in the null model can be obtained, which are $\eta_-(1/(h-1+\xi))$ and $\eta_-(s/(1+|\lambda|+0.05))$, respectively. Therefore, we will vary the value of s (or ξ for hub graph models) in the simulations to control the KL divergence between the true distribution and the null model.

The simplicity of these graphs allows us to illustrate how the signal patterns affect the power of the tests. Appendix F.2 extends the experiments to more complex graph structures, including cases where the null graph is not a subgraph of the true graph. Additionally, Appendix F.1 includes an example with moderately dense null graphs, where the graph degree is not small compared to the sample size. The results from these extended experiments agree with the findings presented in this section.

D.2 Type I error control

We numerically illustrate that the proposed MC-GoF test controls the Type I error regardless of the dimension and the sample size. Specifically, we generate random samples from the GGM with mean 0 and precision matrix from the band graph G with $K = 6$ and $s = 0.2$ as defined in Appendix D.1 and conduct various GoF tests for the GGM w.r.t. G — the null hypothesis is true in this case. We vary the dimension p , the signal magnitude s , and the sample size n for several configurations. We independently repeat each experiment 1200 times and record the p-values given by each method. We then estimate the size of each test at the significance level $\alpha = 0.05$ by its rejection proportion across the replications.

We report the estimated sizes of the tests in Table 2. The first column (M^1P_1) corresponds to the M^1P_1 procedure in Verzelen and Villers [2010], the second (Bonf) is a Bonferroni adjustment of multiple testing for partial correlation in Drton and Perlman [2007]. The other four columns correspond to our proposed MC-GoF testing procedure with different choices of test statistics in Section 3.2.

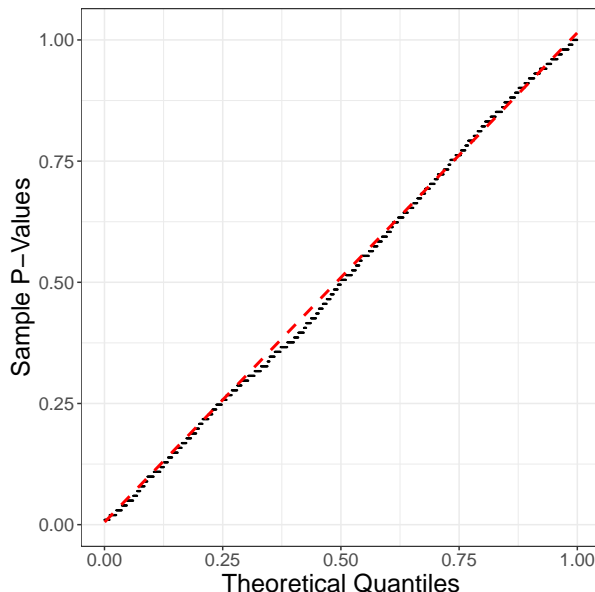
For each setting and each method, we also conduct the one-sample proportion test for the hypothesis that the size is no greater than α and report the p-value in a pair of parentheses. The smallest p-value appears in the result of the MC-GoF test using the GLR- ℓ_1 statistic for the configuration with $(p, s, n) = (20, 0.2, 80)$. In this configuration, we further analyze the p-values from this GoF test and present the QQ plot to compare them with the uniform distribution in Figure 4. Note that Proposition 3 only justifies the validity of any MC-GoF test, but the p-value could be stochastically larger than a uniform random variable. Nonetheless, the QQ plot in Figure 4 shows that the distribution of the simulated p-values is very close to the uniform distribution. The exceedance of some estimated sizes in Table 2 should be attributed to Monte Carlo errors and multiple comparisons.

Table 2: Estimated sizes of various GoF tests at the significance level $\alpha = 0.05$ on band graphs ($K = 6, K_0 = 6$). The p-value of the one-sample proportion test for each size is provided in parentheses.

p	s	n	Method					
			M^1P_1	Bonf	PRC	ERC	F_Σ	GLR- ℓ_1
20	0.2	20	0.037 (0.977)	0.000 (1.000)	0.053 (0.298)	0.045 (0.787)	0.049 (0.553)	0.049 (0.553)
		40	0.053 (0.298)	0.054 (0.254)	0.060 (0.056)	0.051 (0.447)	0.055 (0.213)	0.052 (0.396)
		80	0.044 (0.823)	0.046 (0.746)	0.052 (0.396)	0.052 (0.396)	0.050 (0.500)	0.061 (0.043)
120	0.2	20	0.051 (0.447)	0.000 (1.000)	0.043 (0.883)	0.059 (0.073)	0.060 (0.056)	0.047 (0.702)
		40	0.047 (0.702)	0.040 (0.944)	0.041 (0.927)	0.046 (0.746)	0.049 (0.553)	0.043 (0.855)
		80	0.048 (0.604)	0.043 (0.855)	0.044 (0.823)	0.032 (0.998)	0.042 (0.907)	0.052 (0.346)

The MC-GoF test is guaranteed to control the Type I error when the true graph G is a subgraph of G_0 . As an example, we consider band graphs with $K = 4$ for G and $K_0 = 6$ for G_0 , setting $s = 0.2$ as defined in Appendix D.1. Table 3 presents the estimated sizes of the test. The MC-GoF test controls the sizes at the significance level $\alpha = 0.05$ in all cases, except for tests using PRC or ERC statistics in the

Figure 4: QQ plot comparing the uniform distribution and the p-value of the MC-GoF test using the GLR- ℓ_1 statistic in the setting $(p, s, n) = (20, 0.2, 80)$.



configuration $(p, s, n) = (20, 0.2, 80)$ —again, the deviations are likely caused by Monte Carlo errors and multiple comparisons.

p	s	n	Method					
			M^1P_1	Bonf	PRC	ERC	F_Σ	GLR- ℓ_1
20	0.2	20	0.047 (0.702)	0.000 (1.000)	0.053 (0.298)	0.057 (0.145)	0.053 (0.346)	0.058 (0.117)
		40	0.047 (0.702)	0.039 (0.957)	0.053 (0.346)	0.054 (0.254)	0.047 (0.702)	0.050 (0.500)
		80	0.052 (0.396)	0.047 (0.702)	0.061 (0.043)	0.063 (0.023)	0.060 (0.056)	0.050 (0.500)
120	0.2	20	0.049 (0.553)	0.000 (1.000)	0.043 (0.883)	0.058 (0.117)	0.053 (0.298)	0.046 (0.746)
		40	0.043 (0.855)	0.041 (0.927)	0.054 (0.254)	0.053 (0.298)	0.046 (0.746)	0.043 (0.883)
		80	0.048 (0.654)	0.028 (1.000)	0.040 (0.944)	0.042 (0.907)	0.048 (0.604)	0.058 (0.117)

Table 3: Estimated sizes of various GoF tests at the significance level $\alpha = 0.05$ on band graphs ($K = 4, K_0 = 6$). The p-value of the one-sample proportion test for each size is provided in parentheses.

D.3 Power comparison

We consider each of three graph types in Appendix D.1 with different configurations of population parameters. In each configuration, we generate n random samples from $\mathbf{N}_p(\mathbf{0}, \mathbf{\Omega}^{-1})$ and conduct various GoF tests for the null hypothesis $H_0 : P \in \mathcal{M}_{G_0}$ at the significance level $\alpha = 0.05$. We repeat each experiment 400 times and present the estimated power for different methods in tables. Standard errors are shown in parentheses, and the highest power in each case is indicated in bold type.

Table 4 presents the results for band graphs with $K = 6$ for the true distribution and $K_0 = 1$ for the null hypothesis. The dimension p is either 20 or 120, the sample size n takes value among 20, 40, and 80, while the signal magnitude s among 0.1, 0.15, and 0.2. As expected, the power of each test increases with the sample size n and the signal magnitude s . We also observed that when s is as large as 0.2, F_Σ consistently achieves the highest power in Table 4. When s is 0.1 or 0.15, PRC sometimes slightly outperforms F_Σ . ERC, designed as a computationally efficient alternative to PRC, has slightly lower power than PRC when n is small, but the gap diminishes quickly as n increases. The GLR- ℓ_1 statistic does not perform as well

as the other three statistics when n is 40. This may be due to the violation of the sparsity assumption for GLasso to work well since the degrees of nodes in this band graph are between 6 and 12, which are not negligible relative to $n = 40$. Our GoF testing procedure with any of the four test statistics outperforms the baseline methods across all cases studied in this experiment. In some cases the advantages are significant; for example, when $p = 120$, $s = 0.15$, and $n = 80$, all the four MC-GoF tests achieve power higher than 90%, while M^1P_1 and Bonf have power not exceeding 15%. We also note that for any pair of fixed s and n , increasing the dimension p could boost the power of our MC-GoF test with F_Σ . In contrast, both M^1P_1 and Bonf lose power when the dimension p increases from 20 to 120. This indicates that our proposed method is more applicable to high-dimensional problems than existing methods.

Table 4: Power of various GoF tests on band graphs ($K = 6, K_0 = 1$) at the significance level $\alpha = 0.05$. The first two columns correspond to the baseline methods and the last four columns correspond to the MC-GoF test with four test statistic functions. Standard errors are in parentheses and the highest power in each case is in bold type.

p	s	n	Method					
			M^1P_1	Bonf	PRC	ERC	F_Σ	GLR- ℓ_1
20	0.1	20	0.050 (.011)	0.033 (.009)	0.062 (.012)	0.060 (.012)	0.098 (.015)	0.085 (.014)
		40	0.058 (.012)	0.083 (.014)	0.217 (.021)	0.190 (.020)	0.212 (.020)	0.165 (.019)
		80	0.098 (.015)	0.170 (.019)	0.542 (.025)	0.517 (.025)	0.510 (.025)	0.352 (.024)
	0.15	20	0.052 (.011)	0.065 (.012)	0.125 (.017)	0.115 (.016)	0.133 (.017)	0.135 (.017)
		40	0.083 (.014)	0.138 (.017)	0.490 (.025)	0.465 (.025)	0.532 (.025)	0.365 (.024)
		80	0.182 (.019)	0.280 (.022)	0.960 (.010)	0.948 (.011)	0.958 (.010)	0.810 (.020)
	0.2	20	0.075 (.013)	0.080 (.014)	0.265 (.022)	0.207 (.020)	0.395 (.024)	0.273 (.022)
		40	0.195 (.020)	0.268 (.022)	0.875 (.017)	0.815 (.019)	0.910 (.014)	0.752 (.022)
		80	0.497 (.025)	0.642 (.024)	1.000 (.000)	1.000 (.000)	1.000 (.000)	0.995 (.004)
120	0.1	20	0.055 (.011)	0.055 (.011)	0.125 (.017)	0.128 (.017)	0.115 (.016)	0.070 (.013)
		40	0.062 (.012)	0.055 (.011)	0.225 (.021)	0.215 (.021)	0.260 (.022)	0.160 (.018)
		80	0.055 (.011)	0.085 (.014)	0.723 (.022)	0.685 (.023)	0.705 (.023)	0.370 (.024)
	0.15	20	0.062 (.012)	0.060 (.012)	0.185 (.019)	0.172 (.019)	0.247 (.022)	0.160 (.018)
		40	0.060 (.012)	0.098 (.015)	0.647 (.024)	0.593 (.025)	0.725 (.022)	0.427 (.025)
		80	0.085 (.014)	0.147 (.018)	0.995 (.004)	0.988 (.006)	0.993 (.004)	0.932 (.013)
	0.2	20	0.075 (.013)	0.083 (.014)	0.487 (.025)	0.345 (.024)	0.695 (.023)	0.492 (.025)
		40	0.113 (.016)	0.125 (.017)	0.995 (.004)	0.955 (.010)	1.000 (.000)	0.975 (.008)
		80	0.435 (.025)	0.525 (.025)	1.000 (.000)	1.000 (.000)	1.000 (.000)	1.000 (.000)

Table 5 shows the results for hub graphs. The dimension p is either 20 or 120, the sample size n takes value among 20, 40, and 80, and the noise level ξ among 0.9, 1.4, and 2. A larger value of ξ corresponds to a weaker deviation from the null hypothesis. We observe that F_Σ and GLR- ℓ_1 achieve the highest power across all settings. In general, the performance of GLR- ℓ_1 tends to be better than F_Σ with a large value of n or a small value of ξ . Again, all our methods outperform the existing methods in every case, especially when the dimension $p = 120$. In particular, when $p = 120$, $n = 80$ and $\xi = 2$, the power of either M^1P_1 or Bonf is around 20% whereas our MC-GoF test using either F_Σ or GLR- ℓ_1 could achieve power as high as 70%.

Table 6 presents the results for Erdős–Rényi–Gilbert random graphs. We vary the connection probability q of the true graph G between 0.2 and 0.4, and s between 0.01 and 0.02. The dimension p is either 40 or 120 and the sample size n is either 50 or 100. We observe that F_Σ performs consistently the best across all settings. In the high-dimensional cases, GLR- ℓ_1 has the second best power, with a significant advantage over the rest four tests. Both tests become more powerful when the dimension p increases from 40 to 120. In contrast, the baseline methods M^1P_1 and Bonf suffer from a loss of power in the high-dimensional cases. Notably, when $p = 120$, $q = 0.4$, $s = 0.01$, and $n = 50$, the power of F_Σ is as high as 94% while M^1P_1 and

Table 5: Power of various GoF tests on hub graphs ($\alpha = 0.05$).

p	ξ	n	Method					
			M^1P_1	Bonf	PRC	ERC	F_Σ	GLR- ℓ_1
20	2	20	0.043 (.010)	0.070 (.013)	0.120 (.016)	0.117 (.016)	0.138 (.017)	0.128 (.017)
		40	0.102 (.015)	0.130 (.017)	0.240 (.021)	0.225 (.021)	0.305 (.023)	0.295 (.023)
		80	0.265 (.022)	0.280 (.022)	0.542 (.025)	0.542 (.025)	0.665 (.024)	0.660 (.024)
	1.4	20	0.077 (.013)	0.092 (.015)	0.163 (.018)	0.150 (.018)	0.193 (.020)	0.182 (.019)
		40	0.142 (.017)	0.163 (.018)	0.335 (.024)	0.318 (.023)	0.455 (.025)	0.463 (.025)
		80	0.490 (.025)	0.472 (.025)	0.787 (.020)	0.792 (.020)	0.873 (.017)	0.897 (.015)
	0.9	20	0.085 (.014)	0.095 (.015)	0.205 (.020)	0.185 (.019)	0.302 (.023)	0.315 (.023)
		40	0.333 (.024)	0.305 (.023)	0.603 (.024)	0.578 (.025)	0.770 (.021)	0.772 (.021)
		80	0.855 (.018)	0.765 (.021)	0.943 (.012)	0.938 (.012)	0.995 (.004)	0.995 (.004)
120	2	20	0.037 (.010)	0.048 (.011)	0.090 (.014)	0.095 (.015)	0.115 (.016)	0.105 (.015)
		40	0.065 (.012)	0.062 (.012)	0.215 (.021)	0.212 (.020)	0.292 (.023)	0.255 (.022)
		80	0.203 (.020)	0.212 (.020)	0.603 (.024)	0.580 (.025)	0.700 (.023)	0.782 (.021)
	1.4	20	0.045 (.010)	0.048 (.011)	0.128 (.017)	0.120 (.016)	0.190 (.020)	0.170 (.019)
		40	0.102 (.015)	0.085 (.014)	0.365 (.024)	0.357 (.024)	0.472 (.025)	0.500 (.025)
		80	0.427 (.025)	0.407 (.025)	0.853 (.018)	0.840 (.018)	0.930 (.013)	0.993 (.004)
	0.9	20	0.060 (.012)	0.065 (.012)	0.200 (.020)	0.198 (.020)	0.335 (.024)	0.352 (.024)
		40	0.177 (.019)	0.135 (.017)	0.672 (.023)	0.652 (.024)	0.860 (.017)	0.900 (.015)
		80	0.897 (.015)	0.748 (.022)	0.988 (.006)	0.985 (.006)	1.000 (.000)	1.000 (.000)

Bonf have power lower than 10%.

Table 6: Power of various GoF tests on Erdős–Rényi–Gilbertrandom graphs ($\alpha = 0.05$).

p	q	s	n	Method						
				M^1P_1	Bonf	PRC	ERC	F_Σ	GLR- ℓ_1	
40	0.2	0.01	50	0.075 (.013)	0.095 (.015)	0.245 (.022)	0.215 (.021)	0.323 (.023)	0.312 (.023)	
			100	0.165 (.019)	0.190 (.020)	0.677 (.023)	0.670 (.024)	0.797 (.020)	0.713 (.023)	
		0.02	50	0.180 (.019)	0.155 (.018)	0.550 (.025)	0.500 (.025)	0.800 (.020)	0.740 (.022)	
			100	0.485 (.025)	0.453 (.025)	0.985 (.006)	0.983 (.007)	1.000 (.000)	0.998 (.002)	
		0.4	0.01	50	0.107 (.016)	0.113 (.016)	0.492 (.025)	0.497 (.025)	0.715 (.023)	0.532 (.025)
				100	0.220 (.021)	0.245 (.022)	0.973 (.008)	0.965 (.009)	0.995 (.004)	0.970 (.009)
	0.02	50	50	0.180 (.019)	0.205 (.020)	0.940 (.012)	0.912 (.014)	0.988 (.006)	0.963 (.010)	
			100	0.578 (.025)	0.560 (.025)	1.000 (.000)	1.000 (.000)	1.000 (.000)	1.000 (.000)	
	120	0.2	0.01	50	0.070 (.013)	0.055 (.011)	0.230 (.021)	0.182 (.019)	0.613 (.024)	0.445 (.025)
				100	0.107 (.016)	0.092 (.015)	0.863 (.017)	0.818 (.019)	0.998 (.002)	0.953 (.011)
			0.02	50	0.090 (.014)	0.065 (.012)	0.492 (.025)	0.310 (.023)	0.965 (.009)	0.907 (.015)
		100		0.265 (.022)	0.190 (.020)	0.995 (.004)	0.985 (.006)	1.000 (.000)	1.000 (.000)	
0.4		0.01	50	0.080 (.014)	0.075 (.013)	0.530 (.025)	0.355 (.024)	0.938 (.012)	0.755 (.022)	
			100	0.138 (.017)	0.163 (.018)	1.000 (.000)	1.000 (.000)	1.000 (.000)	1.000 (.000)	
0.02	50	50	0.133 (.017)	0.100 (.015)	0.885 (.016)	0.677 (.023)	1.000 (.000)	0.998 (.002)		
		100	0.282 (.023)	0.260 (.022)	1.000 (.000)	1.000 (.000)	1.000 (.000)	1.000 (.000)		

For each graph type, we identified specific situations where the baseline methods, M^1P_1 and Bonf, perform poorly while our method could achieve high power. These situations occur when the true precision matrix has many nonzero entries that are absent from the null model and the magnitudes of these entries are not large enough for M^1P_1 or Bonf to reject the null hypothesis. In our experiments, we control

these magnitudes using the parameter s in band graphs and Erdős–Rényi–Gilbertrandom graphs, and the inverse of ξ in hub graphs. We refer to this pattern of deviation from the null model as *dense-but-weak* pattern. Conversely, the *strong-but-sparse* pattern occurs when the null model only misses a few entries of the precision matrix, but these entries are large enough for the baseline methods to reject the null hypothesis. Additional simulations in Appendix F.3 confirm that our tests remain competitive and powerful in situations where the strong-but-sparse pattern occurs.

By comparing these two empirical patterns to the theoretical regimes identified in Section 4 of the main paper, we see a clear alignment between practice and theory. The theoretical results on the rate-optimality predict that the MC-GoF test is powerful when the signal pattern is either *dense but weak* or *strong but sparse*, which is confirmed by the empirical studies. Although our theoretical framework in Section 4 focuses on clique-star-shaped graphs, the insights gained from the theory extend to a broader range of graph structures.

In summary, the MC-GoF test achieves higher power than the baseline methods when the signal pattern is dense and weak, and it remains competitive with the M^1P_1 procedure when the signal pattern is strong but sparse. Across all the studied settings, the MC-GoF test with the F_Σ statistic consistently has superior power performance and is thus a promising method for GoF testing in high-dimensional GGMs.

D.4 Performance of M^1P_2 in Verzelen and Villers [2009]

In this section, we evaluate the power properties of the M^1P_2 procedure introduced by Verzelen and Villers [2009]. This analysis complements the discussion in Remark 3, where we highlighted the marginal power improvement of M^1P_2 over M^1P_1 and its computational limitations.

We conducted simulations using the same data-generating process and null hypotheses for the band graphs introduced in Section 5 of the main text. In addition to the methods considered in the main text, we include M^1P_2 in this analysis. For the M^1P_2 procedure, we computed the α_i -quantile as described in Equation (B.18) for each variable i using 2400 Monte Carlo replications (compared to 1000 in the numerical studies of Verzelen and Villers [2009]).

Table 7 extends Table 2 by including the estimated sizes for the M^1P_2 procedure, and Table 8 extends Table 4 to present the power of M^1P_2 . As noted in Remark 3, the power of M^1P_2 is close to that of M^1P_1 across all scenarios, and they are both less competitive compared to the MC-GoF tests. We conclude that the MC-GoF test remains the preferred method in scenarios where the signal pattern is the dense but weak.

Furthermore, a critical limitation of the M^1P_2 procedure is its substantial computational burden. The method relies on Monte Carlo simulations to compute the α_i -quantile, which is computationally intensive, particularly in high-dimensional settings. This results in a total computation time that is significantly higher than that of other methods. As the method does not provide sufficient practical benefits to justify its significant computational demands, we have opted not to include the M^1P_2 procedure in further experimental comparisons.

E Proofs

This section provides the omitted proofs for the theoretical results in the main paper.

E.1 Proofs in Section 2.1

Proposition 1 is based on the following two lemmas, whose proof is given latter

Lemma 1. *Suppose three random elements X , Y , and Z satisfy that conditional on Z , X , and Y are independent and identically distributed. Then for any bounded Borel function g defined on the range of X , it holds that $\mathbf{E}(g(X) | Y, Z) = \mathbf{E}(g(Y) | X, Z)$.*

p	s	n	Method						
			M^1P_1	M^1P_2	Bonf	PRC	ERC	F_Σ	GLR- ℓ_1
20	0.2	20	0.037 (.977)	0.040 (.944)	0.000 (1.000)	0.053 (.298)	0.045 (.787)	0.049 (.553)	0.049 (.553)
		40	0.053 (.298)	0.031 (.999)	0.054 (.254)	0.060 (.056)	0.051 (.447)	0.055 (.213)	0.052 (.396)
		80	0.044 (.823)	0.047 (.702)	0.046 (.746)	0.052 (.396)	0.052 (.396)	0.050 (.500)	0.061 (.043)
120	0.2	20	0.051 (.447)	0.044 (.823)	0.000 (1.000)	0.043 (.883)	0.059 (.073)	0.060 (.056)	0.047 (.702)
		40	0.047 (.702)	0.036 (.988)	0.040 (.944)	0.041 (.927)	0.046 (.746)	0.049 (.553)	0.043 (.855)
		80	0.048 (.604)	0.043 (.883)	0.043 (.855)	0.044 (.823)	0.032 (.998)	0.042 (.907)	0.052 (.346)

Table 7: Estimated sizes of various GoF tests, including the M^1P_2 procedure, at the significance level $\alpha = 0.05$ on band graphs ($K = 6, K_0 = 6$). The p-value of the one-sample proportion test for each size is provided in parentheses.

p	s	n	Method						
			M^1P_1	M^1P_2	Bonf	PRC	ERC	F_Σ	GLR- ℓ_1
20	0.1	20	0.050 (.011)	0.058 (.012)	0.033 (.009)	0.062 (.012)	0.060 (.012)	0.098 (.015)	0.085 (.014)
		40	0.058 (.012)	0.055 (.011)	0.083 (.014)	0.217 (.021)	0.190 (.020)	0.212 (.020)	0.165 (.019)
		80	0.098 (.015)	0.093 (.014)	0.170 (.019)	0.542 (.025)	0.517 (.025)	0.510 (.025)	0.352 (.024)
	0.15	20	0.052 (.011)	0.030 (.009)	0.065 (.012)	0.125 (.017)	0.115 (.016)	0.133 (.017)	0.135 (.017)
		40	0.083 (.014)	0.078 (.013)	0.138 (.017)	0.490 (.025)	0.465 (.025)	0.532 (.025)	0.365 (.024)
		80	0.182 (.019)	0.240 (.021)	0.280 (.022)	0.960 (.010)	0.948 (.011)	0.958 (.010)	0.810 (.020)
	0.2	20	0.075 (.013)	0.063 (.012)	0.080 (.014)	0.265 (.022)	0.207 (.020)	0.395 (.024)	0.273 (.022)
		40	0.195 (.020)	0.195 (.020)	0.268 (.022)	0.875 (.017)	0.815 (.019)	0.910 (.014)	0.752 (.022)
		80	0.497 (.025)	0.475 (.025)	0.642 (.024)	1.000 (.000)	1.000 (.000)	1.000 (.000)	0.995 (.004)
120	0.1	20	0.055 (.011)	0.053 (.011)	0.055 (.011)	0.125 (.017)	0.128 (.017)	0.115 (.016)	0.070 (.013)
		40	0.062 (.012)	0.045 (.010)	0.055 (.011)	0.225 (.021)	0.215 (.021)	0.260 (.022)	0.160 (.018)
		80	0.055 (.011)	0.050 (.011)	0.085 (.014)	0.723 (.022)	0.685 (.023)	0.705 (.023)	0.370 (.024)
	0.15	20	0.062 (.012)	0.048 (.011)	0.060 (.012)	0.185 (.019)	0.172 (.019)	0.247 (.022)	0.160 (.018)
		40	0.060 (.012)	0.035 (.009)	0.098 (.015)	0.647 (.024)	0.593 (.025)	0.725 (.022)	0.427 (.025)
		80	0.085 (.014)	0.073 (.013)	0.147 (.018)	0.995 (.004)	0.988 (.006)	0.993 (.004)	0.932 (.013)
	0.2	20	0.075 (.013)	0.060 (.012)	0.083 (.014)	0.487 (.025)	0.345 (.024)	0.695 (.023)	0.492 (.025)
		40	0.113 (.016)	0.095 (.015)	0.125 (.017)	0.995 (.004)	0.955 (.010)	1.000 (.000)	0.975 (.008)
		80	0.435 (.025)	0.358 (.024)	0.525 (.025)	1.000 (.000)	1.000 (.000)	1.000 (.000)	1.000 (.000)

Table 8: Power of various GoF tests, including the M^1P_2 procedure, on band graphs ($K = 6, K_0 = 1$) at the significance level $\alpha = 0.05$. See the caption of Table 4 for details on methods.

Lemma 2. For any given $i \in [p]$, the distribution of the output $\tilde{\mathbf{X}}_i$ from Algorithm 1 is the uniform distribution on

$$\{\mathbf{x}_i \in \mathbb{R}^n : \mathbf{x}_i^\top \mathbf{1}_n = \mathbf{X}_i^\top \mathbf{1}_n, \mathbf{x}_i^\top \mathbf{x}_i = \mathbf{X}_i^\top \mathbf{X}_i, \mathbf{x}_i^\top \mathbf{X}_j = \mathbf{X}_i^\top \mathbf{X}_j, \forall j \in N_i\}. \quad (\text{E.1})$$

It is straightforward to see that the set in (E.1) is the same as \mathcal{X}_Ψ^i in (B.3). We can now prove Proposition 1 as follows.

Proof of Proposition 1. Lemma 2 shows that both \mathbf{X}_i and $\tilde{\mathbf{X}}_i$ lie on \mathcal{X}_Ψ^i , and thus $\psi_G(\mathbf{X}) = \psi_G(\tilde{\mathbf{X}})$.

We have argued that the conditional distribution of \mathbf{X}_i given (\mathbf{X}_{-i}, Ψ) is the uniform distribution on \mathcal{X}_Ψ^i defined in (B.3). In addition, when $\tilde{\mathbf{X}}_i$ is generated, it only uses the information about (\mathbf{X}_{-i}, Ψ) . Therefore, Lemma 2 implies that conditioning on (\mathbf{X}_{-i}, Ψ) , the output column $\tilde{\mathbf{X}}_i$ and the input column \mathbf{X}_i are independent and they follow the same distribution. We can then apply Lemma 1 to conclude that the conditional distribution of $\tilde{\mathbf{X}}_i \mid (\mathbf{X}_i, \mathbf{X}_{-i}, \Psi)$ is almost surely the same as that of $\mathbf{X}_i \mid (\tilde{\mathbf{X}}_i, \mathbf{X}_{-i}, \Psi)$. By definition of $\tilde{\mathbf{X}}$, we proved the desired statement. \square

Proof of Lemma 2. We only need to show that if the rows of \mathbf{X} are i.i.d. samples from a distribution in \mathcal{M}_G , then conditional on (\mathbf{X}_{-i}, Ψ) , the observed data \mathbf{X}_i and the output $\tilde{\mathbf{X}}_i$ share the same conditional distribution.

By properties of multivariate normal distribution, the conditional distribution of \mathbf{X}_i given \mathbf{X}_{-i} is $\mathcal{N}_n(\mu_i \mathbf{1} + \mathbf{X}_{N_i} \boldsymbol{\alpha}, \boldsymbol{\Omega}_{i,i}^{-1} \mathbf{I}_n)$ for some $|N_i|$ -dimensional parameter $\boldsymbol{\alpha}$ that depends on $\boldsymbol{\Omega}$.

Without loss of generality, we would assume in the following that $[\mathbf{1}, \mathbf{X}_{N_i}]$ has full column rank and $n > 1 + |N_i|$. The first statement here is guaranteed to hold with probability 1 because of the continuity of the Gaussian measure. If $n \leq 1 + |N_i|$, it is clear that the output $\tilde{\mathbf{X}}_i = \mathbf{X}_i$ because the residual of the linear regression is zero.

In the following, we condition on \mathbf{X}_{-i} . Let $\mathbf{U} \in \mathbb{R}^{n \times (1+|N_i|)}$ be a matrix whose columns are an orthonormal basis of the column space of $[\mathbf{1}, \mathbf{X}_{N_i}]$. Let $l_i = n - 1 - |N_i|$ and $\mathbf{V} \in \mathbb{R}^{n \times l_i}$ be a matrix such that $\mathbf{V}^\top \mathbf{U} = \mathbf{0}$ and $\mathbf{V}^\top \mathbf{V} = \mathbf{I}_{l_i}$. By properties of least squares estimation, the fitted vector in Step 2 of Algorithm 1 satisfies that $\mathbf{F} = \mathbf{U} \mathbf{U}^\top \mathbf{X}_i$ and the residual vector satisfies that $\mathbf{R} = \mathbf{V} \mathbf{V}^\top \mathbf{X}_i$. We also have $\mathbf{X}_i = \mathbf{F} + \mathbf{R}$. By properties of Gaussian linear regression models, the following statements hold:

1. \mathbf{F} can be expressed by \mathbf{X}_{-i} and Ψ ;
2. the distribution of $\mathbf{V}^\top \mathbf{X}_i$ is $\mathcal{N}_{l_i}(\mathbf{0}, \boldsymbol{\Omega}_{i,i}^{-1} \mathbf{I}_{l_i})$.

By the statement 1 and the fact that Ψ contains $\mathbf{X}_i^\top \mathbf{X}_i$, we can write $\|\mathbf{V}^\top \mathbf{X}_i\|^2 = \|\mathbf{R}\|^2 = \|\mathbf{X}_i\|^2 - \|\mathbf{F}\|^2$ as a function of \mathbf{X}_{-i} and Ψ .

By the statement 2, $\mathbf{V}^\top \mathbf{X}_i / \|\mathbf{R}\|$ follows the uniform distribution on \mathbb{S}^{l_i-1} , the unit sphere in \mathbb{R}^{l_i} . By Basu's theorem and the properties of exponential families of full rank, we can conclude that $\mathbf{V}^\top \mathbf{X}_i / \|\mathbf{R}\|$ and Ψ are conditionally independent given \mathbf{X}_{-i} .

Let \mathbf{E} be the standard normal n -vector draw in Step 3 of Algorithm 1. We can use a similar argument to show that $\mathbf{V}^\top \mathbf{E} / \|\tilde{\mathbf{R}}\|$ also follows the uniform distribution on \mathbb{S}^{l_i-1} . Therefore, $\mathbf{V}^\top \mathbf{X}_i / \|\mathbf{R}\|$ and $\mathbf{V}^\top \mathbf{E} / \|\tilde{\mathbf{R}}\|$ are conditionally i.i.d. given (\mathbf{X}_{-i}, Ψ) . Furthermore, if $l_i = n - 1 - |N_i| \geq 2$, then w.p. 1, $\mathbf{V}^\top \mathbf{X}_i / \|\mathbf{R}\|$ and $\mathbf{V}^\top \mathbf{E} / \|\tilde{\mathbf{R}}\|$ are different.

Conditional on (\mathbf{X}_{-i}, Ψ) , we have

$$\begin{aligned} \mathbf{X}_i &= \mathbf{F} + \mathbf{R} \\ &= \mathbf{F} + \|\mathbf{R}\| \mathbf{V} \left(\mathbf{V}^\top \mathbf{X}_i / \|\mathbf{R}\| \right) \\ &\stackrel{d.}{=} \mathbf{F} + \|\mathbf{R}\| \mathbf{V} \left(\mathbf{V}^\top \mathbf{E} / \|\tilde{\mathbf{R}}\| \right) \\ &= \mathbf{F} + \frac{\|\mathbf{R}\|}{\|\tilde{\mathbf{R}}\|} \tilde{\mathbf{R}} \\ &= \tilde{\mathbf{X}}_i, \end{aligned}$$

and $\mathbf{X}_i \neq \tilde{\mathbf{X}}_i$ w.p. 1 if $l_i \geq 2$. This completes the proof. \square

Proof of Lemma 1. It is straightforward to see that

$$\begin{aligned} \mathbf{E}(g(X) | Y, Z) &= \mathbf{E}(g(X) | Z) \\ &= \mathbf{E}(g(Y) | Z) \\ &= \mathbf{E}(g(Y) | X, Z), \text{ a.s.} \end{aligned}$$

where the first and last equations are due to the conditional independence between X and Y , and the second one is due to the identical conditional distribution. \square

E.2 Proofs in Section 2.2

Proof of Proposition 2. Denote by P the distribution of the input \mathbf{X} , by \mathcal{C}_0 the (time-inhomogeneous) Markov chain from \mathbf{X} to the hub $\mathbf{X}^{(hub)}$, by $K_i(\mathbf{x}, \mathbf{y})$ the transition kernel of \mathcal{C}_0 at the i -th step, and by $\overleftarrow{\mathcal{C}}_0$ the time-reversed chain of \mathcal{C}_0 .

By Proposition 1, $K_i(\mathbf{x}, \mathbf{y})$ is either 0 or $K_i(\mathbf{x}, \mathbf{y}) = K_i(\mathbf{y}, \mathbf{x})$ with $\psi_G(\mathbf{x}) = \psi_G(\mathbf{y})$. If $P \in \mathcal{M}_G$, we can conclude that

$$f_{\mu, \Omega}(\mathbf{x})K_i(\mathbf{x}, \mathbf{y}) = f_{\mu, \Omega}(\mathbf{y})K_i(\mathbf{y}, \mathbf{x}), \quad \forall \mathbf{x}, \mathbf{y} \in \mathbb{R}^{n \times p}.$$

This means that P satisfies the detailed balance for Markov chain \mathcal{C}_0 . As a result, the end point of \mathcal{C}_0 (i.e. $\mathbf{X}^{(hub)}$) follows the distribution P and K_i is the transition kernel of the reversed chain $\overleftarrow{\mathcal{C}}_0$ at the $(L|\mathcal{Z}| - i + 1)$ -th step.

Consider the Markov chain $\overleftarrow{\mathcal{C}}_m$ that starts from the hub $\mathbf{X}^{(hub)}$ and ends at a generated $\tilde{\mathbf{X}}^{(m)}$ in Step 2 of Algorithm 2. By the procedure of the algorithm and the property of the transition kernel K_i we proved above, $\overleftarrow{\mathcal{C}}_m$ follows the same distribution as $\overleftarrow{\mathcal{C}}_0$.

Furthermore, when conditioning on the initial point $\mathbf{X}^{(hub)}$, the Markov chains $\overleftarrow{\mathcal{C}}_m$ ($m = 0, 1, \dots, M$) are mutually independent. Therefore, $\overleftarrow{\mathcal{C}}_m$ ($m = 0, 1, \dots, M$) are i.i.d. conditional on $\mathbf{X}^{(hub)}$. As a result, the endpoints of these chains are conditionally exchangeable given $\mathbf{X}^{(hub)}$, which can be expressed as follows: for any permutation π of $(m + 1)$ elements and any $(m + 1)$ -variate integral function g , it holds that

$$\mathbf{E} \left[g(\mathbf{X}, \tilde{\mathbf{X}}_1, \dots, \tilde{\mathbf{X}}^{(M)}) | \mathbf{X}^{(hub)} \right] = \mathbf{E} \left[g \circ \pi(\mathbf{X}, \tilde{\mathbf{X}}_1, \dots, \tilde{\mathbf{X}}^{(M)}) | \mathbf{X}^{(hub)} \right], \text{ a.s.} \quad (\text{E.2})$$

Taking the expectation on both sides of Equation (E.2), we conclude that $\mathbf{X}, \tilde{\mathbf{X}}_1, \dots, \tilde{\mathbf{X}}^{(M)}$ are exchangeable.

To prove the second statement, we point out that the coordinates in \mathcal{T}^c remain still during the generation, so $\mathbf{X}_{-\mathcal{T}} = \mathbf{X}_{-\mathcal{T}}^{(hub)} = \tilde{\mathbf{X}}_{-\mathcal{T}}^{(m)}$. We then take the conditional expectation given $\mathbf{X}_{-\mathcal{T}}^{(hub)}$ on both sides of Equation (E.2), which implies the conditional exchangeability as desired. \square

E.3 Validity of the MC-GoF Test

Throughout this section, we simplify the notation $T(\mathbf{X}), T(\tilde{\mathbf{X}}^{(1)}), T(\tilde{\mathbf{X}}^{(2)}), \dots, T(\tilde{\mathbf{X}}^{(M)})$ as $T_0, T_1, T_2, \dots, T_M$.

By Proposition 2, $\mathbf{X}, \tilde{\mathbf{X}}^{(1)}, \tilde{\mathbf{X}}^{(2)}, \dots, \tilde{\mathbf{X}}^{(M)}$ are exchangeable. Therefore, $T_0, T_1, T_2, \dots, T_M$ are exchangeable. This already guarantees the validity of the p-value of Algorithm 3 as stated in Proposition 3 using classic results in statistical inference; see for example [Lehmann and Romano, 2022, Chapter 15.2.1]. For completeness, we prove the validity of the p-values mentioned in Appendix B.3.1.

In the proof, S is a random integer between 1 and $1 + \sum_{m=1}^M \mathbb{I}(T_m = T_0)$.

We use V_1, V_2, \dots, V_K to denote the unique values of T_0, T_1, \dots, T_M sorted in descending order. Let n_1, n_2, \dots, n_K be the respective frequencies of these values. The following two conditions hold:

1. $n_i \geq 1$ for all i
2. $\sum_{i=1}^K n_i = 1 + M$

Denote by $\tilde{\mathbf{P}}(\cdot) = \mathbf{P}(\cdot \mid V_1, \dots, V_K, n_1, \dots, n_K)$ the conditional probability of T_0 being equal to V_j given all distinct values and their frequencies. By exchangeability of T_m 's, it holds that

$$\tilde{\mathbf{P}}(T_0 = V_j) = \frac{n_j}{1 + M}, \quad j = 1, 2, \dots, K.$$

E.3.1 One-sided randomized test

Consider the p-value defined as

$$\text{pVal} = \frac{1}{1 + M} \left(S + \sum_{m=1}^M \mathbb{I}(T_m > T_0) \right).$$

For $\alpha \in (0, 1)$, suppose E is an integer between 1 and K such that

$$\sum_{i=1}^{E-1} n_i < \alpha(1 + M) \leq \sum_{i=1}^E n_i,$$

where the $\sum_{i=1}^0$ is regarded as 0 when E is 1. We have

$$\begin{aligned} \tilde{\mathbf{P}}(\text{reject } H_0) &= \tilde{\mathbf{P}} \left(S + \sum_{m=1}^M \mathbb{I}(T_m > T_0) \leq \alpha(1 + M) \right) \\ &= \tilde{\mathbf{P}} \left(S \leq \alpha(1 + M) - \sum_{m=1}^M \mathbb{I}(T_m > T_0) \right). \end{aligned}$$

We further condition on the event that $T_0 = V_k$ for any $k \in [K]$, so that

$$\begin{aligned} &\tilde{\mathbf{P}} \left(S \leq \alpha(1 + M) - \sum_{m=1}^M \mathbb{I}(T_m > T_0) \mid T_0 = V_k \right) \\ &= \begin{cases} 1, & \text{when } k = 1, \dots, E-1, \\ \frac{\lfloor \alpha(1+M) \rfloor - \sum_{j=1}^{E-1} n_j}{n_E}, & \text{when } k = E, \\ 0, & \text{when } k = E+1, \dots, K. \end{cases} \end{aligned}$$

Therefore, we can compute the rejection probability as follows:

$$\begin{aligned} \tilde{\mathbf{P}}(\text{reject } H_0) &= \sum_{k=1}^K \tilde{\mathbf{P}} \left(S \leq \alpha(1 + M) - \sum_{m=1}^M \mathbb{I}(T_m > T_0), T_0 = V_k \right) \\ &= \sum_{j=1}^K \frac{n_k}{1 + M} \tilde{\mathbf{P}} \left(S \leq \alpha(1 + M) - \sum_{m=1}^M \mathbb{I}(T_m > T_0) \mid T_0 = V_k \right) \\ &= (1 + M)^{-1} \left(\sum_{k=1}^{E-1} n_k + \lfloor \alpha(1 + M) \rfloor - \sum_{j=1}^{E-1} n_j \right) \\ &= (1 + M)^{-1} \lfloor \alpha(1 + M) \rfloor \\ &\leq \alpha. \end{aligned}$$

This proves the validity of the randomized p-value defined in Remark B.3.1.

E.3.2 Two-sided randomized p-value

The two-sided p-value is defined as

$$\frac{2}{1+M} \left[S + \min \left(\sum_{m=1}^M I \{T_m > T_0\}, \sum_{m=1}^M I \{T_m < T_0\} \right) \right].$$

For $\alpha \in (0, 1)$, suppose E and F are two integers between 1 and K such that

$$\begin{aligned} \sum_{i=1}^{E-1} n_i &< \frac{\alpha}{2}(1+M) \leq \sum_{i=1}^E n_i, \\ \sum_{i=F+1}^K n_i &< \frac{\alpha}{2}(1+M) \leq \sum_{i=F}^K n_i, \end{aligned}$$

where the $\sum_{i=1}^0$ is regarded as 0 when E is 1 and the $\sum_{i=K+1}^K$ is regarded as 0 when $F = K$. Summing up the left-hand sides of the two inequalities, we have $\sum_{i=1}^{E-1} n_i + \sum_{i=F+1}^K n_i < \alpha(1+M) < (1+M) = \sum_{i=1}^K n_i$. So $E \leq F$.

We have

$$\tilde{\mathbf{P}}(\text{reject } H_0) = \tilde{\mathbf{P}} \left(S + \min \left(\sum_{m=1}^M I \{T_m > T_0\}, \sum_{m=1}^M I \{T_m < T_0\} \right) \leq \frac{\alpha}{2}(1+M) \right).$$

We first consider the case where $E < F$. If we further condition on $T_0 = V_k$ for any $k \in [K]$, we have

$$\begin{aligned} &\tilde{\mathbf{P}} \left(S + \min \left(\sum_{m=1}^M I \{T_m > T_0\}, \sum_{m=1}^M I \{T_m < T_0\} \right) \leq \frac{\alpha}{2}(1+M) \right) \\ &= \begin{cases} 1, & \text{when } k = 1, \dots, E-1, \\ \frac{[\alpha(1+M)/2] - \sum_{j=1}^{E-1} n_j}{n_E}, & \text{when } k = E, \\ 0, & \text{when } k = E+1, \dots, F-1, \\ \frac{[\alpha(1+M)/2] - \sum_{j=F+1}^K n_j}{n_F}, & \text{when } k = F, \\ 1, & \text{when } k = F+1, \dots, K. \end{cases} \end{aligned}$$

Therefore, we can compute the rejection probability as follows:

$$\begin{aligned} &\tilde{\mathbf{P}}(\text{reject } H_0) \\ &= \sum_{k=1}^K \tilde{\mathbf{P}} \left(S \leq \frac{\alpha}{2}(1+M) - \min \left(\sum_{m=1}^M I \{T_m > T_0\}, \sum_{m=1}^M I \{T_m < T_0\} \right), T_0 = V_k \right) \\ &= \sum_{j=1}^K \frac{n_k}{1+M} \tilde{\mathbf{P}} \left(S \leq \frac{\alpha}{2}(1+M) - \min \left(\sum_{m=1}^M I \{T_m > T_0\}, \sum_{m=1}^M I \{T_m < T_0\} \right) \mid T_0 = V_k \right) \\ &= (1+M)^{-1} \left(\sum_{k=1}^{E-1} n_k + [\alpha(1+M)/2] - \sum_{j=1}^{E-1} n_j + [\alpha(1+M)/2] - \sum_{j=F+1}^K n_j + \sum_{k=F+1}^K n_k \right) \\ &= (1+M)^{-1} 2[\alpha(1+M)/2] \\ &\leq \alpha. \end{aligned}$$

Next, we consider the case where $E = F$. We have

$$\begin{aligned} & \tilde{\mathbf{P}} \left(S + \min \left(\sum_{m=1}^M I \{T_m > T_0\}, \sum_{m=1}^M I \{T_m < T_0\} \right) \leq \frac{\alpha}{2}(1+M) \right) \\ &= \begin{cases} 1, & \text{when } k = 1, \dots, E-1, \\ \frac{[\alpha(1+M)/2] - \min(\sum_{j=1}^{E-1} n_j, \sum_{j=F+1}^K n_j)}{n_E}, & \text{when } k = E = F, \\ 1, & \text{when } k = F+1, \dots, K. \end{cases} \end{aligned}$$

Similar to the previous case, the rejection probability can be computed as follows:

$$\begin{aligned} \tilde{\mathbf{P}}(\text{reject } H_0) &= \sum_{j=1}^K \frac{n_k}{1+M} \tilde{\mathbf{P}} \left(S \leq \frac{\alpha}{2}(1+M) - \min \left(\sum_{m=1}^M I \{T_m > T_0\}, \sum_{m=1}^M I \{T_m < T_0\} \right) \mid T_0 = V_k \right) \\ &= (1+M)^{-1} \left(\sum_{k=1}^{E-1} n_k + [\alpha(1+M)/2] - \min \left(\sum_{j=1}^{E-1} n_j, \sum_{j=F+1}^K n_j \right) + \sum_{k=F+1}^K n_k \right) \\ &= (1+M)^{-1} \left([\alpha(1+M)/2] + \max \left(\sum_{j=1}^{E-1} n_j, \sum_{j=F+1}^K n_j \right) \right) \\ &< (1+M)^{-1} 2[\alpha(1+M)/2] \\ &\leq \alpha, \end{aligned}$$

where the second to last inequality is due to the definition of E and F .

Combining the two cases, we complete the proof of the validity of the randomized two-sided p-value defined in Remark B.3.1.

E.4 Validity of local MC-GoF tests in Section 3.3

In the proof of Proposition 1, we only make use of the neighborhood N_i defined by G (or equivalently, the edges connecting i and any other nodes). Therefore, the result of Proposition 1 still holds for any $i \in \mathcal{T}$ under the hypothesis in (3.1). Since only \mathbf{X}_i with $i \in \mathcal{T}$ will be updated when running Algorithm 2, the same argument in Proposition 2 shows that the generated copies $\tilde{\mathbf{X}}^{(1)}, \dots, \tilde{\mathbf{X}}^{(M)}$ are jointly exchangeable with the input \mathbf{X} under the hypothesis in (3.1). As a result, the p-value computed as in (1.3) remains valid for testing the local graph structure.

E.5 Metric of deviation

Proof of Proposition 4. The equation for $D(\boldsymbol{\Omega}_{\mathcal{C}}, \infty)$ is obvious once we recognize that $\mathbf{R}(\mathbf{A})$ is the correlation matrix of $X_{\mathcal{C}}$ given $X_{\mathcal{H}}$. We focus on the lower bound on $D(\boldsymbol{\Omega}_{\mathcal{C}}, F)$.

Without loss of generality, we rearrange the indices so that $\mathcal{C} = \{1, 2, \dots, q\}$ and $\mathcal{H} = \{q+1, \dots, p\}$. Furthermore, the desired inequality is implied by the following result: Suppose $0 < c_0 \leq \text{var}(X_i \mid X_{\mathcal{H}}) \leq c_1$ and $\|\boldsymbol{\Omega}_{\mathcal{C}}\| \leq c_2$, then it holds that

$$D(\boldsymbol{\Omega}_{\mathcal{C}}, F)^2 \geq \frac{c_0^2}{c_1 c_2} \sum_{i,j \in \mathcal{C}} \boldsymbol{\Omega}_{i,j}^2.$$

Let $\mathbf{A} = \boldsymbol{\Omega}_{\mathcal{C}}^{-1}$ is the conditional covariance matrix of $X_{\mathcal{C}}$ given $X_{\mathcal{H}}$. Let $\mathbf{D} = \text{diag}(\mathbf{A})$ is the diagonal matrix of \mathbf{A} , whose diagonal elements are the conditional variance of X_i ($i \in \mathcal{C}$) given $X_{\mathcal{H}}$. By assumption, we have $c_0 \leq \mathbf{D}_{ii} \leq c_1$.

Define $\mathbf{K} = \mathbf{R}(\mathbf{A}) - \mathbf{I}_q = \mathbf{D}^{-1/2} \mathbf{A} \mathbf{D}^{-1/2} - \mathbf{I}_q$. The diagonal elements of \mathbf{K} are

$$\mathbf{K}_{ii} = \mathbf{D}_{ii}^{-1} \mathbf{A}_{ii} - 1 = 1 - 1 = 0,$$

while the off-diagonal elements are

$$\mathbf{K}_{ij} = \mathbf{D}_{ii}^{-1/2} \mathbf{A}_{ij} \mathbf{D}_{jj}^{-1/2}, \quad \text{for } i \neq j.$$

Since $\mathbf{A} = \mathbf{D}^{1/2}(\mathbf{K} + \mathbf{I}_q)\mathbf{D}^{1/2}$, we have

$$\boldsymbol{\Omega}_{\mathcal{C}} = \mathbf{A}^{-1} = \left(\mathbf{D}^{1/2}(\mathbf{K} + \mathbf{I}_q)\mathbf{D}^{1/2} \right)^{-1} = \mathbf{D}^{-1/2}(\mathbf{K} + \mathbf{I}_q)^{-1}\mathbf{D}^{-1/2}.$$

Therefore, for $i \neq j$, we have

$$\boldsymbol{\Omega}_{i,j} = \mathbf{D}_{ii}^{-1/2} [(\mathbf{K} + \mathbf{I}_q)^{-1}]_{ij} \mathbf{D}_{jj}^{-1/2}.$$

Using the identities $(\mathbf{K} + \mathbf{I}_q)^{-1} - \mathbf{I}_q = -\mathbf{K}(\mathbf{K} + \mathbf{I}_q)^{-1}$ and $(\mathbf{I}_q)_{ij} = 0$, we have:

$$\boldsymbol{\Omega}_{i,j} = -\mathbf{D}_{ii}^{-1/2} [\mathbf{K}(\mathbf{K} + \mathbf{I}_q)^{-1}]_{ij} \mathbf{D}_{jj}^{-1/2}, \quad i \neq j.$$

The sum of squares of $\boldsymbol{\Omega}_{i,j}$ over all pairs of distinct i and j in \mathcal{C} is

$$\begin{aligned} \sum_{i \neq j} (\boldsymbol{\Omega}_{i,j})^2 &= \sum_{i \neq j} \left(\mathbf{D}_{ii}^{-1/2} [-\mathbf{K}(\mathbf{K} + \mathbf{I}_q)^{-1}]_{ij} \mathbf{D}_{jj}^{-1/2} \right)^2 \\ &\leq \|\mathbf{D}^{-1/2} \mathbf{K} (\mathbf{K} + \mathbf{I}_q)^{-1} \mathbf{D}^{-1/2}\|_F^2 \\ &\leq \|\mathbf{D}^{-1/2}\|_F^4 \|(\mathbf{K} + \mathbf{I}_q)^{-1}\|_F^2 \|\mathbf{K}\|_F^2. \end{aligned}$$

Since $D_{ii} \geq c_0$, we have $\|\mathbf{D}^{-1/2}\|_F^4 \leq c_0^{-2}$. By definition, we have $(\mathbf{K} + \mathbf{I}_q)^{-1} = \mathbf{D}^{1/2} \boldsymbol{\Omega}_{\mathcal{C}} \mathbf{D}^{1/2}$. Since $D_{ii} \leq c_1$ and , we have

$$\|(\mathbf{K} + \mathbf{I}_q)^{-1}\|_F^2 \leq \|\mathbf{D}^{1/2}\|_F^2 \|\boldsymbol{\Omega}_{\mathcal{C}}\|_F \leq c_1 c_2,$$

where we have used the assumption that $\|\boldsymbol{\Omega}_{\mathcal{C}}\|_F \leq c_2$. We thus conclude that

$$\sum_{i \neq j} (\boldsymbol{\Omega}_{i,j})^2 \leq \frac{c_1 c_2}{c_0^2} \|\mathbf{K}\|_F^2.$$

By definition, it holds that $\|\mathbf{K}\|_F = D(\boldsymbol{\Omega}_{\mathcal{C}}, F)$ and thus we complete the proof. \square

E.6 Power Guarantee

Recall the assumption that $p > n$, for any $j \in \mathcal{H}$, the size of its neighborhood N_j is larger than or equal to n . Therefore, when running Algorithm 2, the j th column of every generated data matrix remains the same as the observed one. In other words, $\tilde{\mathbf{X}}_{\mathcal{H}}^{(m)} = \mathbf{X}_{\mathcal{H}}$.

Denote by Π_1 the projection matrix onto the column space of the matrix $[\mathbf{1}_n, \mathbf{X}_{\mathcal{H}}]$. Recall that $n \geq 2 + |\mathcal{H}|$, we have the decomposition $\Pi_2 := \mathbf{I}_n - \Pi_1 = \Gamma \Gamma^\top$ where Γ is an orthonormal matrix of dimension $n \times (n - 1 - |\mathcal{H}|)$. Let $\mathbf{W} = \Gamma^\top \mathbf{X}_{\mathcal{C}}$, where $\mathcal{C} = \mathcal{H}^c$. Then we can express the data matrix as

$$\mathbf{X}_{\mathcal{C}} = \Pi_1 \mathbf{X}_{\mathcal{C}} + \Gamma \mathbf{W},$$

and express the partial residual correlation statistics as

$$\hat{\gamma}_{ij} = \frac{(\mathbf{W}_{\cdot,i}^\top \mathbf{W}_{\cdot,j})}{\|\mathbf{W}_{\cdot,i}\|_2 \|\mathbf{W}_{\cdot,j}\|_2} = \left\langle \frac{\mathbf{W}_{\cdot,i}}{\|\mathbf{W}_{\cdot,i}\|_2}, \frac{\mathbf{W}_{\cdot,j}}{\|\mathbf{W}_{\cdot,j}\|_2} \right\rangle, \quad i, j \in \mathcal{C}.$$

For the generated copies, we similarly define $\widetilde{\mathbf{W}}^{(m)} = \Gamma^\top \widetilde{\mathbf{X}}_{\mathcal{C}}^{(m)}$ and express the corresponding partial residual correlations as

$$\tilde{\gamma}_{ij}^{(m)} = \left\langle \frac{\widetilde{\mathbf{W}}_{\cdot,i}^{(m)}}{\|\widetilde{\mathbf{W}}_{\cdot,i}^{(m)}\|_2}, \frac{\widetilde{\mathbf{W}}_{\cdot,j}^{(m)}}{\|\widetilde{\mathbf{W}}_{\cdot,j}^{(m)}\|_2} \right\rangle, \quad i, j \in \mathcal{C}.$$

Our first lemma characterizes the joint distribution of $\{\hat{\gamma}_{ij}, \tilde{\gamma}_{ij}^{(m)} : i, j \in \mathcal{C}, m = 1, \dots, M\}$.

Lemma 3. Consider the notations and assumptions in Section 4. Consider independent random matrices \mathbf{U} and $\tilde{\mathbf{U}}^{(m)}$ ($m = 1, 2, \dots, M$) constructed as follows. \mathbf{U} is a $(n-1-|\mathcal{H}|) \times q$ matrix with i.i.d. rows sampled from $N_q(\mathbf{0}, \mathbf{R}(\boldsymbol{\Omega}_{\mathcal{C}}^{-1}))$, and $\tilde{\mathbf{U}}^{(m)}$ is a $(n-1-|\mathcal{H}|) \times q$ matrix with i.i.d. rows sampled from $N_q(\mathbf{0}, \mathbf{I}_q)$. Then the joint distribution of

$$\left(\frac{\mathbf{W}_{\cdot,i}}{\|\mathbf{W}_{\cdot,i}\|_2} \right)_{i \in \mathcal{C}}, \left(\frac{\tilde{\mathbf{W}}_{\cdot,i}^{(m)}}{\|\tilde{\mathbf{W}}_{\cdot,i}^{(m)}\|_2} \right)_{i \in \mathcal{C}}, m = 1, \dots, M,$$

is the same as the joint distribution of

$$\left(\frac{\mathbf{U}_i}{\|\mathbf{U}_i\|} \right)_{i \leq q}, \left(\frac{\tilde{\mathbf{U}}_i^{(m)}}{\|\tilde{\mathbf{U}}_i^{(m)}\|} \right)_{i \leq q}, m = 1, \dots, M.$$

Furthermore, if $\lambda_{\max}(\boldsymbol{\Omega}_{\mathcal{C}})/\lambda_{\min}(\boldsymbol{\Omega}_{\mathcal{C}}) \leq b_0$, then the spectral norm of $\mathbf{R}(\boldsymbol{\Omega}_{\mathcal{C}}^{-1})$ is bounded by b_0 .

We defer the proof of Lemma 3 in Appendix E.6.4 but discuss the implication. Lemma 3 allows us to analyze the distribution of the statistics $T(\mathbf{X})$ and $T(\tilde{\mathbf{X}}^{(m)})$ using an equivalent version of joint distribution defined using \mathbf{U} and $\tilde{\mathbf{U}}^{(m)}$, provided that if the function $T(\mathbf{x})$ only depends on $\Gamma^\top \mathbf{x}$.

In particular, the distributional equivalence guaranteed by Lemma 3 implies we can represent $\hat{\gamma}_{ij}$ as

$$\hat{\gamma}_{ij} \stackrel{d}{=} \left\langle \frac{\mathbf{U}_i}{\|\mathbf{U}_i\|}, \frac{\mathbf{U}_j}{\|\mathbf{U}_j\|} \right\rangle$$

and similarly for $\tilde{\gamma}_{ij}^{(m)}$ using $\tilde{\mathbf{U}}^{(m)}$. In the following proofs, we abuse the notation $T(\mathbf{U})$ to denote the statistic computed by substituting $\hat{\gamma}_{ij}$ by $\left\langle \frac{\mathbf{U}_i}{\|\mathbf{U}_i\|}, \frac{\mathbf{U}_j}{\|\mathbf{U}_j\|} \right\rangle$ and $T(\tilde{\mathbf{U}}^{(m)})$ to denote the statistic computed by substituting $\hat{\gamma}_{ij}$ by $\left\langle \frac{\tilde{\mathbf{U}}_i^{(m)}}{\|\tilde{\mathbf{U}}_i^{(m)}\|}, \frac{\tilde{\mathbf{U}}_j^{(m)}}{\|\tilde{\mathbf{U}}_j^{(m)}\|} \right\rangle$.

Before we get into the proof, we provide an overview of our strategy.

We will find some constant t depending on the choice of test statistic and we will write

$$\begin{aligned} & \mathbb{P}(\text{Reject } H_0) \tag{E.3} \\ &= \mathbb{P} \left(\frac{1}{M+1} \left[1 + \sum_{m=1}^M \mathbf{1} \{ T(\tilde{\mathbf{U}}^{(m)}) \geq T(\mathbf{U}) \} \right] \leq \alpha \right) \\ &\geq \mathbb{P} \left(T(\mathbf{U}) > t, \frac{1}{M+1} \left[1 + \sum_{m=1}^M \mathbf{1} \{ T(\tilde{\mathbf{U}}^{(m)}) \geq T(\mathbf{U}) \} \right] \leq \alpha \right) \\ &= \mathbb{P}(T(\mathbf{U}) > t) - \mathbb{P} \left(T(\mathbf{U}) > t, \frac{1}{M+1} \left[1 + \sum_{m=1}^M \mathbf{1} \{ T(\tilde{\mathbf{U}}^{(m)}) \geq T(\mathbf{U}) \} \right] > \alpha \right) \\ &\geq \mathbb{P}(T(\mathbf{U}) > t) - \mathbb{P} \left(\frac{1}{M+1} \left[1 + \sum_{m=1}^M \mathbf{1} \{ T(\tilde{\mathbf{U}}^{(m)}) \geq t \} \right] > \alpha \right), \end{aligned}$$

where the last inequality is because if $b > c$ then $\mathbf{1} \{ a \geq b \} \leq \mathbf{1} \{ a \geq c \}$.

Our proof will be dedicated to (1) derive an upper bound on

$$\mathbb{P} \left(\frac{1}{M+1} \left[1 + \sum_{m=1}^M \mathbf{1} \{ T(\tilde{\mathbf{U}}^{(m)}) \geq t \} \right] > \alpha \right), \tag{E.4}$$

and (2) derive a lower bound for $\mathbb{P}(T(\mathbf{U}) > t)$.

The following lemma is useful in the first task.

Lemma 4. *If $M > 2/\alpha$ and if the probability $\theta = P\left(T\left(\tilde{\mathbf{U}}^{(m)}\right) \geq t_n\right)$ satisfies $2(\theta + \sqrt{\theta}) < \alpha$ and $\theta < 0.5$, then*

$$P\left(\frac{1}{M+1} \left[1 + \sum_{m=1}^M \mathbf{1}\left\{T\left(\tilde{\mathbf{U}}^{(m)}\right) \geq t_n\right\}\right] > \alpha\right) \leq e^{-M}.$$

For the second task, it is sufficient to find a value t_n and derive a lower bound on the probability $P(T(\mathbf{U}) > t_n)$ in the proof of either the dense or sparse alternative.

E.6.1 Proof for dense alternative

Proof of Theorem 4. We first consider the test statistic T_1 . Following the argument in the last subsection, we consider

$$T_1(\mathbf{U}) = \sum_{i,j \in \mathcal{C}, i \neq j} \left\langle \frac{\mathbf{U}_i}{\|\mathbf{U}_i\|}, \frac{\mathbf{U}_j}{\|\mathbf{U}_j\|} \right\rangle^2.$$

For this statistic, we first state a result regarding its asymptotic distribution and its first two moments.

Theorem 10. *Suppose \mathbf{U} is a $n \times q$ random matrix with i.i.d. rows sampled from $N_q(\mathbf{0}, \mathbf{R}_n)$ where \mathbf{R}_n is a correlation matrix with spectral norm bounded by a constant b_0 . Suppose q increases along with n and $\lim \frac{q}{n} \in (0, \infty)$. Let $\mu_n = \mathbb{E}T_1(\mathbf{U})$. We can choose a sequence of positive numbers σ_n^2 such that the followings hold:*

1. *As $n, q \rightarrow \infty$, it holds that*

$$\frac{T_1(\mathbf{U}) - \mu_n}{\sigma_n} \xrightarrow{D} N(0, 1);$$

2. *When $\mathbf{R}_n = \mathbf{I}_q$, we have*

$$\mu_n = \frac{q(q-1)}{n}, \quad \sigma_n^2 = (2q/n)^2.$$

3. *For a general \mathbf{R}_n ,*

$$\mu_n \geq \frac{q(q-1)}{n} + \left(1 - \frac{4}{n}\right) \|\mathbf{R}_n - \mathbf{I}_q\|_F^2$$

and

$$\sigma_n^2 \leq b_0^4 \left[(2q/n)^2 + 8n^{-1} \|\mathbf{R}_n - \mathbf{I}_q\|_F^2 \right].$$

We defer the proof of Theorem 10 at the end of this subsection.

Denote by z the $(\alpha^2/16)$ -upper quantile of the standard normal distribution. For any n , we take

$$t_n = z \frac{2q}{n} + \frac{q(q-1)}{n}.$$

Theorem 10 implies that

$$\mathbb{P}(T_1(\tilde{\mathbf{U}}) \geq t_n) \rightarrow \alpha^2/16, \quad (q, n \rightarrow \infty).$$

Since $2(\alpha^2/16 + \sqrt{\alpha^2/16}) < \alpha$, when n is sufficiently large, the probability $\theta = \mathbb{P}\left(T_1\left(\tilde{\mathbf{U}}^{(m)}\right) \geq t_n\right)$ satisfies $2(\theta + \sqrt{\theta}) < \alpha$ and $\theta < 0.5$.

Therefore, we can apply Lemma 4 to get

$$\mathbb{P}\left(\frac{1}{M+1} \left[1 + \sum_{m=1}^M \mathbf{1}\left\{T_1\left(\tilde{\mathbf{U}}^{(m)}\right) \geq t_n\right\}\right] > \alpha\right) \leq e^{-M} \leq \epsilon/2, \quad (\text{E.5})$$

since $M > \log(2\epsilon^{-1})$.

Recall that the rows of \mathbf{U} are i.i.d. sampled from $N_q(\mathbf{0}, \mathbf{R}(\boldsymbol{\Omega}_C^{-1}))$. Let μ_n and σ_n be the quantities define in Theorem 10 with \mathbf{R}_n being $\mathbf{R}(\boldsymbol{\Omega}_C^{-1})$. If $(1 - 4/n)b^2 > 2z$, then Theorem 10 implies that $\mu_n \geq t_n$. Furthermore, if we denote by $\delta = \|\mathbf{R}_n - \mathbf{I}_q\|_F^2/(q/n)$, we have $\delta \geq b^2$ and

$$\begin{aligned} & \frac{\mu_n - t_n}{\sigma_n} \\ & \geq \frac{(1 - \frac{4}{n})\delta - 2z}{\sigma_n} \times \frac{q}{n} \\ & \geq \frac{(1 - \frac{4}{n})\delta - 2z}{b_0^4 [(2q/n)^2 + 8n^{-1}\delta]} \times \frac{q}{n}. \end{aligned}$$

Note that the right hand side of the above display is an increasing function in δ , so it is lower bounded by

$$\frac{(1 - \frac{4}{n})b^2 - 2z}{b_0^4 [(2q/n)^2 + 8n^{-1}b^2]} \times \frac{q}{n},$$

whose limit is

$$\frac{b^2 - 2z}{4b_0^4\gamma}.$$

It then follows from the asymptotic normality in Theorem 10 that

$$\begin{aligned} & \liminf_n \mathbb{P}(T_1(\mathbf{U}) > t_n) \\ & = \liminf_n \mathbb{P}\left(\frac{T_1(\mathbf{U}) - \mu_n}{\sigma_n} > \frac{t_n - \mu_n}{\sigma_n}\right) \\ & \geq 1 - \Phi\left(-\frac{b^2 - 2z}{4b_0^4\gamma}\right), \end{aligned}$$

where Φ denotes the standard normal CDF. For any given ϵ , if we choose $b^2 > 2z + 4b_0^4\gamma\tilde{z}$ where \tilde{z} is the $(\epsilon/2)$ -upper quantile of the standard normal distribution, we can conclude that

$$\begin{aligned} & \liminf_n \mathbb{P}(\text{Reject } H_0) \\ & \geq \liminf_n \left\{ \mathbb{P}(T_1(\mathbf{U}) > t_n) - \mathbb{P}\left(\frac{1}{M+1} \left[1 + \sum_{m=1}^M \mathbf{1}\{T_1(\tilde{\mathbf{U}}^{(m)}) \geq t_n\}\right] > \alpha\right) \right\} \\ & \geq 1 - \epsilon/2 - \epsilon/2, \end{aligned}$$

where we have used (E.5). □

Proof of Theorem 10. The asymptotic normality and the expression for σ_n^2 are adapted from Theorem 2.2 in Zheng et al. [2019] with \mathbf{R}_* there being \mathbf{I}_q and \mathbf{R} being \mathbf{R}_n . Furthermore, using the elementary identities that $\text{tr}(\mathbf{A} \text{diag}(\mathbf{B})) = \text{tr}(\text{diag}(\mathbf{A}) \text{diag}(\mathbf{B})) = \text{tr}(\text{diag}(\mathbf{A})\mathbf{B})$ and $\text{diag}(\mathbf{R}) = \mathbf{I}_q$, we can reduce the expression of the asymptotic variance given in [Zheng et al., 2019, Section A.1] to

$$\begin{aligned} \sigma_n^2 = & 4n^{-1} \left[2 \text{tr}(\mathbf{R}^4) + n^{-1} [\text{tr}(\mathbf{R}^2)]^2 \right. \\ & + 2 \text{tr}(\text{diag}(\mathbf{R}^2) \mathbf{R}^2 \text{diag}(\mathbf{R}^2)) \\ & \left. - 4 \text{tr}(\mathbf{R}^2 \text{diag}(\mathbf{R}^3)) \right]. \end{aligned}$$

The last expression can be further reduce as follows:

$$\begin{aligned}
& 8^{-1}n\sigma_n^2 - (2n)^{-1} [\text{tr}(\mathbf{R}^2)]^2 \\
&= \text{tr}(\mathbf{R}^4) + \text{tr}(\text{diag}(\mathbf{R}^2)^2 \mathbf{R}^2) - 2 \text{tr}(\text{diag}(\mathbf{R}^2) \text{diag}(\mathbf{R}^3)) \\
&= \text{tr}([\mathbf{R}^2 - \text{diag}(\mathbf{R}^2)]^2) + 2 \text{tr}(\mathbf{R}^2 \text{diag}(\mathbf{R}^2)) - \text{tr}(\text{diag}(\mathbf{R}^2)^2) \\
&\quad - 2 \text{tr}(\text{diag}(\mathbf{R}^2) \text{diag}(\mathbf{R}^3)) + \text{tr}(\text{diag}(\mathbf{R}^2)^2 \mathbf{R}^2) \\
&= \text{tr}([\mathbf{R}^2 - \text{diag}(\mathbf{R}^2)]^2) \\
&\quad + \text{tr}(\mathbf{R}^2 \text{diag}(\mathbf{R}^2)) - 2 \text{tr}(\text{diag}(\mathbf{R}^2) \mathbf{R}^3) + \text{tr}(\mathbf{R}^4 \text{diag}(\mathbf{R}^2)) \\
&\quad - \text{tr}(\mathbf{R}^4 \text{diag}(\mathbf{R}^2)) + \text{tr}(\text{diag}(\mathbf{R}^2)^2 \mathbf{R}^2) \\
&= \text{tr}([\mathbf{R}^2 - \text{diag}(\mathbf{R}^2)]^2) + \text{tr}(\mathbf{R}^2[\mathbf{R} - \mathbf{I}]^2 \text{diag}(\mathbf{R}^2)) \\
&\quad - \text{tr}(\mathbf{R}^2 [\mathbf{R}^2 - \text{diag}(\mathbf{R}^2)] \text{diag}(\mathbf{R}^2)) \\
&= \text{tr}([\mathbf{R}^2 - \text{diag}(\mathbf{R}^2)]^2) + \text{tr}(\mathbf{R}^2[\mathbf{R} - \mathbf{I}]^2 \text{diag}(\mathbf{R}^2)) \\
&\quad - \text{tr}([\mathbf{R}^2 - \text{diag}(\mathbf{R}^2)]^2 \text{diag}(\mathbf{R}^2)) \\
&\quad + \text{tr}([\mathbf{R}^2 - \text{diag}(\mathbf{R}^2)] \text{diag}(\mathbf{R}^2)^2). \tag{E.6}
\end{aligned}$$

Since the diagonal entries of $\mathbf{R}^2 - \text{diag}(\mathbf{R}^2)$ are zero while $\text{diag}(\mathbf{R}^2)^2$ is a diagonal matrix, we have $\text{tr}([\mathbf{R}^2 - \text{diag}(\mathbf{R}^2)] \text{diag}(\mathbf{R}^2)^2) = 0$. Furthermore, the diagonal entries of $\text{diag}(\mathbf{R}^2)$ are all greater than or equal to 1. Therefore, the right hand side of (E.6) can be bounded as

$$\begin{aligned}
8^{-1}n\sigma_n^2 - (2n)^{-1} [\text{tr}(\mathbf{R}^2)]^2 &= \text{tr}(\mathbf{R}^2[\mathbf{R} - \mathbf{I}]^2 \text{diag}(\mathbf{R}^2)) \\
&\quad - \text{tr}([\mathbf{R}^2 - \text{diag}(\mathbf{R}^2)]^2 [\text{diag}(\mathbf{R}^2) - \mathbf{I}]) \\
&\leq \text{tr}(\mathbf{R}^2[\mathbf{R} - \mathbf{I}]^2 \text{diag}(\mathbf{R}^2)) \\
&\leq \|\mathbf{R}^2\|_2 \|\text{diag}(\mathbf{R}^2)\|_2 \text{tr}([\mathbf{R} - \mathbf{I}]^2) \\
&\leq b_0^4 \|\mathbf{R} - \mathbf{I}\|_F^2,
\end{aligned}$$

since $\|\mathbf{R}\|_2 \leq b_0$ by assumption. Furthermore, since $\text{tr}(\mathbf{R}^2) \leq q\|\mathbf{R}^2\|_2 \leq qb_0^2$, we have

$$\sigma_n^2 \leq 4b_0^4(q/n)^2 + 8n^{-1}b_0^4\|\mathbf{R} - \mathbf{I}\|_F^2.$$

It remains to derive the expression for $\mu_n = \mathbb{E}T_1(\mathbf{U})$ using properties of normal distributions. By linearity of expectation, we only need to compute the expectation for each $\left\langle \frac{\mathbf{U}_i}{\|\mathbf{U}_i\|}, \frac{\mathbf{U}_j}{\|\mathbf{U}_j\|} \right\rangle^2$. We denote this by r^2 , where r is the sample correlation coefficient for a pair of bivariate normal variables with correlation ρ .

When $\mathbf{R}_n = \mathbf{I}_q$, it is well-known that r^2 follows a Beta(1, $n - 1$) distribution and the expectation is $1/n$. For a general \mathbf{R}_n , one can compute the second moment of using Theorem 4.4.5 in Anderson [2007] to lower bound $\mathbb{E}r^2$. More concretely,

$$\mathbb{E}(r^2) = 1 - \frac{n-1}{n}(1-\rho^2) \left[1 + \sum_{k=1}^{\infty} \frac{\rho^{2k} \cdot \prod_{i=1}^k (2i)}{\prod_{i=1}^k (2i-1+n)} \right].$$

For $n > 10$ and $|\rho| < 1$, we have

$$\begin{aligned} \sum_{k=1}^{\infty} \frac{\rho^{2k} \cdot \prod_{i=1}^k (2i)}{\prod_{i=1}^k (2i-1+n)} &= \frac{2\rho^2}{n+1} + \frac{1}{n+1} \sum_{k=2}^{\infty} \frac{\rho^{2k} \cdot \prod_{i=1}^k (2i)}{\prod_{i=2}^k (2i-1+n)} \\ &\leq \frac{2\rho^2}{n+1} + \frac{1}{n+1} \sum_{k=2}^{\infty} \rho^{2k} \\ &= \frac{2\rho^2}{n+1} + \frac{\rho^4}{(n+1)(1-\rho^2)}. \end{aligned}$$

Then we have

$$\begin{aligned} \mathbb{E}(r^2) &= \frac{1}{n} + \frac{n-1}{n} \rho^2 - \frac{n-1}{n} (1-\rho^2) \sum_{k=1}^{\infty} \frac{\rho^{2k} \cdot \prod_{i=1}^k (2i)}{\prod_{i=1}^k (2i-1+n)} \\ &\geq \frac{1}{n} + \frac{n-1}{n} \rho^2 - \frac{n-1}{n} (1-\rho^2) \left[\frac{2\rho^2}{n+1} + \frac{\rho^4}{(n+1)(1-\rho^2)} \right] \\ &\geq \frac{1}{n} + \rho^2 - \frac{4\rho^2}{n} \end{aligned}$$

Summing up the expectation of $\left\langle \frac{\mathbf{U}_i}{\|\mathbf{U}_i\|}, \frac{\mathbf{U}_j}{\|\mathbf{U}_j\|} \right\rangle^2$ for all distinct pairs of (i, j) , we obtain the desired equation and inequality for μ_n . \square

E.6.2 Proof for strong alternative

We consider the test statistic T_2 . Following the argument in the Appendix E.6, we consider

$$T_2(\mathbf{U}) = \max_{i,j \leq q, i \neq j} \left\langle \frac{\mathbf{U}_i}{\|\mathbf{U}_i\|}, \frac{\mathbf{U}_j}{\|\mathbf{U}_j\|} \right\rangle^2.$$

For this statistic, we first state a result regarding the tail behavior and the concentration of $T_2(\mathbf{U})$. In the following, $(q \vee n)$ is a shorthand for $\max(q, n)$.

Theorem 11. *Suppose \mathbf{U} is a $n \times q$ random matrix with i.i.d. rows sampled from $N_q(\mathbf{0}, \mathbf{R}_n)$ where \mathbf{R}_n is a correlation matrix. Suppose q increases along with n , then the followings hold:*

1. When $\mathbf{R}_n = \mathbf{I}_q$, for $t \in (0, 1)$, we have

$$\mathbb{P}(T_2(\mathbf{U}) > t) \leq 6 \exp\left(-\frac{nt}{16} + 2 \log q\right);$$

2. When $\mathbf{R}_n \neq \mathbf{I}_q$, if $|\max_{i < j} |\mathbf{R}_n(i, j)|| \geq \sqrt{\frac{64}{n} \log\left(\frac{96(q \vee n)^2}{\alpha^2}\right)}$, then we have

$$\mathbb{P}\left(T_2(\mathbf{U}) \leq \frac{16}{n} \log\left(\frac{96q^2}{\alpha^2}\right)\right) \leq \frac{2}{(q \vee n)} + 4 \exp\left(-\frac{n}{32}\right).$$

We defer the proof of Theorem 11 at the end of this subsection.

For any n , we take

$$t_n = \frac{16}{n} \log\left(\frac{96q^2}{\alpha^2}\right).$$

Recall that the rows of $\tilde{\mathbf{U}}$ are i.i.d. sampled from $N_q(\mathbf{0}, \mathbf{I}_q)$. Statement 1 in Theorem 11 implies that

$$\mathbb{P}(T_2(\tilde{\mathbf{U}}) \geq t_n) \leq \alpha^2/16.$$

Since $2(\alpha^2/16 + \sqrt{\alpha^2/16}) < \alpha$, the probability $\theta = \mathbb{P}\left(T_2\left(\tilde{\mathbf{U}}^{(m)}\right) \geq t_n\right)$ satisfies $2(\theta + \sqrt{\theta}) < \alpha$ and $\theta < 0.5$.

Therefore, we can apply Lemma 4 to get

$$\mathbb{P}\left(\frac{1}{M+1} \left[1 + \sum_{m=1}^M \mathbf{1}\left\{T_2\left(\tilde{\mathbf{U}}^{(m)}\right) \geq t_n\right\}\right] > \alpha\right) \leq e^{-M} \leq \epsilon/2, \quad (\text{E.7})$$

since $M > \log(2\epsilon^{-1})$.

Recall that the rows of \mathbf{U} are i.i.d. sampled from $N_q(\mathbf{0}, \mathbf{R}(\boldsymbol{\Omega}_C^{-1}))$ and we are about to apply Statement 2 in Theorem 11. Consider $n > \max(10/\alpha, 32 \log(16/\epsilon), 8/\epsilon)$. We have $\log\left(\frac{96(q \vee n)^2}{\alpha^2}\right) \leq 4 \log(q \vee n)$. As a result, for \mathbf{R}_n being $\mathbf{R}(\boldsymbol{\Omega}_{C,C}^{-1})$, we have $\max_{i < j} |\mathbf{R}_n(i, j)| \geq 16 \sqrt{\frac{\log(q \vee n)}{n}} \geq \sqrt{\frac{64}{n} \log\left(\frac{96(q \vee n)^2}{\alpha^2}\right)}$. Theorem 11 implies that

$$P(T_2(\mathbf{U}) < t_n) \leq \frac{2}{(q \vee n)} + 4 \exp\left(-\frac{n}{32}\right) \leq \epsilon/4. \quad (\text{E.8})$$

Combining the inequalities in (E.3, E.7, E.8), we have

$$\mathbb{P}(\text{Reject } H_0) \geq 1 - \epsilon/2 - \epsilon/2 = 1 - \epsilon.$$

Proof of Theorem 11. When $\mathbf{R}_n = \mathbf{I}_q$, we first introduce an event which will happen with high probability. For any two distinct column indices i and j , define

$$\mathcal{E}_1(i, j) = \{|\|\mathbf{U}_i\|^2 - n| \leq \sqrt{2}/2n, \|\mathbf{U}_j\|^2 - n| \leq \sqrt{2}/2n\}.$$

According to Statement 1 in Lemma 5, we have $\mathbb{P}(\mathcal{E}_1(i, j)) \geq 1 - 4 \exp(-n/16)$. For any $t \in (0, 1)$, we have

$$\begin{aligned} \mathbb{P}(T_2(\mathbf{U}) > t) &\leq \sum_{1 \leq i < j \leq q} \mathbb{P}\left(\frac{(\mathbf{U}_i^\top \mathbf{U}_j)^2}{\|\mathbf{U}_i\|_2^2 \|\mathbf{U}_j\|_2^2} > t\right) \\ &\leq \sum_{1 \leq i < j \leq q} \left[\mathbb{P}\left(\frac{(\mathbf{U}_i^\top \mathbf{U}_j)^2}{\|\mathbf{U}_i\|_2^2 \|\mathbf{U}_j\|_2^2} > t, \mathcal{E}_1(i, j)\right) + \mathbb{P}(\mathcal{E}_1(i, j)^c)\right] \\ &\stackrel{(1)}{\leq} 2q^2 \mathbb{P}\left(\frac{1}{n^2} (\mathbf{U}_1^\top \mathbf{U}_2)^2 > \frac{1}{2}t\right) + 2q^2 \exp(-n/16) \\ &= 2q^2 \mathbb{P}\left(\left|\frac{1}{n} \sum_{k=1}^n U_{k,1} U_{k,2}\right| > \sqrt{\frac{1}{2}t}\right) + 2q^2 \exp(-n/16) \\ &\stackrel{(2)}{\leq} 4 \exp\left(-\frac{nt}{16} + 2 \log q\right) + 2 \exp\left(-\frac{n}{16} + 2 \log q\right) \\ &\leq 6 \exp\left(-\frac{nt}{16} + 2 \log q\right), \end{aligned}$$

where (1) is due to the symmetry across the pairs of (i, j) and (2) follows from Statement 2 in Lemma 5 with $\rho = 0$.

For a general \mathbf{R}_n , suppose $i_* \in [q], j_* \in [q], i_* \neq j_*$ such that $|\mathbf{R}_n(i_*, j_*)| = \max_{i < j} |\mathbf{R}_n(i, j)|$. We introduce the following events:

$$\begin{aligned} \mathcal{E}_1 &= \{|\|\mathbf{U}_{i_*}\|^2 - n| \leq 1/2n, \|\mathbf{U}_{j_*}\|^2 - n| \leq 1/2n\}, \\ \mathcal{E}_2 &= \left\{\left|\frac{(\mathbf{U}_{i_*}^\top \mathbf{U}_{j_*})}{n} - \mathbf{R}_n(i_*, j_*)\right| \leq \sqrt{\frac{8 \log(q \vee n)}{n}}\right\}. \end{aligned}$$

Based on Lemma 5, we have $\mathbb{P}(\mathcal{E}_1) \geq 1 - 4 \exp(-n/32)$ and $\mathbb{P}(\mathcal{E}_2) \geq 1 - 2/(q \vee n)$. Note that the event \mathcal{E}_1 implies $\|\mathbf{U}_{i_*}\|_2 \|\mathbf{U}_{j_*}\|_2 \leq 3/2$. When both \mathcal{E}_1 and \mathcal{E}_2 occurs, we have

$$\begin{aligned} \left| \frac{\mathbf{U}_{i_*}^\top \mathbf{U}_{j_*}}{\|\mathbf{U}_{i_*}\|_2 \|\mathbf{U}_{j_*}\|_2} \right| &\geq \frac{2}{3} \left| \mathbf{U}_{i_*}^\top \mathbf{U}_{j_*} \right| \\ &\geq \frac{2}{3} \left(\mathbf{R}_n(i_*, j_*) - \sqrt{\frac{8 \log(q \vee n)}{n}} \right) \\ &> \sqrt{\frac{16}{n} \log \left(\frac{96q^2}{\alpha^2} \right)}, \end{aligned}$$

where the last inequality is because by assumption $\mathbf{R}_n(i_*, j_*) \geq 8\sqrt{\frac{1}{n} \log \left(\frac{96(q \vee n)^2}{\alpha^2} \right)} > \sqrt{\frac{8 \log(q \vee n)}{n}} + \frac{3}{2} \sqrt{\frac{16}{n} \log \left(\frac{96q^2}{\alpha^2} \right)}$. Therefore, we have

$$\begin{aligned} &\mathbb{P} \left(T_2(\mathbf{U}) \leq \frac{16}{n} \log \left(\frac{96q^2}{\alpha^2} \right) \right) \\ &\stackrel{(1)}{\leq} \mathbb{P} \left(\left| \frac{(\mathbf{U}_{i_*}^\top \mathbf{U}_{j_*})}{\|\mathbf{U}_{i_*}\|_2 \|\mathbf{U}_{j_*}\|_2} \right| \leq \sqrt{\frac{16}{n} \log \left(\frac{96q^2}{\alpha^2} \right)} \right) \\ &\leq \mathbb{P}(\mathcal{E}_1^c \cup \mathcal{E}_2^c) \\ &\leq \mathbb{P}(\mathcal{E}_1^c) + \mathbb{P}(\mathcal{E}_2^c) \leq 4e^{-n/32} + 2/(q \vee n), \end{aligned}$$

where the inequality (1) follows from $T_2(\mathbf{U}) \geq \left(\frac{(\mathbf{U}_{i_*}^\top \mathbf{U}_{j_*})}{\|\mathbf{U}_{i_*}\|_2 \|\mathbf{U}_{j_*}\|_2} \right)^2$. □

Lemma 5. Let $\mathbf{X} = (X_1, X_2, \dots, X_n)$ and $\mathbf{Y} = (Y_1, Y_2, \dots, Y_n)$ be n -dimensional random vectors. Assume that each pair (X_i, Y_i) for $i = 1, 2, \dots, n$, is independently sampled from a zero mean bivariate normal distribution. Specifically, $\text{Var}(X_i) = \text{Var}(Y_i) = 1, \mathbb{E}(X_i Y_i) = \rho$. Then we have:

1. For \mathbf{W} equals to either \mathbf{X} or \mathbf{Y} ,

$$\mathbb{P} \left(\left| \frac{\|\mathbf{W}\|_2^2}{n} - 1 \right| > t \right) \leq 2 \exp \left(-\frac{nt^2}{8} \right) \quad \text{for all } t \in (0, 1) \quad (\text{E.9})$$

2.

$$\mathbb{P} \left(\left| \frac{1}{n} \sum_{i=1}^n X_i Y_i - \rho \right| \geq t \right) \leq 2 \exp \left(-\frac{nt^2}{8} \right) \quad \text{for all } t \in (0, 1) \quad (\text{E.10})$$

Proof of Lemma 5. Direct consequence of $\mathbb{E}(e^{\lambda(W_i^2-1)}) \leq e^{2\lambda^2}$ and $\mathbb{E}(e^{\lambda(X_i Y_i - \rho)}) \leq e^{2\lambda^2}$, for all $|\lambda| < 1/4$. □

E.6.3 Proof for union alternative

Proof of Theorem 8. Denote by z the $(\alpha^2/16)$ -upper quantile of the standard normal distribution. Denote by u_0 the solution of $\exp[-(8\pi)^{-1/2} \exp(-u_0/2)] = 1 - \alpha^2/16$. Note that both z and u_0 are constants.

For any n , we take

$$t_n = \max\{z, u_0\}.$$

Theorem 10 and Theorem 3 in Cai and Jiang [2011] implies that

$$\begin{aligned}\mathbb{P}\left(\frac{n}{2q}\left(T_1(\tilde{\mathbf{U}}^{(m)}) - q(q-1)/n\right) \geq z\right) &\rightarrow \frac{\alpha^2}{16}, \quad (q, n \rightarrow \infty), \\ \mathbb{P}\left(nT_2(\tilde{\mathbf{U}}^{(m)}) - 4\log q + \log \log q \geq u_0\right) &\rightarrow \frac{\alpha^2}{16}, \quad (q, n \rightarrow \infty).\end{aligned}$$

Since $2(\alpha^2/8 + \sqrt{\alpha^2/8}) < \alpha$, when n is sufficiently large together, we can use the union bound to see that the probability $\theta = \mathbb{P}\left(T_3(\tilde{\mathbf{U}}^{(m)}) \geq t_n\right)$ satisfies $2(\theta + \sqrt{\theta}) < \alpha$ and $\theta < 0.5$. Therefore, we can apply Lemma 4 to get

$$\mathbb{P}\left(\frac{1}{M+1}\left[1 + \sum_{m=1}^M \mathbf{1}\left\{T_3(\tilde{\mathbf{U}}^{(m)}) \geq t_n\right\}\right] > \alpha\right) \leq e^{-M} \leq \epsilon/2,$$

since $M > \log(2\epsilon^{-1})$.

Next, we will show

$$\liminf_n \mathbb{P}(T_3(\mathbf{U}) > t_n) \geq 1 - \epsilon/2. \quad (\text{E.11})$$

Since it is assumed that $\Omega \in \Theta_{n3}(b) = \Theta_{n1}(b) \cup \Theta_{n2}(16)$, we can divide the sequence of populations into two subsequences (possibly finite) so that either of the followings

- **Case 1:** $\Omega \in \Theta_{n1}(b)$,
- **Case 2:** $\Omega \in \Theta_{n2}(16)$

holds for the whole subsequence. Therefore, it suffices to prove (E.11) for both cases.

For Case 1, following a similar argument as in the proof of Theorem 4, and setting $b = \sqrt{2 \max\{z, u_0\} + 4b_0^4 \gamma z_2}$, where z_2 is the $(\epsilon/2)$ -upper quantile of the standard normal distribution, we can conclude that

$$\liminf_n \mathbb{P}(T_3(\mathbf{U}) > t_n) \geq \liminf_n \mathbb{P}\left(\frac{n}{2q}\left(T_1(\mathbf{U}) - q(q-1)/n\right) > \max\{z, u_0\}\right) \geq 1 - \epsilon/2.$$

For Case 2,

$$\begin{aligned}\liminf_n \mathbb{P}(T_3(\mathbf{U}) > t_n) &\geq \liminf_n \mathbb{P}(nT_2(\mathbf{U}) - 4\log q + \log \log q > \max\{z, u_0\}) \\ &= \liminf_n \mathbb{P}\left(T_2(\mathbf{U}) \geq \frac{\max\{z, u_0\} + 4\log q - \log \log q}{n}\right).\end{aligned}$$

Recall from Theorem 6, we have

$$\liminf_n \mathbb{P}\left(T_2(\mathbf{U}) \geq \frac{16}{n} \log\left(\frac{96q^2}{\alpha^2}\right)\right) \geq 1 - \epsilon/2.$$

Then, it suffices to show that

$$\frac{16}{n} \log\left(\frac{96q^2}{\alpha^2}\right) \geq \frac{\max\{z, u_0\} + 4\log q - \log \log q}{n},$$

which is a direct consequence of Lemma 6. □

Lemma 6. Let $0 < \alpha < 1$. Denote by z the $(\alpha^2/16)$ -upper quantile of the standard normal distribution. and let u_0 be the solution of $\exp[-(8\pi)^{-1/2} \exp(-u_0/2)] = 1 - \alpha^2/16$. Then we have

$$u_0 \leq -2 \log \left(\frac{\alpha^2}{16} \right), \quad (\text{E.12})$$

$$z \leq \sqrt{2 \log \left(\frac{16}{\alpha^2 \sqrt{2\pi}} \right)} \quad (\text{E.13})$$

Proof of Lemma 6. First, we solve the equation $\exp[-(8\pi)^{-1/2} \exp(-u_0/2)] = 1 - \alpha^2/16$. This yields

$$u_0 = -2 \log \left(-\log \left(1 - \frac{\alpha^2}{16} \right) \sqrt{8\pi} \right).$$

Using the inequality $\log(1-x) \leq -x$ for $0 < x < 1$ and the monotonicity of $-\log(x)$, we find that

$$\begin{aligned} u_0 &= -2 \log \left(-\log \left(1 - \frac{\alpha^2}{16} \right) \right) - 2 \log \left(\sqrt{8\pi} \right) \\ &\leq -2 \log \left(-\log \left(1 - \frac{\alpha^2}{16} \right) \right) \\ &\leq -2 \log \left(\frac{\alpha^2}{16} \right). \end{aligned}$$

Next, we establish an inequality for the tail probability of the standard normal distribution. Let $X \sim N(0, 1)$ and for $t \geq x > 0$, we have that $1 \leq t/x$ and

$$\mathbb{P}(X > x) = \frac{1}{\sqrt{2\pi}} \int_x^\infty 1 \cdot e^{-t^2/2} dt \leq \frac{1}{\sqrt{2\pi}} \int_x^\infty \frac{t}{x} e^{-t^2/2} dt = \frac{e^{-x^2/2}}{x\sqrt{2\pi}}.$$

Since $\frac{\alpha^2}{16} < 1/16$, we have $z > 1$, which implies that $\exp(z^2/2) \leq z \exp(z^2/2) \leq \frac{16}{\alpha^2 \sqrt{2\pi}}$. □

E.6.4 Proof of Lemma 3

The proof is divided into three steps.

Step 1. We characterize the randomness of any sampled $\tilde{\mathbf{X}}$ when running Algorithm 1. Let $\tilde{\mathbf{W}} := \Gamma^\top \tilde{\mathbf{X}}_{\mathcal{C}}$. Then we have

$$\tilde{\mathbf{X}}_{\mathcal{C}} = \Pi_1 \tilde{\mathbf{X}}_{\mathcal{C}} + \Gamma \tilde{\mathbf{W}}.$$

Consider running Algorithm 1 with index i . (1) if $i \in \mathcal{H}$, then $|N_i| > n$ and we have $\tilde{\mathbf{X}}_i = \mathbf{X}_i$. (2) If $i \in \mathcal{C}$, then $N_i = \mathcal{H}$, so we have

$$\mathbf{F} + \tilde{\mathbf{R}} \frac{\|\mathbf{R}\|}{\|\tilde{\mathbf{R}}\|},$$

where $\mathbf{F} = \Pi_1 \mathbf{X}_i$ and $\|\mathbf{R}\| = \|\Gamma \mathbf{X}_i\|$ both remain unchanged over iterations, and $\|\tilde{\mathbf{R}}\|^{-1} \tilde{\mathbf{R}}$ is a uniformly distributed unit vector that is orthogonal to the column space of $[\mathbf{1}_n, \mathbf{X}_{\mathcal{H}}]$. Therefore, we have

$$\tilde{\mathbf{W}}_i = \|\mathbf{R}\| \Gamma^\top \frac{\tilde{\mathbf{R}}}{\|\tilde{\mathbf{R}}\|}$$

is uniformly distributed on the sphere in $\mathbb{R}^{n-1-|\mathcal{H}|}$ with radius $\|\Gamma \mathbf{X}_i\|$ and is independent with $\{\tilde{\mathbf{X}}_j : j \in \mathcal{C} \setminus \{i\}\}$. It follows that

$$\frac{\tilde{\mathbf{W}}_i}{\|\tilde{\mathbf{W}}_i\|} \sim \text{Unif}(\mathbb{S}^{n-1-|\mathcal{H}|-1}),$$

that is, the uniform distribution w.r.t. the Haar measure on the unit sphere in $\mathbb{R}^{n-1-|\mathcal{H}|}$ and is independent with all other random variables.

Step 2. Now we characterize the sampled copies in Algorithm 3. Since $\mathcal{I} = (1, 2, \dots, p)$, every column of any copies $\tilde{\mathbf{X}}$ in Step 1 has been updated by Algorithm 1 at least one. By the analysis above for Algorithm 1, we know that for every $i \in \mathcal{C}$, $\frac{\tilde{\mathbf{W}}_i}{\|\tilde{\mathbf{W}}_i\|} \sim \text{Unif}(\mathbb{S}^{n-1-|\mathcal{H}|-1})$ and they are mutually independent and independent with all other random variables. In fact, if $\tilde{\mathbf{U}}$ is a $(n-1-|\mathcal{H}|) \times q$ matrix with i.i.d. rows sampled from $N_q(\mathbf{0}, \mathbf{I}_q)$, then

$$\left(\frac{\tilde{\mathbf{W}}_i}{\|\tilde{\mathbf{W}}_i\|} \right)_{i \in \mathcal{C}} \stackrel{d}{=} \left(\frac{\tilde{\mathbf{U}}_i}{\|\tilde{\mathbf{U}}_i\|} \right)_{i \leq q}.$$

Step 3.

Since $\Gamma^\top[\mathbf{1}_n, \mathbf{X}, \mathcal{H}] = 0$, it is easy to show that $\mathbf{W} := \Gamma^\top \mathbf{X}_{\mathcal{C}} \sim N(0, \mathbf{I}_{n-1-|\mathcal{H}|} \otimes \Omega_{\mathcal{C}}^{-1})$. Recall the diagonal normalization $\mathbf{R}(\mathbf{M}) = \text{diag}(\mathbf{M})^{-1/2} \mathbf{M} \text{diag}(\mathbf{M})^{-1/2}$. We claim that if \mathbf{U} is a $(n-1-|\mathcal{H}|) \times q$ matrix with i.i.d. rows sampled from $N_q(\mathbf{0}, \mathbf{R}(\Omega_{\mathcal{C}}^{-1}))$, then

$$\left(\frac{\mathbf{W}_i}{\|\mathbf{W}_i\|} \right)_{i \in \mathcal{C}} \stackrel{d}{=} \left(\frac{\mathbf{U}_i}{\|\mathbf{U}_i\|} \right)_{i \leq q}. \quad (\text{E.14})$$

This is because for any $q \times q$ diagonal matrix \mathbf{D} with $D_{i,i} > 0$, the value of $\frac{\mathbf{U}_i}{\|\mathbf{U}_i\|}$ remains invariant under the transformation of \mathbf{U} to $\mathbf{U}\mathbf{D}$. In particular, we set $\mathbf{D} = \text{diag}(\Omega_{\mathcal{C}}^{-1})^{1/2}$ and $\mathbf{U} = \mathbf{W}\mathbf{D}^{-1}$ to get (E.14).

Lastly, the spectral norm of $\mathbf{R}(\Omega_{\mathcal{C}}^{-1})$ can be bounded as

$$\begin{aligned} & \lambda_{\max}(\mathbf{R}(\Omega_{\mathcal{C}}^{-1})) \\ & \leq \lambda_{\max}(\Omega_{\mathcal{C}}^{-1}) \lambda_{\max}(\mathbf{D}^{-1})^2 \\ & = \frac{1}{\lambda_{\min}(\Omega_{\mathcal{C}})} \max_{i \in \mathcal{C}} \frac{1}{(\mathbf{D}_{ii})^2} \\ & = \frac{1}{\lambda_{\min}(\Omega_{\mathcal{C}})} \max_{i \in \mathcal{C}} ([\Omega_{\mathcal{C}}^{-1}]_{ii}^{-1}). \end{aligned}$$

Using Schur complement, it is easy to see that $[\Omega_{\mathcal{C}}^{-1}]_{ii}^{-1} \leq \Omega_{ii} \leq \lambda_{\max}(\Omega_{\mathcal{C}})$ for any $i \in \mathcal{C}$. Therefore, if

$$\lambda_{\max}(\Omega_{\mathcal{C}}) / \lambda_{\min}(\Omega_{\mathcal{C}}) \leq b_0,$$

then $\lambda_{\max}(\mathbf{R}(\Omega_{\mathcal{C}}^{-1}))$ is bounded by b_0 .

E.6.5 Proof of Lemma 4

We first state the following concentration inequality resulting from Kearns–Saul inequality Kearns and Saul [1998].

Lemma 7. *Suppose $\{\xi_i\}_{i=1}^M$ are i.i.d. Bernoulli random variables with probability θ . If $\theta < 0.5$, then it holds that*

$$\mathbb{P} \left(\frac{1}{M} \sum_{i=1}^M \xi_i - \theta \geq x \right) \leq \exp(-\theta^{-1} M x^2), \forall x > 0.$$

We apply Lemma 7 with $\xi_m = \mathbf{1} \left\{ T \left(\tilde{\mathbf{U}}^{(m)} \right) \geq t \right\}$ and $x = [(1+M)\alpha - 1]/M - \theta$. Since $M > 2/\alpha$ and

$2(\theta + \sqrt{\theta}) < \alpha$, we can show $x^2 > \theta$. Therefore, we have

$$\begin{aligned} & \mathbb{P} \left(\frac{1}{M+1} \left[1 + \sum_{m=1}^M \mathbf{1} \{ T(\tilde{\mathbf{U}}^{(m)}) \geq t_n \} \right] > \alpha \right) \\ &= \mathbb{P} \left(\frac{1}{M} \sum_{i=1}^M \xi_i - \theta \geq x \right) \\ &\leq \exp(-Mx^2/\theta) \\ &\leq e^{-M}. \end{aligned}$$

The proof of Lemma 4 is completed.

Proof of Lemma 7. By Lemma 1 in Kearns and Saul [1998], the moment generating function of $(\xi_i - \theta)$ satisfies

$$\ln \left[(1 - \theta)e^{-t\theta} + \theta e^{\theta(1-\theta)} \right] \leq \frac{t^2}{4} g(\theta), \quad t \in \mathbb{R},$$

where $g(\theta) = \frac{(1-2\theta)}{\log((1-\theta)/\theta)}$. By Markov inequality, for any $t > 0$ and $x > 0$, we have

$$\mathbb{P} \left(\frac{1}{M} \sum_{i=1}^M \xi_i - \theta \geq x \right) \leq \exp \left(-txM + M \frac{t^2}{4} g(\theta) \right).$$

In particular, taking $t = 2x/g(\theta)$, we have

$$\mathbb{P} \left(\frac{1}{M} \sum_{i=1}^M \xi_i - \theta \geq x \right) \leq \exp(-Mx^2/g(\theta)), \quad x > 0.$$

To prove the lemma, it suffices to show $g(\theta) \leq \theta^{-1}$. This can be proved using elementary calculus. Consider $h(x) = \log((1-x)/x) - x(1-2x)$ for any $x \in (0, 1/2]$. We can show that the derivative of h is $-(1-x)^{-1} - x^{-1} - 1 + 4x < 0$, since $x(1-x) < 1/4 < 1/3$. So $h(x)$ attains the minimal value 0 at $x = 1/2$. From $\log((1-\theta)/\theta) - \theta(1-2\theta) \geq 0$, we have $\theta g(\theta) \leq 1$ for $\theta \in (0, 1/2]$. \square

E.7 Lower bound of separation rate

Proof of Theorem 5. Denote by $\rho = b/\sqrt{n(q-1)}$. Consider the following subset of $\Theta_{n1}(b)$:

$$\begin{aligned} \Theta_{n1}^*(b) &= \left\{ \mathbf{A}^{(v)} : \mathbf{A}_{\mathcal{H},\mathcal{H}}^{(v)} = \mathbf{I}_{p-q}, \mathbf{A}_{\mathcal{H},\mathcal{C}}^{(v)} = \left(\mathbf{A}_{\mathcal{C},\mathcal{H}}^{(v)} \right)^\top = \mathbf{0}_{(p-q) \times q}, \right. \\ &\quad \left. \mathbf{A}_{\mathcal{C},\mathcal{C}}^{(v)} = \frac{1}{1-\rho} \mathbf{I}_q - \left[\frac{1}{1-\rho} - \frac{1}{1+(q-1)\rho} \right] \frac{1}{q} \mathbf{v}\mathbf{v}', \mathbf{v} \in \{-1, 1\}^q \right\}. \end{aligned} \quad (\text{E.15})$$

For any $\mathbf{A}^{(v)} \in \Theta_{n1}^*(b)$, it is straightforward to see that $\left[\mathbf{A}_{\mathcal{C},\mathcal{C}}^{(v)} \right]^{-1} = (1-\rho)\mathbf{I}_q + \rho\mathbf{v}\mathbf{v}'$ and thus $D(\mathbf{A}_{\mathcal{C},\mathcal{C}}^{(v)}, F) = \sqrt{\rho^2 q(q-1)} = b\sqrt{q/n}$. Since the eigenvalues of $\mathbf{A}_{\mathcal{C},\mathcal{C}}^{(v)}$ are either $1/(1-\rho)$ or $1/(1+(q-1)\rho)$, the condition number is $1 + q\rho/(1-\rho)$ and is bounded by $1 + 2b\sqrt{\kappa}$ (for q large, we have $1-\rho > 1/2$). Therefore, $\Theta_{n1}^*(b) \subset \Theta_{n1}(b)$.

Let P_0 be the probability measure when the rows of \mathbf{X} are i.i.d. $\mathbf{N}_p(\mathbf{0}, \mathbf{I}_p)$ and let $P_{\mathbf{v}}$ be the probability measure when the rows of \mathbf{X} are i.i.d. $\mathbf{N}_p(\mathbf{0}, (\mathbf{A}^{(v)})^{-1})$ for any $\mathbf{v} \in \{-1, 1\}^q$. Let f_0 and $f_{\mathbf{v}}$ be the

respective Lebesgue density functions. A direct computation yields

$$\begin{aligned} \forall \mathbf{x} \in \mathbb{R}^{n \times p}, \quad \frac{f_{\mathbf{v}}(\mathbf{x})}{f_0(\mathbf{x})} &= \left(\det \mathbf{A}_{\mathcal{C}, \mathcal{C}}^{(\mathbf{v})} \right)^{n/2} \exp \left(-\frac{1}{2} \mathbf{x}_{\mathcal{C}}^{\top} \left(\mathbf{A}_{\mathcal{C}, \mathcal{C}}^{(\mathbf{v})} - \mathbf{I}_q \right) \mathbf{x}_{\mathcal{C}} \right) \\ &=: g_{\mathbf{v}}(\mathbf{x}, \mathcal{C}). \end{aligned}$$

Let P_1 be the mixture measure $P_1 = \frac{1}{2^q} \sum_{\mathbf{v}} P_{\mathbf{v}}$ and let f_1 be the Lebesgue density function. Since $f_1 = \frac{1}{2^q} \sum_{\mathbf{v}} f_{\mathbf{v}}$, we have

$$\forall \mathbf{x} \in \mathbb{R}^{n \times p}, \quad \left(\frac{f_1(\mathbf{x})}{f_0(\mathbf{x})} \right)^2 = \frac{1}{2^{2q}} \sum_{\mathbf{u}, \mathbf{v}} g_{\mathbf{u}}(\mathbf{x}, \mathcal{C}) g_{\mathbf{v}}(\mathbf{x}, \mathcal{C}). \quad (\text{E.16})$$

The rest of the proof is an adaption of the proof of Theorem 1 in Cai and Ma [2013] in our setting. We highlight the key steps below to be self-contained.

Note that the marginal distribution of $\mathbf{X}_{\mathcal{C}}$ under P_0 is $N_{n \times q}(\mathbf{0}_q, \mathbf{I}_q)$. For this marginal distribution, we can follow the proof of Theorem 1 in Cai and Ma [2013] and use the expression in (E.16) to compute

$$\mathbb{E}_{P_0} \left(\frac{f_1(\mathbf{X})}{f_0(\mathbf{X})} \right)^2 = \frac{(1 - \rho^2)^{n-nq/2}}{[1 + (q-1)\rho^2]^n} \mathbb{E}_V \left[1 - \left(\frac{q\rho}{1 + (q-1)\rho^2} \right)^2 \left(\frac{\mathbf{1}'V}{q} \right)^2 \right]^{-n/2}, \quad (\text{E.17})$$

where the random vector $V \in \{-1, 1\}^q$ has i.i.d. symmetric Rademacher entries. The condition needed is

$$b \leq 1/\sqrt{2\kappa}, \quad b < 1.$$

This condition implies $2(q-1) > b^2 q \log 2$ when q is large enough. Then the proof of Theorem 1 in Cai and Ma [2013] also suggests that

$$\mathbb{E}_V \left[1 - \left(\frac{q\rho}{1 + (q-1)\rho^2} \right)^2 \left(\frac{\mathbf{1}'V}{q} \right)^2 \right]^{-n/2} \leq 1 + \frac{2b^2 q \log 2}{2(q-1) - b^2 q \log 2}. \quad (\text{E.18})$$

Since $b^2 \leq 1$, we can see by calculus that there is some constant x_0 such that for any $x, y \geq x_0$, it holds that

$$(1 - b^2/x)^{-x} < e^{b^2} \sqrt{1 + b^2 \log 2}, \quad (1 + b^2/y)^y > e^{b^2} / \sqrt{1 + b^2 \log 2}.$$

Therefore, $n \geq 2x_0$, we have

$$\frac{(1 - \rho^2)^{n-nq/2}}{[1 + (q-1)\rho^2]^n} \leq (1 + b^2 \log 2). \quad (\text{E.19})$$

Combining the inequalities (E.19) and (E.18), we obtain from (E.17) that

$$\mathbb{E}_{P_0} \left(\frac{f_1(\mathbf{X})}{f_0(\mathbf{X})} \right)^2 - 1 < \frac{8b^2 q \log 2}{2(q-1) - b^2 q \log 2}.$$

Given any $0 < \alpha < \beta < 1$, there is some b_0 such that for all $b \leq b_0$, we have

$$\mathbb{E}_{P_0} \left(\frac{f_1(\mathbf{X})}{f_0(\mathbf{X})} \right)^2 - 1 < 4(\beta - \alpha)^2. \quad (\text{E.20})$$

Finally, for any test ϕ , the sum of probabilities of its two types of errors satisfies

$$\begin{aligned} \sup_{\mathbf{v}} (\mathbb{E}_{P_0} \phi + \mathbb{E}_{P_{\mathbf{v}}} (1 - \phi)) &\geq \frac{1}{2^p} \sum_{\mathbf{v}} (\mathbb{E}_{P_0} \phi + \mathbb{E}_{P_{\mathbf{v}}} (1 - \phi)) \\ &= \mathbb{E}_{P_0} \phi + \mathbb{E}_{P_1} (1 - \phi) \\ &\geq \inf_{\psi} (\mathbb{E}_{P_0} \psi + \mathbb{E}_{P_1} (1 - \psi)) \\ &= 1 - d_{TV}(P_0, P_1), \end{aligned}$$

where $d_{TV}(P_0, P_1)$ is the total variation distance, which is in turn bounded by the chi-square divergence as

$$d_{TV}^2(P_0, P_1) \leq \frac{1}{4} \left[\mathbb{E}_{P_0} \left(\frac{f_1(\mathbf{X})}{f_0(\mathbf{X})} \right)^2 - 1 \right] < (\beta - \alpha)^2,$$

where the last inequality is due to (E.20). Hence, for any test ϕ , we have

$$\sup_{\mathbf{v}} (\mathbb{E}_{P_0} \phi + \mathbb{E}_{P_{\mathbf{v}}} (1 - \phi)) > 1 - \beta + \alpha,$$

which implies

$$\inf_{\Omega \in \Theta_{n1}(b)} \mathbb{E}(\phi) \leq \inf_{\Omega \in \Theta_{n1}^*(b)} \mathbb{E}(\phi) \leq \beta.$$

□

Proof of Theorem 7. Our strategy of this proof is the same as the proof of Theorem 5 except that we need to construct another least favorable subset for the sparse alternative and compute the chi-square divergence.

Denote by $\rho = b\sqrt{\frac{\log q}{n}}$. Let $\mathcal{C}^2 = \{(i, j) : i < j, i, j \in \mathcal{C}\}$. For any $(i, j) \in \mathcal{C}^2$, let $\mathbf{E}_{ij} = \mathbf{e}_i \mathbf{e}'_j + \mathbf{e}_j \mathbf{e}'_i$. Consider the following subset of $\Theta_{n2}(b)$:

$$\begin{aligned} \Theta_{n2}^*(b) = & \left\{ \mathbf{A}^{(ij)} : \mathbf{A}_{\mathcal{H}, \mathcal{H}}^{(ij)} = \mathbf{I}_{p-q}, \mathbf{A}_{\mathcal{H}, \mathcal{C}}^{(ij)} = \left(\mathbf{A}_{\mathcal{C}, \mathcal{H}}^{(ij)} \right)^\top = \mathbf{0}_{(p-q) \times q}, \right. \\ & \left. \mathbf{A}_{\mathcal{C}, \mathcal{C}}^{(ij)} = [\mathbf{I}_q + \rho \mathbf{E}_{ij}]^{-1}, (ij) \in \mathcal{C}^2 \right\}. \end{aligned} \quad (\text{E.21})$$

For any $\mathbf{A}^{(ij)} \in \Theta_{n2}^*(b)$, it is straightforward to see that $D(\mathbf{A}_{\mathcal{C}, \mathcal{C}}^{(ij)}, \infty) = \rho = b\sqrt{\log(q)/n}$. Therefore, $\Theta_{n2}^*(b) \subset \Theta_{n2}(b)$.

Let P_0 be the probability measure when the rows of \mathbf{X} are i.i.d. $\mathbf{N}_p(\mathbf{0}, \mathbf{I}_p)$ and let P_{ij} be the probability measure when the rows of \mathbf{X} are i.i.d. $\mathbf{N}_p(\mathbf{0}, (\mathbf{A}^{(ij)})^{-1})$ for any $(i, j) \in \mathcal{C}^2$. Let f_0 and f_{ij} be the respective Lebesgue density functions. A direct computation yields

$$\begin{aligned} \forall \mathbf{x} \in \mathbb{R}^{n \times p}, \quad \frac{f_{ij}(\mathbf{x})}{f_0(\mathbf{x})} &= \left(\det \mathbf{A}_{\mathcal{C}, \mathcal{C}}^{(ij)} \right)^{n/2} \exp \left(-\frac{1}{2} \sum_{k=1}^n \mathbf{x}_{k, \mathcal{C}}^\top \left(\mathbf{A}_{\mathcal{C}, \mathcal{C}}^{(ij)} - \mathbf{I}_q \right) \mathbf{x}_{k, \mathcal{C}} \right) \\ &= \left(\det \mathbf{A}_{\mathcal{C}, \mathcal{C}}^{(ij)} \right)^{n/2} \exp \left(-\frac{1}{2} \sum_{k=1}^n \mathbf{x}_{k, \mathcal{C}}^\top \left(\mathbf{A}_{\mathcal{C}, \mathcal{C}}^{(ij)} - \mathbf{I}_q \right) \mathbf{x}_{k, \mathcal{C}} \right) \\ &=: g_{ij}(\mathbf{x}_{(i, j)}), \end{aligned}$$

since the only nonzero entries of $\mathbf{A}_{\mathcal{C}, \mathcal{C}}^{(ij)} - \mathbf{I}_q$ are on the (i, j) row and the (i, j) columns.

Let P_1 be the mixture measure $P_1 = \frac{2}{q(q-1)} \sum_{(i, j) \in \mathcal{C}^2} P_{ij}$ and let f_1 be the Lebesgue density function. Since $f_1 = \frac{2}{q(q-1)} \sum_{(i, j) \in \mathcal{C}^2} f_{ij}$, we have

$$\forall \mathbf{x} \in \mathbb{R}^{n \times p}, \quad \left(\frac{f_1(\mathbf{x})}{f_0(\mathbf{x})} \right)^2 = \left(\frac{2}{q(q-1)} \right)^2 \sum_{(i, j), (i', j')} g_{ij}(\mathbf{x}_{(i, j)}) g_{i'j'}(\mathbf{x}_{(i', j')}). \quad (\text{E.22})$$

Note that the marginal distribution of $\mathbf{X}_{\mathcal{C}}$ under P_0 is $N_{n \times q}(\mathbf{0}_q, \mathbf{I}_q)$. We will compute the expectation under P_0 of each term in (E.22).

Case 1: For any (i, j) and (i', j') without overlap, the submatrices $\mathbf{X}_{(i, j)}$ and $\mathbf{X}_{(i', j')}$ are independent under P_0 , and thus

$$\mathbb{E}_{P_0} [g_{ij}(\mathbf{X}_{(i, j)}) g_{i'j'}(\mathbf{X}_{(i', j')})] = \mathbb{E}_{P_0} [g_{ij}(\mathbf{X}_{(i, j)})] \mathbb{E}_{P_0} [g_{i'j'}(\mathbf{X}_{(i', j')})] = 1,$$

since $\mathbb{E}_{P_0}[g_{ij}(\mathbf{X}_{(i,j)})] = \mathbb{E}_{P_0}[\frac{f_{ij}(\mathbf{X})}{f_0(\mathbf{X})}] = 1$ for any (i, j) .

Case 2: For $(i, j) = (i', j')$, by property the normal distribution, we can compute as

$$\begin{aligned}\mathbb{E}_{P_0}[g_{ij}(\mathbf{X}_{(i,j)})^2] &= \left(\frac{\det(\mathbf{A}_{\mathcal{C},\mathcal{C}}^{(ij)})^2}{\det(2\mathbf{A}_{\mathcal{C},\mathcal{C}}^{(ij)} - \mathbf{I}_q)} \right)^{n/2} \\ &= \left(\frac{\det(\mathbf{A}_{\mathcal{C},\mathcal{C}}^{(ij)})}{\det(2\mathbf{I}_q - [\mathbf{A}_{\mathcal{C},\mathcal{C}}^{(ij)}]^{-1})} \right)^{n/2} \\ &= \left(\frac{1}{\det(\mathbf{I}_q + \rho\mathbf{E}_{ij}) \det(\mathbf{I}_q - \rho\mathbf{E}_{ij})} \right)^{n/2} \\ &= (1 - \rho^2)^{-n}.\end{aligned}$$

Case 3: If (i, j) and (i', j') has one common element, (without loss of generality, assume $j = j'$ and $i \neq i'$), we have

$$\begin{aligned}&\mathbb{E}_{P_0}[g_{ij}(\mathbf{X}_{\mathcal{C}})g_{i'j}(\mathbf{X}_{\mathcal{C}})] \\ &= \int_{\mathbb{R}^{n \times q}} \left((2\pi)^{-q/2} \det(\mathbf{A}_{\mathcal{C},\mathcal{C}}^{(ij)}) \det(\mathbf{A}_{\mathcal{C},\mathcal{C}}^{(i'j)}) \right)^{n/2} \exp \left(-\frac{1}{2} \sum_{k=1}^n \mathbf{x}_k^\top (\mathbf{A}_{\mathcal{C},\mathcal{C}}^{(ij)} + \mathbf{A}_{\mathcal{C},\mathcal{C}}^{(i'j)} - \mathbf{I}_q) \mathbf{x}_k \right) \mathbf{d}\mathbf{x} \\ &= \left(\frac{\det(\mathbf{A}_{\mathcal{C},\mathcal{C}}^{(ij)}) \det(\mathbf{A}_{\mathcal{C},\mathcal{C}}^{(i'j)})}{\det(\mathbf{A}_{\mathcal{C},\mathcal{C}}^{(ij)} + \mathbf{A}_{\mathcal{C},\mathcal{C}}^{(i'j)} - \mathbf{I}_q)} \right)^{n/2} \\ &= \left(\frac{1}{\det([\mathbf{A}_{\mathcal{C},\mathcal{C}}^{(ij)}]^{-1} + [\mathbf{A}_{\mathcal{C},\mathcal{C}}^{(i'j)}]^{-1} - [\mathbf{A}_{\mathcal{C},\mathcal{C}}^{(ij)}]^{-1}[\mathbf{A}_{\mathcal{C},\mathcal{C}}^{(i'j)}]^{-1})} \right)^{n/2} \\ &= (\det(\mathbf{I}_q - \rho^2\mathbf{E}_{ij}\mathbf{E}_{i'j}))^{-n/2} \\ &= (\det(\mathbf{I}_q - \rho^2\mathbf{e}_i\mathbf{e}_{i'}'))^{-n/2} \\ &= 1.\end{aligned}$$

We now combine the three cases together and note that if

$$b^2\kappa < 0.5, \text{ and } b^2 < 1,$$

we have $\rho^2 < 0.5$ and we can then compute

$$\begin{aligned}&\mathbb{E}_{P_0} \left(\frac{f_1(\mathbf{X})}{f_0(\mathbf{X})} \right)^2 \tag{E.23} \\ &= 1 + \left(\frac{2}{q(q-1)} \right)^2 \frac{q(q-1)}{2} [(1 - \rho^2)^{-n} - 1] \\ &\leq 1 + \frac{2}{q(q-1)} [(1 + 2\rho^2)^n - 1] \\ &\leq 1 + \frac{2}{q(q-1)} \exp(2b^2 \log q) \\ &\leq 1 + 4q^{-2(1-b^2)},\end{aligned}$$

where the first inequality is because $(1 - \rho^2)^{-1} \leq 1 + 2\rho^2$ since $\rho^2 < 0.5$, the second inequality is because the inequality $1 + x \leq e^x$, the last inequality is because $q > 2$ implies $q - 1 > q/2$.

Since $b^2 < 1$, we have

$$\limsup_{n,q \rightarrow \infty} \mathbb{E}_{P_0} \left(\frac{f_1(\mathbf{X})}{f_0(\mathbf{X})} \right)^2 \leq 1.$$

Following the same argument at the end of the proof for Theorem 5, we can derive an lower bound for the sum of error rates of two types for any test ϕ , and obtain

$$\liminf_{n,q \rightarrow \infty} \inf_{\phi} \sup_{(i,j) \in \mathcal{C}^2} (\mathbb{E}_{P_0} \phi + \mathbb{E}_{P_{ij}}(1 - \phi)) \geq 1,$$

which implies

$$\begin{aligned} \alpha &\geq \limsup_{n,q \rightarrow \infty} \sup_{\phi} \inf_{(i,j) \in \mathcal{C}^2} (\mathbb{E}_{P_{ij}} \phi) \\ &\geq \limsup_{n,q \rightarrow \infty} \sup_{\phi} \inf_{\Omega \in \Theta_{n^2}^*(b)} (\mathbb{E} \phi). \end{aligned}$$

This completes the proof. □

F Additional Simulations

In this section, we provide additional simulation results. Appendix F.1 examines the effect of the parameter L in Algorithm 2. Appendix F.2 explores more complicated graph structures. Appendix F.3 conducts our methods in the setting of an experiment in Verzelen and Villers [2009]. Appendix F.4 explores the use of prior information for constructing test statistics in the framework of the MC-GoF test.

F.1 Selection of L

The number of iterations L in Algorithm 2 determines the length of the generated Markov chains. The main text argues that $L = 1$ is sufficient for both theoretical and practical purposes. This appendix provides more empirical evidence to support this claim.

Specifically, we present two experiments:

1. Analyze the dependence structure using the autocorrelation function for the generated Markov chain with $L = 2,000$.
2. Compare the power performance of the MC-GoF test with $L = 1$, $L = 3$, and $L = 20$.

In both experiments, we consider running the algorithm with G_0 being a cyclic graph with $p = 120$ nodes, where each node is connected to its $d = 20$ nearest neighbors (10 on each side). Concretely, the adjacency matrix of this graph is constructed such that:

$$\mathbf{A}_{G_0}(i, j) = \begin{cases} 1 & \text{if } \min(|i - j|, p - |i - j|) \leq d/2, i \neq j \\ 0 & \text{otherwise} \end{cases}$$

The sample size n is set to 50, which is around the same magnitude as d —this is a high-dimensional scenarios with a dense null graph. The true precision matrix Ω has nonzero off-diagonal entries at (i, j) if $5 \leq \min(|i - j|, p - |i - j|) \leq 14$. In other words, on the true graph, each node is connected to its 6-th to 15-th neighboring nodes on each side. These nonzero entries are randomly and independently assigned values of either 1 or -1 . The diagonal entries of Ω are set to be a constant such that the smallest eigenvalue of Ω is 1. We then normalize Ω so that the resulting covariance matrix Σ has unit diagonal entries.

Dependence of Markov Chains. Given n samples from $N(\mathbf{0}, \Sigma)$, we implement Step 1 of Algorithm 2 with $L = 2000$ and obtain the Markov chain $\mathcal{C} = \{\mathbf{X}^{(t)}\}_{t=1}^L$ where each $\mathbf{X}^{(t)}$ is the output of Algorithm 1 according to $\mathcal{I} = \{1, 2, \dots, p\}$. Based on the algorithm, \mathcal{C} is a stationary process and all $\mathbf{X}^{(t)}$ share the same sufficient statistic for the GGM \mathcal{M}_{G_0} .

We observe that the process \mathcal{C} behaves as if it is i.i.d., rather than correlated. Specifically, we compute the Gram matrices $\mathbf{S}^t = (\mathbf{X}^{(t)})^\top \mathbf{X}^{(t)}$ and for each fixed pair of (i, j) absent from G_0 , we examine the autocorrelation of the process $\{\mathbf{S}^t(i, j)\}_{t=1}^L$. See Figure 5 for some examples of these processes. We note that there is no significant autocorrelation for $\{\mathbf{S}^t(i, j)\}_{t=1}^L$: we examine the first 1188 pairs of (i, j) absent from G_0 , among which only 2% of the calculated lag-1 autocorrelation coefficients exceed 0.05 in absolute value. This suggests that the \mathbf{S}^t and \mathbf{S}^{t-1} exhibit minimal dependence and the generated data are almost independent.

Power performance. We further analyze the power properties of the resulting MC-GoF test with various values of L . For simplicity, we focus on the F_Σ statistic. We implement the tests with $L \in \{1, 3, 20\}$ as well as the two baseline methods discussed in Section 5 of the main paper.

The results, computed based on 400 replications, are summarized in Table 9. It is clear that the MC-GoF test with any L outperforms the baseline methods, and there is no significant difference in power performance across different values of L . These observations, along with additional unreported numerical results, suggest that choosing L as small as 1 is often sufficient.

Method	Power	SE
M^1P_1	0.062	0.012
Bonf	0.043	0.010
MC-GoF ($L = 1$)	0.762	0.021
MC-GoF ($L = 3$)	0.770	0.021
MC-GoF ($L = 20$)	0.748	0.022

Table 9: Power of different goodness-of-fit tests for the dense cycle graph G_0 with degree 20. The dimension $p = 120$ and the sample size $n = 50$. Power and standard errors are estimated based on 400 replications.

F.2 More Complicated Graph Structures

We extend the experiments in Section 5 of the main paper to evaluate the power of the proposed MC-GoF tests on more diverse and challenging graph structures. Unlike the scenarios in Section 5, where true graphs were supergraphs of the null, we consider cases where the null graph may contain many false edges not present in the true graph. This null graph could have a dense graph structure relative to the sample size which is challenging for GoF testing. Furthermore, we will explore various graph structures, including tree graphs, spatial graphs, small-world graphs, and scale-free graphs, which may be more commonly seen in real-world applications.

All experiments use $N_p(\mathbf{0}, \Omega^{-1})$ as the data-generating population, with $p = 120$, $n = 50$, and are repeated for 400 times. The null graph G_0 and the true graph associated with the precision matrix Ω are specified as follows so that they have different graphical structures.

- **Tree vs. Star**

We begin with the case where G_0 is a tree graph where each parent has 3 children, and G is a star graph. The tree graph is a block graph where each pair of a parent and one of its child form a block. A star graph is a special tree graph where there is only one parent and all other nodes are its children. Note that G_0 and G are not nested: most of the edges in one graph are absent from the other graph. This experiment is designed to examine the ability of GoF tests to detect structural differences between fundamentally distinct graph topologies.

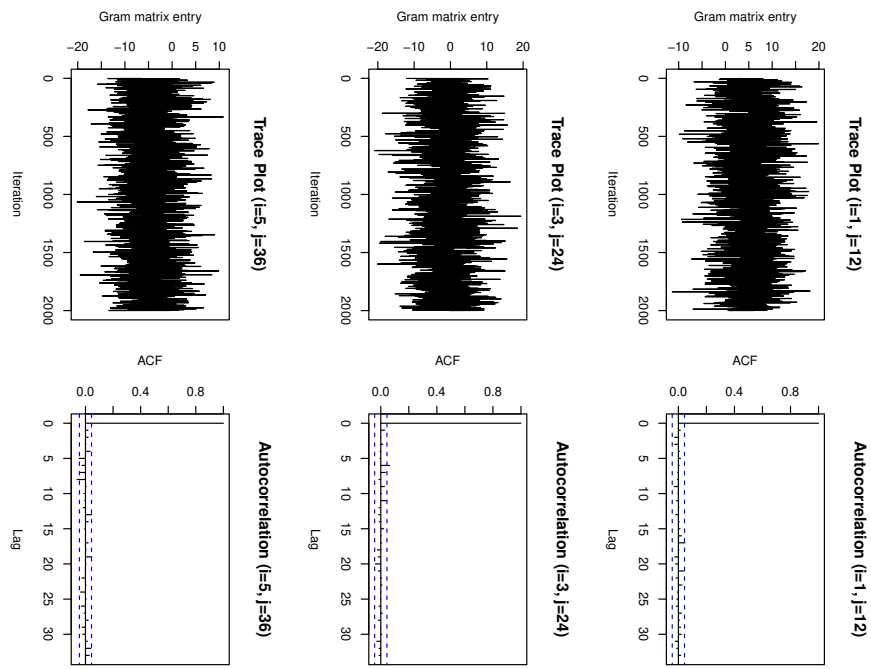


Figure 5: Generated values of $(\mathbf{X}^{(t)})^\top \mathbf{X}^{(t)}(i, j)$ for selected pairs of (i, j) absent from G_0 . Left: Trace plots. Right: Autocorrelation functions.

- **Spatial Graph**

A spatial lattice graph captures local dependencies typical in physical systems. We consider a 2D spatial lattice graph, where nodes are arranged in a 10×12 grid on \mathbb{Z}^2 and distance between nodes is defined as the ℓ_1 -distance. The null graph G_0 connects the pairs of nodes with distance equals to 1, and the true graph G connects the pairs of nodes with distance equal to 2.

- **Small-World Graph**

A small-world graph is a graph with high clustering and short path lengths [Watts and Strogatz, 1998], which are two of the characteristics shared by many real-world networks. We can use a small-world graph using the Watts-Strogatz algorithm with K being an even number and q being the rewiring probability: 1. Construct a regular ring lattice with each node connected to its K nearest neighbors ($K/2$ on each side); 2. At the j th iteration ($1 \leq j \leq K/2$), consider each node i and its j th rightmost neighbor k . With probability q , the edge (i, k) is replaced by another edge (i, k') where k' is chosen uniformly random over all nodes except for i, k , and those connected to i . We refer to Figure 1 in Watts and Strogatz [1998] for the specific procedure.

We implement this algorithm with $K = 8$ and $q = 0.3$ to get the null graph G_0 . The true graph G is obtained by removing edges in G_0 with probability 0.2 and adding edges absent in G_0 with probability 0.1.

- **Scale-free Graph**

A scale-free graph is a graph whose node degrees follow a power-law distribution [Barabási and Albert, 1999]. We can use the preferential attachment algorithm to generate a scale-free graph. For two integers m and $m_0 \geq m$, we start with a completely connected subgraph with m_0 nodes, and update the graph incrementally. At each time, we add a new node and m edges connecting this node with m of the existing nodes with probability proportional to the current node degrees. This preferential attachment ensures that high-degree nodes emerge so that the degree distribution is heavy tail. We implement this algorithm with $m = 2$ and $m_0 = 3$ to get the null graph G_0 . The true graph G is obtained in the same way as in the setting of Small-World Graph.

Given the true graph G , the precision matrix $\mathbf{\Omega}$ is obtained by assigning symmetric Bernoulli random variables on the entries associated with G and set the diagonal to be a positive constant so that the smallest eigenvalue of $\mathbf{\Omega}$ is 2. The results are summarized in Table 10. We recognize that the MC-GoF tests with any of the four test statistics significantly outperform the baseline methods across all types of graphs. In particular, F_Σ consistently achieves the highest power. These experiments consolidate the superior performance of our proposed method for various graphical structures.

F.3 Experiments in Verzelen and Villers [2009]

To test the GoF of GGMs, we additionally consider an experimental setup in Verzelen and Villers [2009] for a balanced comparison with existing methods. According to the setting of the first simulation experiment in Verzelen and Villers [2009, Section 3], the parameter η controls the percentages of edges in the true graph G , and the positions of edges are chosen uniformly.¹ Then we generate a random symmetric $p \times p$ matrix U , where for each pair of $i < j$, the element $U[i, j]$ is either sampled uniformly from the interval $[-1, 1]$ if an edge connects nodes i and j , or it is set to zero otherwise. Each diagonal entry of U is set to the sum of the absolute values of its row’s off-diagonal entries plus a small constant, ensuring that U is diagonally dominant and positive definite. Finally, U is standardized so that the diagonal entries all equal 1 to obtain the partial correlation matrix $\mathbf{\Pi}$, which is then used for sample generation.

¹Verzelen and Villers [2009] did not mention how a non-integer is rounded, so we decide to set the number of edges equal to $\lfloor \eta \times C_p^2 \rfloor$.

Model	$M^1 P_1$	Bonf	PRC	ERC	F_Σ	$GLR-\ell_1$
Tree vs. Star	0.040 (0.010)	0.058 (0.012)	0.395 (0.024)	0.385 (0.024)	0.532 (0.025)	0.362 (0.024)
Lattice	0.117 (0.016)	0.117 (0.016)	0.700 (0.023)	0.672 (0.023)	0.917 (0.014)	0.782 (0.021)
Small World	0.117 (0.016)	0.068 (0.013)	0.590 (0.025)	0.407 (0.025)	0.995 (0.004)	0.953 (0.011)
Scale Free	0.095 (0.015)	0.020 (0.007)	0.177 (0.019)	0.877 (0.016)	0.993 (0.004)	0.948 (0.011)

Table 10: Power of various GoF tests in for different graphical models at the significance level $\alpha = 0.05$. The dimension $p = 120$ and the sample size $n = 50$. See the text in Appendix F.2 for detailed description of the null graphs and the true population. The first two columns correspond to the baseline methods and the last four columns correspond to the MC-GoF test with four test statistic functions. Standard errors are in parentheses.

Their null graph G_0 is built from G by randomly deleting the existing edges at the proportion of q . In other words, $\lceil q \eta C_p^2 \rceil$ edges are randomly removed from G to define G_0 . In their simulations, the dimension p is fixed at 15, the sample size n varies among 10, 15, and 30, η is either 0.1 or 0.15, and q ranges from 0.1 to 1.

In this experiment, the sample size is so small that the GLasso algorithm does not provide any meaningful estimates, so we do not consider using the GLR- ℓ_1 statistic for the MC-GoF test here. Instead, we replace it with the F_{\max} statistic, which resembles the test statistic used in the M^1P_1 procedure proposed by Verzelen and Villers [2009].

The significance level of each test is set to $\alpha = 0.05$. We repeat the experiment 400 times and report the estimated power in Table 11 in a similar format as in Table 4. As the sample size n increases, the power of every method improves as expected. Furthermore, we observe that when q is 1 (i.e., the null graph G_0 is an empty graph), all testing methods, including the Bonferroni adjustment of partial correlation tests (Bonf), work exceptionally well even with a small sample size $n = 10$. This is very different from the experiments in Section 5 of the main paper, where Bonf substantially underperforms our methods regardless of the sample size.

The parameter q controls the number of different edges between the true graph G and the null graph G_0 . We observe that as q increases, every method works better because the deviation between G and G_0 increases. In addition, the M^1P_1 procedure (VV) stands out in every setting and can achieve higher power than our MC-GoF test with the statistics PRC and ERC. The gap is especially large in the cases with $q = 0.1$; in these cases, with either value of η , G_0 has two fewer edges than G . Although the number of edges omitted by G_0 is so small in these cases, the signal is strong enough for M^1P_1 to reject the null hypothesis with a probability of at least 36% (the minimum appears when $\eta = 0.15$ and $n = 10$). We call this pattern as *strong but sparse* to describe the deviation of the true distribution from the null hypothesis in these cases. This is in contrast to some of the experimental settings in Section 5, where the pattern of the deviation is dense but weak, and both M^1P_1 and Bonf underperform our methods by a large amount.

Overall, the MC-GoF tests with the F_Σ and F_{\max} statistics remain competitive to M^1P_1 in every case. These comparisons further justify our recommendations in Appendix B.4.2 of using F_Σ as the default test statistic for the MC-GoF test, because the simulation results here and the ones in Section 5 of the main paper together demonstrate its efficiency in power and its robustness to signal patterns.

F.4 Additional simulations on GoF tests with prior information

We examine the power of the MC-GoF test using the statistic function PRC-w formulated in Equation B.22 by extending the simulation shown in Table 4. Here we focus on a small signal magnitude $s = 0.1$ since our methods already perform sufficiently well when s takes a larger value as shown in Table 4. Assuming that we have the prior information that the true graph G might be a band graph with $K = 6$, we design a weight matrix $\mathbf{W} = (w_{ij})_{1 \leq i, j \leq p}$, where $w_{ij} = 0.8$ for $i \in \{1, \dots, p\}$ and $1 \leq |i - j| \leq 6$, and the other off-diagonal entries are equal to 0.2. Note that this prior information does not depend on \mathbf{X} , so the MC-GoF test using the PRC-w statistic remains valid.

To investigate the assistance of the prior information, we repeat the experiment in Table 4 using the MC-GoF test with the PRC-w statistic 400 times and report the results in Table 12, where we keep the results of the other MC-GoF tests in Table 4 for the same settings. We omit the results for M^1P_1 and Bonf since they underperform in these settings. The results demonstrate that the MC-GoF tests using statistics incorporated with the weight matrix \mathbf{W} achieve higher power than the original ones. In most cases, either PRC-w or ERC-w is the most powerful among these tests.

G Details of Real-World Examples

In this section, we provide detailed information about the applications of our testing methods to real-world datasets.

Table 11: Power of various GoF tests for the first experiment in Verzelen and Villers [2009]. $p = 15$. Significance level $\alpha = 0.05$.

(a) $\eta = 0.1$

q	n	Method					
		M^1P_1	Bonf	PRC	ERC	F- Σ	F-max
0.1	10	0.852 (.032)	0.352 (.042)	0.289 (.040)	0.367 (.043)	0.852 (.032)	0.844 (.032)
	15	0.922 (.024)	0.523 (.044)	0.453 (.044)	0.391 (.043)	0.922 (.024)	0.930 (.023)
	30	0.977 (.013)	0.758 (.038)	0.609 (.043)	0.453 (.044)	0.961 (.017)	0.977 (.013)
0.4	10	0.961 (.017)	0.867 (.030)	0.883 (.029)	0.930 (.023)	0.969 (.015)	0.961 (.017)
	15	0.992 (.008)	0.977 (.013)	0.953 (.019)	0.930 (.023)	0.992 (.008)	0.992 (.008)
	30	0.992 (.008)	1.000 (.000)	0.977 (.013)	0.945 (.020)	0.992 (.008)	0.992 (.008)
1	10	0.992 (.008)	0.992 (.008)	1.000 (.000)	0.992 (.008)	0.992 (.008)	0.992 (.008)
	15	0.992 (.008)	1.000 (.000)	1.000 (.000)	1.000 (.000)	1.000 (.000)	1.000 (.000)
	30	1.000 (.000)	1.000 (.000)	1.000 (.000)	1.000 (.000)	1.000 (.000)	1.000 (.000)

(b) $\eta = 0.15$

q	n	Method					
		M^1P_1	Bonf	PRC	ERC	F- Σ	F-max
0.1	10	0.367 (.043)	0.031 (.015)	0.055 (.020)	0.125 (.029)	0.414 (.044)	0.305 (.041)
	15	0.570 (.044)	0.195 (.035)	0.164 (.033)	0.148 (.032)	0.586 (.044)	0.578 (.044)
	30	0.781 (.037)	0.406 (.044)	0.258 (.039)	0.180 (.034)	0.789 (.036)	0.797 (.036)
0.4	10	0.750 (.038)	0.469 (.044)	0.430 (.044)	0.500 (.044)	0.852 (.032)	0.680 (.041)
	15	0.930 (.023)	0.758 (.038)	0.805 (.035)	0.695 (.041)	0.984 (.011)	0.930 (.023)
	30	0.992 (.008)	0.969 (.015)	0.953 (.019)	0.883 (.029)	0.992 (.008)	0.992 (.008)
1	10	0.883 (.029)	0.914 (.025)	1.000 (.000)	1.000 (.000)	0.992 (.008)	0.898 (.027)
	15	0.969 (.015)	0.992 (.008)	1.000 (.000)	1.000 (.000)	1.000 (.000)	1.000 (.000)
	30	1.000 (.000)	1.000 (.000)	1.000 (.000)	1.000 (.000)	1.000 (.000)	1.000 (.000)

Table 12: Boosting power by incorporating prior information in MC-GoF tests using the weighted statistics. The graphs are band graphs with $K = 6, K_0 = 1, s = 0.1$. Significance level $\alpha = 0.05$.

p	n	Method					
		PRC	PRC-w	ERC	ERC-w	F- Σ	GLR- ℓ_1
20	20	0.062 (.012)	0.085 (.014)	0.060 (.012)	0.095 (.015)	0.098 (.015)	0.085 (.014)
	40	0.217 (.021)	0.280 (.022)	0.190 (.020)	0.320 (.023)	0.212 (.020)	0.165 (.019)
	80	0.542 (.025)	0.725 (.022)	0.517 (.025)	0.785 (.020)	0.510 (.025)	0.352 (.024)
120	20	0.125 (.017)	0.268 (.022)	0.128 (.017)	0.263 (.022)	0.115 (.016)	0.070 (.013)
	40	0.225 (.021)	0.830 (.019)	0.215 (.021)	0.888 (.016)	0.260 (.022)	0.160 (.018)
	80	0.723 (.022)	1.000 (.000)	0.685 (.023)	1.000 (.000)	0.705 (.023)	0.370 (.024)

G.1 Average Daily Precipitation in the United States

Average daily precipitation, measured in mm, is collected from the North America Land Data Assimilation System (see [NLDAS] or the system's homepage: <https://wonder.cdc.gov/NASA-Precipitation.html>). Our dataset spans from 1979 to 2011 and comprises 48 states, excluding Alaska, Hawaii, and Puerto Rico due to their geographical isolation, and the District of Columbia due to its encirclement by Maryland and Virginia. The data range has sample size $n = 33$ and dimension $p = 48$. Figure 6 displays the map of the average daily precipitation in the contiguous United States in 2011 generated by [NLDAS].

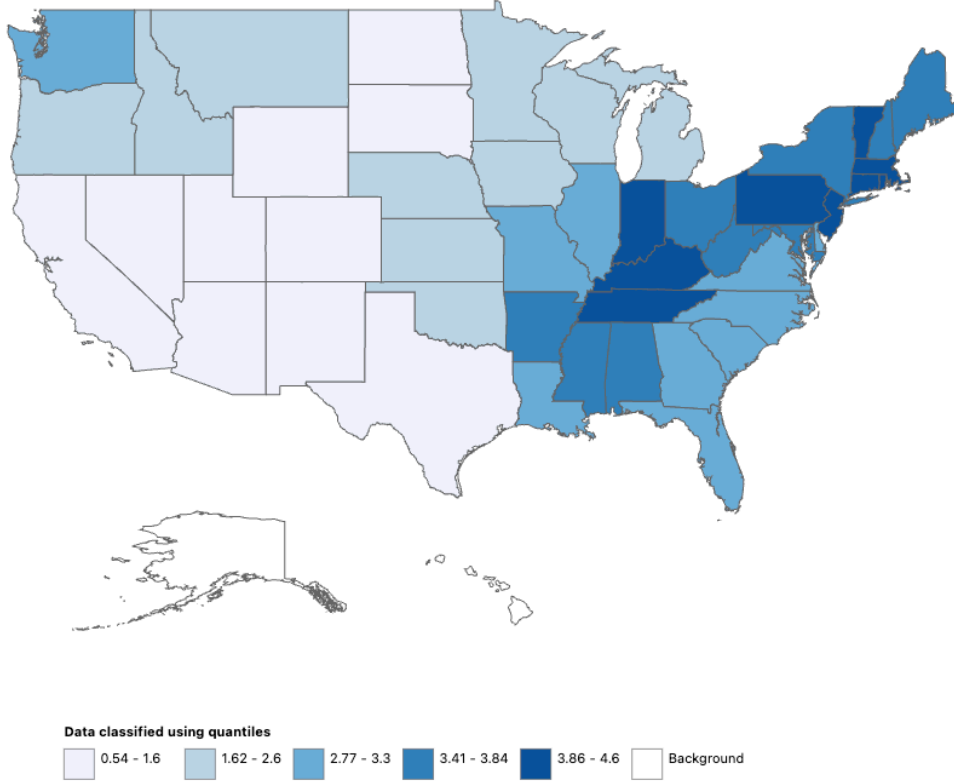


Figure 6: Map of Contiguous United States average daily precipitation in 2011 by [NLDAS]

Assuming the yearly averaged data are independent and identically distributed, we conduct the Box–Cox transformation to normalize the data. For any state, suppose the data are Z_i ($i \in [n]$). we first shift the data using $\tilde{Z}_i = Z_i - Z_{\min} + 0.01 \times (Z_{\max} - Z_{\min})$, where Z_{\max} and Z_{\min} are the maximum and the minimum of Z_i 's. We then transform the shifted data through the following function

$$\varphi(z) = \begin{cases} \frac{z^\lambda - 1}{\lambda}, & \text{if } \lambda \neq 0, \\ \ln(z), & \text{if } \lambda = 0, \end{cases} \quad (\text{G.1})$$

where the parameter λ is tuned by using the `boxcox()` function in the **R** package `MASS`. For each state, the transformed data pass the Shapiro–Wilk test with a p-value larger than the significance level $\alpha = 0.05$. This ensures that the distributions of the transformed data are approximately following some normal distributions.

Before our analysis, we perform a simulation study to assess the validity of these tests. We simulate data from the GGM with parameters estimated from the data under the null hypothesis. The precision matrix is estimated using a modified GLasso as in (B.20) but with λ set to be extremely large. We repeat this experiment 400 times and report the results in Table 13, which confirms that all methods control the Type-I error at the nominal level $\alpha = 0.05$.

Table 13: Estimated sizes of GoF tests using simulated data from the fitted model for US precipitation data ($\alpha = 0.05$).

	Method					
	M^1P_1	Bonf	PRC	ERC	F_Σ	GLR- ℓ_1
Size	0.062 (0.012)	0.050 (0.011)	0.052 (0.011)	0.055 (0.011)	0.055 (0.011)	0.045 (0.010)

The testing procedures considered here are identical to those in Section 5, specifically, our MC-GoF tests with statistics F_Σ , $GLR-\ell_1$, PRC, and ERC, as well as the benchmark methods M^1P_1 and Bonf. Table 14 summarizes the p-values of the GoF tests. The MC-GoF test using the F_Σ and the $GLR-\ell_1$ statistic reject the null hypothesis with p-values smaller than 0.05, which suggests that a GGM defined by the geographic adjacency of the states falls short of modeling the precipitation. A plausible explanation is that the data are strongly associated with precipitation in neighboring regions outside the U.S. such as Canada, Mexico, and the oceans, and the absence of the precipitation data in these regions breaks the conditional independence between non-adjacent states. Besides, the other tests fail to reject the null hypothesis. This is consistent with our simulation results in Section 5 that the MC-GoF test using F_Σ or $GLR-\ell_1$ can often achieve the highest power.

Table 14: Results of GoF tests for modeling precipitation using geographic adjacency.

	Method					
	M^1P_1	Bonf	PRC	ERC	F_Σ	$GLR-\ell_1$
p-value	1.000	0.252	0.059	0.317	0.030	0.010

We further investigate the influence of the sample size on the power of the GoF tests. To do this, we repeatedly draw a subsample of size n_s from the full dataset and perform the tests on this smaller dataset. For each subsample size n_s , we repeat the experiment 400 times and compute the fraction of times each test rejects the null hypothesis. Since these subsamples are not independently drawn from the population, the rejection rate in this experiment cannot be interpreted as power. Nonetheless, the rejection rate is an informative indicator of the influence of the sample size. The results are shown in Table 15. As n_s increases, the rejection rate of the MC-GoF test using the F_Σ statistic exhibits a clear increasing trend, whereas the MC-GoF test using the $GLR-\ell_1$ statistic almost always rejects the null hypothesis. The rejection rate resulting from the PRC statistic increases to 22% when n_s increases to 21 but remains lower than 30%. The other three tests all have rejection rates lower than 10%. In conclusion, the rejection decision given by the MC-GoF test using the $GLR-\ell_1$ statistic is robust with respect to the sample size, and the MC-GoF test using the F_Σ statistic is able to recover its decision more often when the subsample size increases.

Table 15: Rejection rates of GoF tests for modeling U.S. precipitation by geographic adjacency using a subsample of size n_s across 400 replications ($\alpha = 0.05$). Standard errors are placed in parentheses.

n_s	Method					
	M^1P_1	Bonf	PRC	ERC	F_Σ	$GLR-\ell_1$
18	0.065 (.012)	0.000 (.000)	0.060 (.012)	0.068 (.013)	0.310 (.023)	0.973 (.008)
21	0.085 (.014)	0.022 (.007)	0.215 (.021)	0.065 (.012)	0.420 (.025)	0.993 (.004)
24	0.080 (.014)	0.028 (.008)	0.255 (.022)	0.055 (.011)	0.530 (.025)	1.000 (.000)
27	0.072 (.013)	0.043 (.010)	0.278 (.022)	0.030 (.009)	0.645 (.024)	1.000 (.000)

G.2 Dependence of fund return

In the context of stock market analysis, building a graphical model for stock returns can uncover dependencies among stocks and identify clusters or sector-specific interactions. Such insights are valuable for portfolio management, risk assessment, and market structure analysis.

We consider the weekly average returns of 103 large-cap U.S. stocks, comprising 101 stocks from the Standard & Poor’s 100 Index (SP100) and the Dow Jones Industrial Average (DJIA). The return is defined as $(P_t - P_{t-1})/P_{t-1}$, where P_t and P_{t-1} are the adjusted closing prices of the current day and the last trading day on the stock market, respectively. We then apply a carefully chosen transformation to enhance the normality shown in the data (details on the transformation are deferred to the end). This results in $n = 92$ observations of averaged stock return X and the dimension p of X is 103.

Our analysis begins with a graphical modeling for the stock returns X . Suppose the observations of X are i.i.d. sampled from a normal distribution, and we want to find a graph G so that the distribution belongs to a GGM w.r.t. G . Here we aim at getting a super-graph G of the true graph so that even if the G includes some false edges, the model remains adequate for modeling the data. To facilitate the selection of such a super-graph, we incorporate the prior knowledge that the stocks can be classified into 11 sectors based on their industries (details on the sectors are deferred to the end). We estimate G using GLasso with regularization parameter $\lambda = 0.15$ and with no penalty on edges between stocks in the same sector. This approach yields a graph \hat{G} (Figure 7 in Appendix G.2), with a maximal degree of 30, a median degree of 19, and around 18.4% pairs of nodes are connected.

To validate the adequacy of the estimated graph \hat{G} for modeling the stock returns, we perform the MC-GoF test (Algorithm 3) with $G_0 = \hat{G}$ and statistic F_Σ (the overall winner in the simulation studies) as well as the two existing benchmarks M^1P_1 and Bonf to test the goodness-of-fit of the GGM with \hat{G} . The p-values are listed in Table 16 and are all above 0.3, which indicates that the GGM with \hat{G} is sufficient for modeling the stock data. This validation supports the suitability of the estimated graph for downstream analysis. For instance, if we are interested in a stock-related quantity, such as the return of a particular fund, we can leverage the GGM to conduct model-X inference.

Table 16: Results of GoF tests for modeling the stock returns by the GGM with the estimated graph.

	Method		
	M^1P_1	Bonf	F_Σ
p-value	1.000	0.352	0.321

Information of data collection, transformation, and sectors. An exchange-traded fund (ETF) is a basket of securities that tracks a specific index. The SPDR Dow Jones Industrial Average ETF Trust (DIA) was introduced in January 1998 and has been proven popular in the market [Hegde and McDermott, 2004]. The Standard and Poor’s 100 Index (SP100) includes 101 stocks (there are two classes of stock corresponding to one of the component companies). The holdings of the SP100 can be found on the homepage of the index-linked product iShares S&P 100 ETF (<https://www.ishares.com/us/products/239723/ishares-sp-100-etf>). We used the version of the holdings on September 29, 2023 for our analysis. We define sectors of these stocks almost the same as shown on the webpage but put the three stocks MA, PYPL, and V of payment technology companies in the sector of Information Technology rather than Financial, and put TGT in Consumer Discretionary rather than Consumer Staples. In our analysis, we have also included the two stocks TRV and WBA that are included by DJIA but not by the SP100. In total, we consider 103 stocks and they are divided into 11 sectors:

1. Communication Services (10): CHTR, CMCSA, DIS, GOOG, GOOGL, META, NFLX, T, TMUS, VZ
2. Consumer Discretionary (12): AMZN, BKNG, F, GM, HD, LOW, MCD, NKE, SBUX, TGT, TRV, TSLA
3. Consumer Staples (10): CL, COST, KHC, KO, MDLZ, MO, PEP, PG, PM, WMT
4. Energy (3): COP, CVX, XOM
5. Financials (15): AIG, AXP, BAC, BK, BLK, BRK-B, C, COF, GS, JPM, MET, MS, SCHW, USB, WFC
6. Health Care (15): ABBV, ABT, AMGN, BMY, CVS, DHR, GILD, JNJ, LLY, MDT, MRK, PFE, TMO, UNH, WBA

7. Industrials (13): BA, CAT, DE, EMR, FDX, GD, GE, HON, LMT, MMM, RTX, UNP, UPS
8. Information Technology (17): AAPL, ACN, ADBE, AMD, AVGO, CRM, CSCO, IBM, INTC, MA, MSFT, NVDA, ORCL, PYPL, QCOM, TXN, V
9. Materials (2): DOW, LIN
10. Real Estate (2): AMT, SPG
11. Utilities (4): DUK, EXC, NEE, SO

For any stock, denoted by Z_i 's the 5-day averages of returns. We then consider transformation using a piece-wise function

$$\psi(z) = \begin{cases} \text{sign}(z) \cdot |z|^\lambda, & \text{if } |z| < c, \\ \text{sign}(z) \cdot (a + 0.01 \cdot \log(|z|)), & \text{otherwise,} \end{cases} \quad (\text{G.2})$$

where $a = c^\lambda - 0.01 \cdot \log(c)$. The parameter λ is tuned over a grid from 0.1 to 2, and the parameter c is tuned over a grid between the 80% quantile and the maximum of the observed values of Z_i . The criteria to be maximized is the p-value of the Shapiro–Wilk test on the transformed data. After this transformation, only two stocks have p-values from the Shapiro–Wilk tests smaller than 0.05, and we alternatively use the Box–Cox transformation for these two stocks as described in Appendix G.1.

The graph \widehat{G} we estimated using GLasso is shown in Figure 7, where nodes are colored according to their sectors.

Figure 7: Estimated Graph with Color for Sector

